Quantum Hydrodynamic Models for Semiconductors with and without Collisions

Dissertation
zur Erlangung des Grades
Doktor der Naturwissenschaften

Am Fachbereich Physik, Mathematik und Informatik
der Johannes Gutenberg-Universität Mainz

Josipa Pina Milišić,
geboren in Split (Kroatien)

Mainz, 2007

Tag der mündlichen Prüfung: 21. August 2007

D77 - Mainzer Dissertation

Abstract

In this thesis we study quantum hydrodynamic (QHD) models, particularly the ones used in semiconductor device modeling. The QHD model consists of the conservation laws for the particle density, momentum, and energy density, including quantum corrections from the Bohm potential.
We start with a review of the known results on collisionless QHD models derived from the mixed-state Schrödinger system or from the Wigner equation. Using the reformulation of the one-dimensional stationary QHD equations with the linear potential as a stationary Schrödinger equation, the semi-analytical expressions for current-voltage curves are studied.
Further on, we consider viscous stabilizations of the QHD model. The numerical viscosity for the upwind finite-difference discretization of the QHD model proposed by C. Gardner is computed. On the other side, starting from the Wigner equation with the Fokker-Planck collision operator we derive the viscous QHD model. This model contains the physical viscosity introduced by the collision operator. The existence of solutions (with strictly positive particle density) to the isothermal, stationary, one-dimensional viscous model for general data and non-homogeneous boundary conditions is shown. The estimates depend on the viscosity and do not allow to perform the inviscid limit. By numerical simulations of the resonant tunneling diode using the non-isothermal, stationary, one-dimensional viscous QHD model, we show the influence of the physical viscosity on the solution.
Applying the quantum entropy minimization method, recently developed by P. Degond and C. Ringhofer, we derive the general QHD equations, starting from a Wigner-Boltzmann equation with the BGK-type collision operator. The derivation is based on a careful expansion of the quantum Maxwellian in powers of the scaled Planck constant. The general QHD model includes also vorticity terms and a dispersive term for the velocity. Current-voltage curve of the resonant tunneling diode for the simplified general QHD equations in one dimension is studied by numerical simulations. The results indicate that the dispersive velocity term regularizes the solution of the system.

Zusammenfassung

In dieser Arbeit werden Quantum-Hydrodynamische (QHD) Modelle betrachtet, die ihren Einsatz besonders in der Modellierung von Halbleiterbauteilen finden. Das QHD Modell besteht aus den Erhaltungsgleichungen für die Teilchendichte, das Momentum und die Energiedichte, inklusive der Quanten-Korrekturen durch das Bohmsche Potential.
Zu Beginn wird eine Übersicht über die bekannten Ergebnisse der QHD Modelle unter Vernachlässigung von Kollisionseffekten gegeben, die aus einem Schrödinger-System für den gemischten-Zustand oder aus der Wigner-Gleichung hergeleitet werden können. Nach der Reformulierung der eindimensionalen QHD Gleichungen mit linearem Potential als stationäre Schrödinger-Gleichung werden die semianalytischen Fassungen der QHD Gleichungen für die Gleichspannungs-Kurve betrachtet.
Weiterhin werden die viskosen Stabilisierungen des QHD Modells berücksichtigt, sowie die von Gardner vorgeschlagene numerische Viskosität für das upwind Finite-Differenzen Schema berechnet. Im Weiteren wird das viskose QHD Modell aus der Wigner-Gleichung mit Fokker-Planck Kollisions-Operator hergeleitet. Dieses Modell enthält die physikalische Viskosität, die durch den Kollision-Operator eingeführt wird. Die Existenz der Lösungen (mit strikt positiver Teilchendichte) für das isotherme, stationäre, eindimensionale, viskose Modell für allgemeine Daten und nichthomogene Randbedingungen wird gezeigt. Die dafür notwendigen Abschätzungen hängen von der Viskosität ab und erlauben daher den Grenzübergang zum nicht-viskosen Fall nicht. Numerische Simulationen der Resonanz-Tunneldiode modelliert mit dem nichtisothermen, stationären, eindimensionalen, viskosen QHD Modell zeigen den Einfluss der Viskosität auf die Lösung.
Unter Verwendung des von Degond und Ringhofer entwickelten Quanten-Entropie-Minimierungs-Verfahren werden die allgemeinen QHD-Gleichungen aus der Wigner-Boltzmann-Gleichung mit dem BGK-Kollisions-Operator hergeleitet. Die Herleitung basiert auf der vorsichtige Entwicklung des Quanten-Maxwellians in Potenzen der skalierten Plankschen Konstante. Das so erhaltene Modell enthält auch vertex-Terme und dispersive Terme für die Geschwindigkeit. Dadurch bleibt die Gleichspannungs-Kurve für die Resonanz-Tunneldiode unter Verwendung des allgemeinen QHD Modells in einer Dimension numerisch erhalten. Die Ergebnisse zeigen, dass der dispersive Geschwindigkeits-Term die Lösung des Systems stabilisiert.

Contents

List of Figures

List of Tables

Chapter 1

Introduction

In this work we are concerned with the modeling, mathematical analysis and numerical approximation of quantum hydrodynamic models for semiconductors.

Semiconductor devices, electronic components made of semiconductor materials, are essential in digital technologies, from computers to cellular phones. Semiconductors are materials whose ability to transport electricity is somewhere between conductors and insulators. At low temperatures semiconductors behave like insulators, but with some additional input their ability to conduct electricity can be greatly changed. The speciality of semiconductors lies in the fact that their current flow can be controlled (using external control voltages or adding impurities). Due to this fact, semiconductors are ideal for construction of electronic components, such are for example transistors. Transistors can serve as switches (on/off) or amplifiers, and are the key elements in integrated circuits. The first transistor, made of germanium, was developed in 1947. by Bardeen, Brattain and Schockley who were awarded the 1956. Nobel Prize in Physics, *for their research on semiconductors and their discovery of the transistor effect*. Since then semiconductor devices have evolved tremendously. Important fact which contributed to the success of the semiconductor technology is miniaturization[1] of the device length: from $20\mu m$ of the first transistor towards to the $90nm$ of the transistors in Pentium 4 processor. Modern quantum-based devices, like tunneling diodes, have structures of only few nanometer length.

[1] According to the International Technology Roadmap for Semiconductors, http://www.itrs.net/.

Clearly, on such scales, physical models should include quantum mechanical approaches. The hierarchy of quantum models for semiconductors is shown in the Figure 1.1. Formally, in the semi-classical limit, one obtains well known classical counterparts of mentioned models: Boltzmann, Vlasov and Liouville equation as the kinetic models and hydrodynamic, drift-diffusion and energy-transport equations in the group of classical fluid-type models for semiconductors. Detailed description of classical models can be found in [**64, 84**]. In the literature, the quantum Liouville equation is usually called the (many-particle) Wigner equation. This convention will be used also in this thesis.

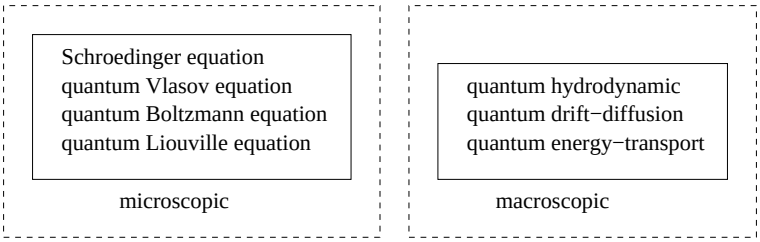

Figure 1.1: Hierarchy of quantum models for semiconductors

Besides mathematical modeling, the simulation of charge transport in semiconductor devices is also important research area. In order to produce devices at low cost and to reduce the production time, efficient computer simulations are necessary. However, simulations using quantum *microscopic* models, like the Schrödinger or Wigner equation, are very time consuming. Furthermore, since the problems of interest are defined on the bounded semiconductor domain, we encounter the problem of defining physically acceptable boundary conditions for microscopic variables.
In the literature, *macroscopic* quantum models have been proposed [**3, 33, 34, 40, 47**] and they seem to represent a compromise between requirements of physical accuracy and computational efficiency. In quantum fluid models the flow of the electrons in the semiconductor is considered as a gas of charged particles. These models have several advantages: they are formulated in terms of macroscopic quantities, like for example, the particle density, the fluid velocity or the temperature and consequently fluid-type boundary conditions can be imposed.
Roughly speaking, quantum macroscopic models belong either to the class of quantum hydrodynamic equations or to the class of quantum diffusion models (quantum drift-diffusion and quantum energy-transport models). As we have already pointed out at the beginning of the section, our aim is to

consider hydrodynamic rather then the diffusive models.

Quantum hydrodynamic models can be obtained through the moment expansion of the Wigner equation closed by quantum equilibrium distribution. Central to the kinetic theory is the collision operator, which models the interactions between the particles or their interactions with the surrounding environment (crystal lattice of the semiconductor). Here we mention that a quantum theory of collisions is still at a rather early stage and in fact there is no complete quantum collision theory up to now. There are many derivations of collision operators modeling the interactions of electrons with phonons [**8, 13, 35, 39, 43**], but none of them lead to a form which is computationally tractable and, at the same time, is usable for fluid approximations. However, for the derivation of quantum hydrodynamic models with collisions, in this work we use two simple collision models which have been derived in the literature. The first is the Fokker-Planck collision operator, derived by Caldeira and Leggett in [**23**] and later improved by Castella et al. in [**24**]. The second simple collision operator used in this thesis is given by a BGK approach (Bhatnagar, Gross and Krook [**16**]).

The collision operator is the source of entropy dissipation which induces the relaxation of the system towards local thermodynamical equilibrium. When this relaxation is achieved, the system evolves according to the fluid equations. Fluid-dynamical descriptions of gases rest on the assumption that the average distance travelled between the collisions is much smaller then the macroscopic length scales of interest. Here we mention that in some physical situations when the mean momentum of equilibrium vanishes, the motion of the mobile species must be observed at longer time scales. In this regimes the limit hydrodynamic model is not well adapted to capture the transport properties of the system and one needs the diffusive models.

The investigation of quantum hydrodynamic models, both from the analytical and numerical point of view attracts recently the attention of the scientific community. The quantum hydrodynamic equations are highly nonlinear, dispersive regularization of the classical Euler equations and due to their complicated mathematical structure there are still many open problems in their analysis. On the other side, using quantum hydrodynamic models in simulations of ultra-integrated semiconductor devices purely based on quantum effects, it is possible to describe quantum phenomena, such as negative differential resistance in a resonant tunneling diode.

Finally, we notice that the models similar to the quantum hydrodynamic equations also appear in application areas other than semiconductor theory, for example in superfluidity [**80, 81**] and thermistor theory, [**29, 98**].

1.1 Basic semiconductor physics

This section gives a short summary of the semiconductor physics. The aim here is just to motivate some concepts relevant to the material presented in the following chapters. In order to get the detailed view in this matter, we refer to textbooks on semiconductor physics, e.g., [**11, 19, 93**].
A semiconductor is a solid with an energy gap larger than zero and smaller than about $4eV$ (electron volt). In order to define the energy gap we describe briefly the crystal structure of solids. Solids are made of an infinite three-dimensional array of atoms arranged according to a lattice

$$L = \{n_1\vec{a}_1 + n_2\vec{a}_2 + n_3\vec{a}_3 \colon n_1, n_2, n_3 \in \mathbb{Z}\} \subset \mathbb{R}^3,$$

where $\vec{a}_1$, $\vec{a}_2$, $\vec{a}_3$ are basis vectors of the lattice. The set L is also called a Bravais lattice. The connected set $D \subset \mathbb{R}^3$ is called the primitive cell of L if

$$\mathrm{vol}(D) = \vec{a}_1 \cdot (\vec{a}_2 \times \vec{a}_3),$$

and if the whole space $\mathbb{R}^3$ is covered with the union of translates of D by the basis vectors. The reciprocal lattice L^* is defined by

$$L^* = \{n_1\vec{a}_1^* + n_2\vec{a}_2^* + n_3\vec{a}_3^* \colon n_1, n_2, n_3 \in \mathbb{Z}\} \subset \mathbb{R}^3,$$

where

$$\vec{a}_j \cdot \vec{a}_r^* = 2\pi\delta_{jr}, \quad j, r = 1, 2, 3.$$

The Brillouin zone $B \subset \mathbb{R}^3$ is the primitive cell of the reciprocal lattice L^* which is defined as (see Figure 1.2):

$$B = \{k \in \mathbb{R}^3 \colon |k| \leq \min_{l \in L^*} |k + l|,\ l \neq 0\}.$$

The lattice atoms generate a periodic electrostatic potential V_L,

$$V_L(x + y) = V_L(x), \qquad \text{for all } x \in \mathbb{R}^3,\ y \in L.$$

The state of an electron moving in this periodic potential is described by an eigenfunction $\psi(x)$ of the stationary Schrödinger equation

$$-\frac{\hbar^2}{2m}\Delta\psi - qV_L(x)\psi = E\psi, \quad x \in \mathbb{R}^3, \tag{1.1}$$

where $\psi \colon \mathbb{R}^3 \to \mathbb{C}$ is the (stationary) wave function, $\hbar$ is the reduced Planck constant, m the electron mass (at rest), q the elementary charge and E the energy.

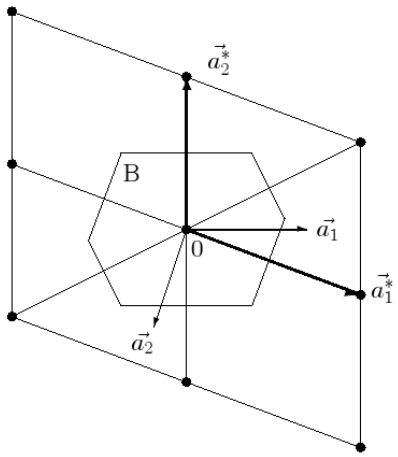

Figure 1.2: The primitive vectors of a two-dimensional lattice L and its reciprocal lattice L^* and the Brillouin zone (from [**64**], Figure 2.4).

Due to the Bloch theorem [**11**], the whole-space Schrödinger problem (1.1) can be reduced to an eigenvalue problem on a cell of the lattice. More precisely, the Bloch theorem says that the eigenfunctions of the problem (1.1) can be written as

$$\psi(x) = \mathrm{e}^{ik\cdot x}u(x), \tag{1.2}$$

(where $i^2 = -1$), for some $k \in B$ and some function $u(x)$ satisfying

$$u(x) = u(x+y), \qquad \text{for all } x \in \mathbb{R}^3,\ y \in L. \tag{1.3}$$

Inserting the decomposition (1.2) into the Schrödinger equation (1.1), one obtains that $u(x)$ satisfies the eigenvalue problem

$$-\frac{\hbar^2}{2m}(\Delta u + 2ik\cdot\nabla u) + \Big(\frac{\hbar^2}{2m}|k|^2 - qV_L(x)\Big)u = Eu, \qquad \text{in } D, \tag{1.4}$$

with the periodicity condition (1.3). Because of the self-adjointness of the operator defined by the left-hand side of (1.4), for each $k \in B$ there exists a sequence of eigenfunctions $u = u_{n,k}$ and eigenvalues $E = E_n(k)$ of (1.4)-(1.3). Since, in particular the functions $(u_{n,k})_{n\in\mathbb{N}}$ form an orthonormal basis of the underlying Hilbert space $L^2(D)$, one introduce the so-called Bloch functions

$$\psi_{n,k}(x) = \mathrm{e}^{ik\cdot x}u_{n,k}(x).$$

The Bloch pair $(\psi_{n,k}(x), E_n(k))_{n\in\mathbb{N}}$ is a solution of the eigenvalue problem for Schrödinger equation (1.1) in the primitive cell D of L with pseudo-periodic boundary conditions

$$\psi_{n,k}(x+y) = \mathrm{e}^{ik\cdot y}\psi_{n,k}(x), \quad x, x+y \in \partial D.$$

The continuous function $k \mapsto E_n(k)$ represents the n-th energy band. The ranges of all energy bands do not fill the whole energy space $\mathbb{R}$. There may exist energies E^* for which there is no $n \in \mathbb{N}$ and no $k \in B$ such that $E_n(k) = E^*$. Every connected component of the set of such energies is called an energy gap. The nearest energy band below the energy gap is called the valence band whereas the nearest one above is named the conduction band. So, the energy gap separates the top of the valence band and the bottom of the conduction band (see Figure 1.3).

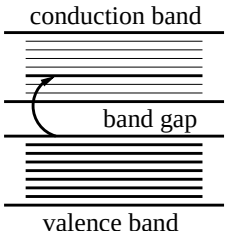

Figure 1.3: Simplified band diagram of a semiconductor

In a semiconductor, the energy gap is fairly small. At a low temperature the semiconductor has a completely filled valence band. There are no empty energy positions available for electrons to be accelerated in. Therefore, at low temperatures the semiconductor behaves like an insulator. At room temperature, the atoms in the semiconductor material vibrate enough so that a few electrons may escape from their positions in the valence band into unoccupied positions in the conduction band. The conduction at room temperature, however, is so small that no significant current can be said to pass. Finally, the electrical conductance happens when the energy level of a semiconductor crystal is moderately raised by, e.g., applying an electric field or increasing the temperature, since then many valence electrons became the conduction ones.
Semiconductors may be elemental materials such as silicon and germanium, or compound semiconductors such as gallium arsenide and indium phosphide, or alloys such as silicon germanium or aluminium gallium arsenide. The values of the energy gaps for some commonly used semiconductor materials can be seen in Table 1.1.

Material	Symbol	Energy gap in eV
silicon	Si	1.12
germanium	Ge	0.67
gallium arsenide	GaAl	1.42
aluminium gallium arsenide	$Al_{0.3}Ga_{0.7}As$	1.80
gallium phosphide	GaP	2.20

Table 1.1: Energy gaps of selected semiconductors (from [**11**], Table 28.1 and [**82**], Fig.1.14).

The mean velocity of the electron belonging to the n-th energy band is identified with the group velocity of the corresponding wave packet

$$v_n(k) = \frac{1}{\hbar}\nabla_k E_n(k). \tag{1.5}$$

The expression (1.5) has some important consequences. First, it is well known that the change of energy with respect to time equals the product of a force F and the velocity v_n. Combining this fact with (1.5), one obtains

$$\partial_t E_n(k) = \hbar^{-1} F \nabla_k E_n(k).$$

On the other side, using the chain rule $\partial_t E_n(k) = \nabla_k E_n(k)\partial_t k$ we conclude that

$$F = \partial_t(\hbar k). \tag{1.6}$$

Differentiating the expression (1.5) and using (1.6) leads to

$$\partial_t v_n = \frac{1}{\hbar^2}(\nabla_k^2 E_n)F.$$

Then, by Newton's law $F = \partial_t p = m^* \partial_t v_n$, and we infer that

$$(m^*)^{-1} = \frac{1}{\hbar^2}\nabla_k^2 E_n. \tag{1.7}$$

The expression (1.7) is considered as a definition of the effective mass m^*. We note here that symbol $(m^*)^{-1}$ is $\mathbb{R}^{3\times 3}$ matrix. Let k^0 be a local minimum of the conduction band, i.e. $\nabla_k E_n(k^0) = 0$. Then, since the Hessian matrix $\nabla_k^2 E_n(k^0)$ is symmetric, positive definite, it can be diagonalized and the

diagonal elements are positive. Assuming that the coordinates are chosen such that $\nabla_k^2 E_n(k^0)$ is already diagonal, we can write

$$\frac{1}{\hbar^2}\nabla_k^2 E_n(k^0) = \begin{bmatrix} 1/m_1^* & 0 & 0 \\ 0 & 1/m_2^* & 0 \\ 0 & 0 & 1/m_3^*. \end{bmatrix} \tag{1.8}$$

If the function $k \mapsto E_n(k)$ is smooth, Taylor's formula gives

$$E_n(k) = E_n(k^0) + \frac{\hbar^2}{2}\Big[\frac{(k_1-k_1^0)^2}{m_1^*} + \frac{(k_2-k_2^0)^2}{m_2^*} + \frac{(k_3-k_3^0)^2}{m_3^*}\Big] + O(|k-k^0|^3),$$

where $k = (k_1, k_2, k_3)^T$. In the case when $k^0 = 0$ and $m_1^* = m_2^* = m_3^* = m^*$, we can write, neglecting higher-order terms

$$E_n(k) = E_n(0) + \frac{\hbar^2}{2m^*}|k|^2. \tag{1.9}$$

Expression (1.9) is called the parabolic band approximation.
Up to now we saw that semiconductors exhibit an energy gap according to the band theory of solids. The population of the conduction band is described by the Fermi-Dirac distribution function, i.e. the electron probability of occupying an available energy state E is given by

$$f_{FD}(E) = \frac{1}{1 + e^{\frac{E-q\mu}{k_B T}}}, \tag{1.10}$$

where k_B is the Boltzmann constant, T the (electron) temperature and μ the chemical potential. We notice that, in the semiconductor theory, the product $q\mu$ is usually referred to as the Fermi level and it is noted by E_F. For energies much larger than the Fermi level in the sense of $E - E_F \gg k_B T$, the Fermi-Dirac distribution can be approximated by the Maxwell-Boltzmann distribution

$$f_{MB}(E) = e^{-\frac{E-E_F}{k_B T}}.$$

A pure semiconductor with no impurities is called an intrinsic semiconductor. In this case, electrons in the conduction band can only come from valence band levels leaving a vacancy behind them. Vacancies in the valence band are called holes. Therefore, the number of electrons in the conduction band is equal to the number of holes in the valence band,

$$n = p = n_i,$$

where n_i is the intrinsic density. Replacing some atoms in the semiconductor crystal by atoms which provide free electrons in the conduction band or free holes in the valence band, allows to increase the conductivity. Such process is called doping. Impurities are called donors, if they supply additional electrons and acceptors, if they supply the additional holes. Let $N_D(x)$ and $N_A(x)$ denote the densities of the donor and acceptor impurities, respectively. The doping profile or doping concentration is

$$C(x) = N_A(x) - N_D(x),$$

and the total space charge ρ is given by $\rho = -q(n - p - C(x))$. It remains to write the equation for the electrostatic potential. Electrons and holes interact on long-ranges via the Coulomb force

$$F(x, y) = -\frac{q}{4\pi\epsilon_S}\frac{x-y}{|x-y|^3},$$

where ϵ_S denotes the material constant called electrical permittivity. The resulting electric field is

$$E_{ef}(x,t) = \frac{1}{4\pi\epsilon_S}\int_{\mathbb{R}^3}\rho(y,t)\frac{x-y}{|x-y|^3}dy.$$

The electrostatic potential V, defined via $E_{ef} = -\nabla V$, is the solution of the Poisson equation

$$\epsilon_S \Delta V = q(n - p - C) \text{ in } \mathbb{R}^3.$$

1.2 Resonant tunneling diode

The resonant tunneling diode (RTD) is a device whose behaviour is dominated by quantum effects. Quantum hydrodynamical models derived in Chapters 3 and 4 are used in the simulations of simple one-dimensional resonant tunneling diode.

The resonant tunneling diode consists of the GaAs quantum well sandwiched between two very thin AlGaAs layers and heavily doped GaAs n^+-regions, called source and drain, situated at the contacts. The substrate of the n-channel between the n^+-regions is usually weakly doped. Figure 1.4 shows the cross section of the resonant tunneling diode. Applying a bias voltage to the device contacts, the resonant tunneling diode produces the certain current. The dependence of the obtained current upon the applied voltage is described with the current-voltage characteristics. The typical current-voltage curve for the resonant tunneling diode and the corresponding potential diagram are shown in the Figure 1.5. We observe that the current

Figure 1.4: Resonant tunneling diode

depends non-monotonically on the applied potential: there is a part of the current-voltage curve where the current decreases with increasing voltage. This is called the negative differential resistance (NDR) and it is caused by the quantum effect of tunneling. The tunneling process in the resonant tunneling diode is described here schematically following [**41**] and observing the Figure 1.5, without going into any deeper details. Firstly, a size-quantized state is confined in the well; its energy is indicated by the dashed line. The structure in equilibrium is denoted with (a). When a voltage is applied, electrons can resonantly tunnel out of occupied states (shaded region) through the confined state, (b). Finally, as the voltage is increased, the resonant state is pulled below the occupied levels and the tunneling current decreases, leading to the negative differential resistance. The goal of our nu-

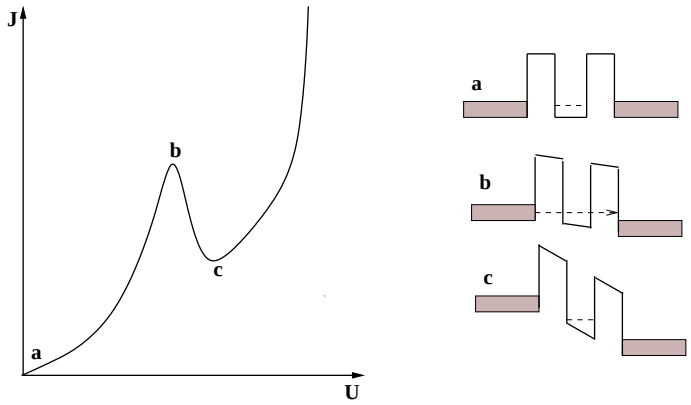

Figure 1.5: The schematic current-voltage curve of a resonant tunneling diode with the corresponding applied bias potential

merical simulations is to obtain, using the quantum hydrodynamic models derived in this thesis, the current-voltage curves for the resonant tunneling diode which reproduce the negative differential resistance effect. The experimental current-voltage curves for resonant tunneling diode can be found, for example, in [**74, 89**].

We note that the phenomenon of resonant tunneling in double barrier het-

erostructures was first investigated in the seminal work of Chang, Esaki, and Tsu [**26**]. It is worth to mention that Esaki received in 1973. the Nobel Prize in physics *for discovering the electron tunneling effect* used in tunnel diodes. Due to their intrinsically high-speed negative differential characteristics at room temperatures, resonant tunneling diodes are very promising nanoelectronic devices for digital logic circuit applications [**85**]. They are also used at very high frequencies as amplifiers or oscillators.

1.3 Overview of the main results

A fluid-dynamics formulation of the Schrödinger equation is known since the early years of quantum mechanics. In [**83**] Madelung assumed that the wave function can be written as

$$\psi(x,t) = \sqrt{n(x,t)}\mathrm{e}^{\frac{iS(x,t)}{\varepsilon}}, \tag{1.11}$$

where $n(x,t)$ is the electron density, $S(x,t)$ the phase and ε the scaled Planck constant. By performing elementary calculations (see Section 2.1 and Section 2.4), separating the real and the imaginary part of the single-state Schrödinger equation and defining the current density as $J(x,t) = n(x,t)\nabla S(x,t)$, one obtains the (scaled) zero-temperature quantum hydrodynamic equations:

$$\begin{aligned}
&\partial_t n - \mathrm{div} J = 0,\\
&\partial_t J - \mathrm{div}\left(\frac{J\otimes J}{n}\right) + n\nabla V + \frac{\varepsilon^2}{2} n\nabla\left(\frac{\Delta\sqrt{n}}{\sqrt{n}}\right) = 0, \quad x\in\mathbb{R}^d,\ t>0,
\end{aligned}$$

which are usually coupled with the Poisson equation for the potential

$$\lambda^2\Delta V = n - C(x), \tag{1.12}$$

where λ is the scaled Debye length and $C(x)$ the concentration of fixed charged background ions (the doping profile). Here, the unknowns are the electron density $n(x,t)$, the electron current density $J(x,t)$, and the electrostatic potential $V(x,t)$. Naturally, we impose initial conditions on the variables n and J. The velocity of the system can be defined as $u = J/n$. The matrix $J\otimes J$ consists of the elements $J_l J_k$, $l,k = 1,\dots,d$. The above equations are quantum analogue of the pressureless Euler equations under an electric force $E = \nabla V$ and with an additional third-order term. This quantum term can be interpreted either as an internal self-potential,

so-called Bohm potential, $\Delta\sqrt{n}/\sqrt{n}$, or as a non-diagonal pressure tensor, $(\nabla \otimes \nabla) \log n$, since

$$\frac{1}{2}\mathrm{div}(n(\nabla \otimes \nabla) \log n) = n\nabla\Big(\frac{\Delta\sqrt{n}}{\sqrt{n}}\Big). \tag{1.13}$$

In order to include temperature effects we abandon the Madelung's ansatz, since it is essentially devoted to the pure-state mechanics and cannot be adapted to include many-body effects. We are aware of two approaches of incorporating many-particle effects. The first approach starts from the mixed-state Schrödinger-Poisson system [**56, 63**]. Defining the particle and current densities as the superpositions of all single-state densities, quantum equations for the macroscopic variables (particle density, current density, and energy density) are derived. The system of equations is closed by expressing the heat flux heuristically in terms of the macroscopic variables. This approach is mentioned in Section 2.3 and it will not be used later in the thesis.
The second approach concerns the Wigner formalism together with the moment-method and it is used in this work in the derivation of the quantum hydrodynamic models. The schematic view of the quantum hydrodynamic models considered here together with the derivation techniques is presented in the Figure 1.6. The original contribution of this thesis concerns different

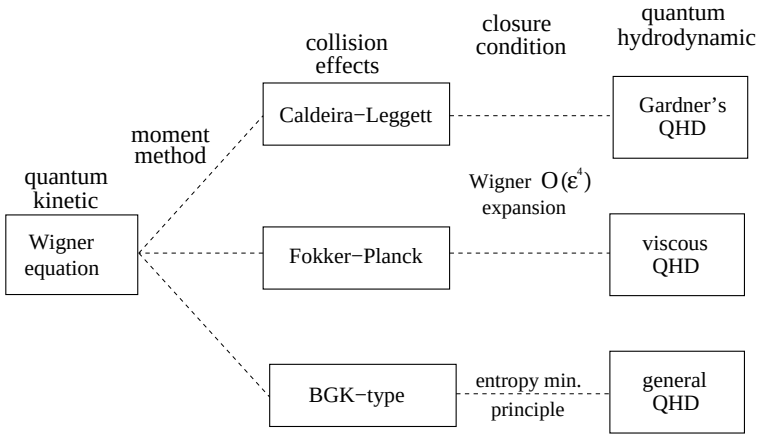

Figure 1.6: The summary of derivation methods, collision operators and models considered in this thesis.

aspects related to the analysis and numerics for the Gardner's QHD, the viscous QHD, and the general QHD model. More precisely, we studied the upwind scheme for the one-dimensional Gardner's QHD model, proposed

in [47]. Next, we derived the viscous quantum hydrodynamic model and performed the numerical simulations for a one-dimensional resonant tunneling diode. Moreover, for the isothermal version of this model in one space dimension we showed the existence of steady-state solutions. Finally, using the entropy minimization principle we derived the general quantum hydrodynamic model and for its simplified, one-dimensional version we made numerical simulations of a resonant tunneling diode.
Now, following the schematic view shown in the Figure 1.6, we explain the main steps in the derivation of quantum hydrodynamic models considered in the thesis. We start with the (collisional) Wigner equation in position-momentum phase space,

$$\partial_t f + p\cdot\nabla_x f + \theta[V]f = Q(f), \quad (x,p)\in\mathbb{R}^{2d},\ t>0, \tag{1.14}$$

where (x,p) is the position-momentum variable, $t>0$ is the time, and $\theta[V]$ is a pseudo-differential operator defined by

$$(\theta[V]f)(x,p,t) = \frac{i}{(2\pi)^{d/2}}\int_{\mathbb{R}^{2d}}\frac{1}{\varepsilon}\left[V\Big(x+\frac{\varepsilon}{2}\eta,t\Big)-V\Big(x-\frac{\varepsilon}{2}\eta,t\Big)\right]f(x,p',t)e^{i\eta\cdot(p-p')}d\eta dp'.$$

The operator $Q(f)$ on the right-hand side of the equation (1.14) is a quantum collision operator and models the interactions of electrons with the semiconductor crystal lattice. We leave this operator unspecified for the moment. The electric potential $V=V(x,t)$ is self-consistently coupled to the Wigner function $f(x,p,t)$ via Poisson's equation (1.12), where $n(x,t)=\int_{\mathbb{R}^d}f(x,p,t)dp$. The macroscopic variables are defined as the moments of the Wigner function f over momentum space; more precisely, we consider the particle density $n=\langle 1\rangle$, the fluid-dynamical momentum density $nu=\langle p\rangle$, and the energy density $e=\langle\frac{1}{2}|p|^2\rangle$, where we have used the notation $\langle g(p)\rangle=\int f(\cdot,p)g(p)dp$ for functions $g(p)$. In order to obtain macroscopic equations, a moment method is applied to (1.14): we multiply the equation by 1, p, and $\frac{1}{2}|p|^2$ and integrate over the momentum space. This yields evolution equations for n, nu and ne:

$$\frac{\partial}{\partial t}\begin{pmatrix} n\\ nu\\ 2ne\end{pmatrix} + \nabla_x\int_{\mathbb{R}^d} f\begin{pmatrix} p\\ p\otimes p\\ |p|^2 p\end{pmatrix}dp + \begin{pmatrix} 0\\ n\nabla_x V\\ nu\cdot\nabla_x V\end{pmatrix} = \int_{\mathbb{R}^d} Q(f)\begin{pmatrix} 1\\ p\\ |p|^2\end{pmatrix}dp. \tag{1.15}$$

However, the above equations contain the integrals

$$\int_{\mathbb{R}^d} f(x,p,t)p\otimes p\,dp \quad \text{and} \quad \int_{\mathbb{R}^d} f(x,p,t)|p|^2 p\,dp \tag{1.16}$$

which generally cannot be expressed in terms of macroscopic variables n, nu and ne without the additional assumption on the Wigner function f, i.e. the system (1.15) is not closed. In order to pass from the microscopic to the macroscopic level, we need to specify the collision operator and to close the system. We achieve the closure by approximating the Wigner function with the thermal equilibrium distribution function.
Roughly speaking, certain definitions of the collision operator and the thermal equilibrium distribution lead us to different quantum hydrodynamic models. We start our introductory overview of the models studied in this thesis with the Gardner's quantum hydrodynamic model.

Gardner's quantum hydrodynamic model

Very important work on the quantum hydrodynamics for semiconductors is given in the article of Gardner [**47**] where he derived the quantum hydrodynamic equations, performed an upwind numerical scheme and made the simulations of the resonant tunneling diode. In Section 3.3.2 we analyze the Gardner's finite-difference scheme. Furthermore, in Section 3.3.3 and Section 4.5 we compare numerical results achieved using the quantum hydrodynamic models derived originally in this thesis with the model of Gardner.
The main steps in the derivation of the Gardner's model can be seen in Section 2.3 (there presented without the collision operator). For modelling the collisions Gardner used the Caldeira-Leggett operator [**23**]. Namely, Caldeira and Leggett derived a Wigner equation in the large-temperature limit (1.14) with the operator

$$(Q(f))(x,p,t) = \Delta_p f(x,p,t) + \frac{1}{\tau}\mathrm{div}_p(pf(x,p,t)), \tag{1.17}$$

where $\tau > 0$ is the relaxation time. As a closure condition Gardner employed a quantum-corrected thermal equilibrium distribution function (2.15), based on the result of Wigner [**97**], in place of f in the derivation of the moment equations. Arguing that the electric potential is close to $\log n$ near equilibrium, Gardner replaces V by $\log n$, which is the origin of the Bohm potential. The main mathematical difficulty in the analysis of quantum hydrodynamic models is the treatment of highly nonlinear third-order quantum term and

the proof of the nonnegativity of the particle density, since in general maximum principles cannot be applied here. The mathematical difficulties influence also the numerical approximation of the equations. There is strong numerical evidence that the equations, discretized by finite differences or finite elements, need some kind of stabilization. In view of the similarity of the (transient) quantum hydrodynamic model to the Euler equations, the use of a hyperbolic scheme, treating the third-order quantum part as a perturbation, seems to be appropriate. In this sense, as we have already mentioned, Gardner [**47**] employed the upwind scheme to the stationary one-dimensional quantum model, which introduces numerical viscosity. In Section 3.3.2 is shown that the numerical viscosity is (in one space dimension) of the form $h(|u|n_x)_x/2$ in the continuity equation and $h(|u|(nu)_x)_x$ in the momentum equation, where h is the mesh size and u is the velocity. Moreover, numerical results show that the static current-voltage curve of a tunneling diode is strongly mesh-depending.

Viscous quantum hydrodynamic model

Chapter 3 is devoted to the analytical and numerical considerations of the viscous quantum hydrodynamic model. Instead of employing a *numerical viscosity* stabilization of quantum hydrodynamic equations, we are interested in the stabilization by a *physical viscosity* which will be introduced in the model by appropriate collision operator. This was the motivation for deriving the viscous quantum hydrodynamic model. For modelling the collisions we used the Fokker-Planck operator proposed by Castella et al., in [**24**] as an improvement of the Caldeira-Leggett operator [**23**]. Namely, the corresponding Wigner equation in the large-temperature limit (1.14) with the Caldeira-Leggett operator on the right hand side was not in Lindblad form and hence, the positivity of the density operator was not preserved under temporal evolution. Castella et al. improved the derivation of the Caldeira-Leggett model and derived a Wigner-Fokker-Planck model belonging to the Lindblad class. This model reads as (1.14) with the collision operator

$$\begin{aligned}(Q(f))(x,p,t) &= \nu_0\Delta_x f(x,p,t) + \nu_1\Delta_p f(x,p,t)\\ &\quad + \nu_2\mathrm{div}_x(\nabla_p f(x,p,t)) + \frac{1}{\tau}\mathrm{div}_p(pf(x,p,t)).\end{aligned} \tag{1.18}$$

The parameters ν_0, ν_1, $\nu_2 \geq 0$ constitute the phase-space diffusion matrix of the system, and $\tau > 0$ is like before a friction parameter, the relaxation time. We notice that in the semi-classical limit $\varepsilon \to 0$, where ε is the (scaled) Planck constant, it holds $\nu_0 \to 0$ and $\nu_2 \to 0$, and the scattering operator reduces to the Caldeira-Leggett operator (1.17).

In order to close the system, we employed the shifted-equilibrium distribution (2.15) in the corresponding Wigner model. The isothermal quantum hydrodynamic model containing viscous terms has been already derived in [**58, 72**]. Moreover, in this thesis we proceed one step further and derive the *nonisothermal viscous quantum hydrodynamic model* for the particle density n, the current density J, and the energy density ne:

$$\partial_t n + \operatorname{div} J = F_1, \tag{1.19}$$

$$\partial_t J + \operatorname{div}\Big(\frac{J\otimes J}{n}\Big) + \operatorname{div} P - n\nabla V = F_2, \tag{1.20}$$

$$\partial_t (ne) + \operatorname{div}\Big(\frac{J}{n}(P+neI)\Big) - J\cdot\nabla V = F_3, \quad x\in\Omega,\ t>0, \tag{1.21}$$

where $\Omega\subset\mathbb{R}^3$ is a bounded domain, I is the identity matrix, the (scaled) stress tensor P and energy density ne are given by

$$P = nTI - \frac{\varepsilon^2}{12}n(\nabla\otimes\nabla)\log n, \quad ne = \frac{|J|^2}{2n} + \frac{3}{2}nT - \frac{\varepsilon^2}{24}n\Delta\log n,$$

with the (scaled) Planck constant ε and the particle temperature T. We note here that the stress tensor P is given as a sum of the classical pressure term followed by the quantum correction. In the same sense, the energy e is given as a sum of the kinetic energy, thermal energy and the quantum correction. The source terms F_1, F_2, and F_3 are given as

$$F_1 = \nu\Delta n, \quad F_2 = -\frac{J}{\tau} + \nu\Delta J - \mu\nabla n,$$
$$F_3 = -\frac{2}{\tau}\Big(ne - \frac{3}{2}n\Big) + \nu\Delta(ne) - \mu\operatorname{div} J,$$

where $\nu>0$ is the (scaled) viscosity constant and μ is proportional to ν/ε (see Section 3.1 for details on the derivation and the scaling of the equations). The electric potential V is self-consistently coupled to the Poisson equation (1.12). Equations (1.19)-(1.21), (1.12) are to be supplemented with boundary conditions for n, J, ne, and V. Notice that the viscous terms in F_1 and F_2 are similar to the numerical viscosity calculated for Gardner's upwind scheme (in one space dimension) with ν replaced by $h|u|$. The effective current density is given by $J_0 = J - \nu\nabla n$ such that J_0 is divergence-free.
The use of physical viscosity has some important consequences. First, we are able to show the existence of steady-state solutions to the one-dimensional isothermal model with physically motivated boundary conditions for *any* value of $\nu>0$ and *any* value for the applied voltage. Namely, we assume that the particle density n is given at the boundary, that n satisfies as in [**47**]

homogeneous Neumann boundary conditions, and that the second derivative n_{xx} is periodic at the boundary. Furthermore, the electric potential on the boundary is given by the applied voltage. Up to now only partial existence results were available for the viscous quantum hydrodynamic equations [58]. The main difficulties which we needed to overcome in mathematical analysis of the isothermal model are: (i) the third-order differential operator, (ii) the strong nonlinearities, and (iii) the nonhomogeneous boundary conditions. The first idea of the proof of the existence result is to formulate the quantum hydrodynamic equations as in [54] as a *fourth-order* differential equation for the exponential variable $n = e^w$. This avoids the difficulty (i). The fixed-point operator in the existence proof is then defined in $w = \ln n$ with domain $H^2_{\rm per}$, the space of periodic H^2 functions. The second idea, which allows to treat the difficulty (ii), consists in estimating the energy production

$$E_P = \nu\int_0^1 \Big(nu_x^2 + \frac{\varepsilon^2}{3}(\sqrt{n})_{xx}^2 + \frac{\varepsilon^2}{144}\frac{n_x^4}{n^3} + \frac{n^2}{2\nu\lambda^2} + 4\Big(T+\frac{\nu}{\tau}\Big)(\sqrt{n})_x^2 + \frac{J_0^2}{\nu\tau n}\Big)dx,$$

where $J_0 = J - \nu n_x$, using the *third-order* formulation of the viscous quantum hydrodynamic model. Because of the boundary conditions (difficulty (iii)), we only obtain the estimate $E_P \le J_0U/\nu + c$, where $c > 0$ is a constant. However, the electric power J_0U/ν can be estimated, thanks to the Poisson equation, in terms of the integral $\int n^2dx$ which can be absorbed by the energy production. The bound on the energy production only provides an estimate for $\sqrt{n}$ in H^2; however, the definition of the fixed-point operator makes necessary an estimate for $w = \ln n$ in H^2. This is achieved by first estimating the velocity J_0/n, employing the energy production bound, and then carefully proving a bound on w_{xx} in L^2, by using the fourth-order formulation of the equation. These estimates are sufficient to apply the Leray-Schauder fixed-point theorem.

We notice that the proof of the existence result makes use of both the original third-order *and* the fourth-order formulation of the quantum hydrodynamic model. Furthermore, we remark that all a priori bounds depend on ν and become useless in the limit $\nu \to 0$. The above energy estimate shows the regularizing effect of the viscosity since we obtain (viscosity-dependent) a priori H^2 bounds. Our proof seems to be only valid in the one-dimensional setting since we use the embedding $H^1 \hookrightarrow L^\infty$. Moreover, it seems to be difficult to generalize the proof to the viscous quantum hydrodynamic model including the energy equation (1.21).

The second consequence of the viscous terms concerns the numerical approximation of the quantum hydrodynamic model. In the literature, the quantum hydrodynamic equations have been discretized employing an upwind

finite-difference approximation [47], a Runge-Kutta discontinuous Galerkin method [27, 28], and a relaxation scheme [72]. As mentioned above, these hyperbolic-type schemes lead to possibly large numerical viscosity. On the other side, the physical viscosity included in the viscous quantum hydrodynamic equations enables to discretize the model using central finite differences. Moreover, in Section 3.3.2 we show that the numerical dispersion, introduced by the central scheme, is much smaller than the physical dispersion, given by the third-order quantum terms. In particular, we show that the numerical results are much less mesh-depending than the upwind scheme employed for the Gardner's quantum hydrodynamic equations. However, we claim that the quantum hydrodynamic model is very sensitive with respect to any change of physical or numerical viscosity. The central finite-difference approximation is a rather simple numerical method and usually it has some stability problems, but here it gives good results, at least in one space dimension, when the mesh is fine enough. In Section 3.3.2 we give a consistency analysis which allows to interpret the numerical results for both the central and the upwind discretization. Notice that the numerical approximation of the quantum hydrodynamic equations, with or without viscosity, is still not well understood.
The analytical results do not allow for the inviscid limit $\nu \to 0$. Numerically this can be seen by the fact that the viscosity cannot be chosen arbitrarily small in our scheme (although the physical value for ν can be used). This indicates that the physical viscosity is indeed needed for stabilization.
There is also a drawback of the viscous model. One of the interests of the quantum hydrodynamic equations is the simulation of resonant tunneling diode whose current-voltage characteristics exhibit negative differential resistance effects, i.e., the current density is monotonically decreasing in a certain voltage range. An important quantity is the peak-to-valley ratio, i.e. the quotient of local maximum to local minimum current densities. Our numerical experiments for the nonisothermal model show that the peak-to-valley ratio is too small compared to physical experiments. Thus, the physical viscosity strongly influences the quantum behavior of the model.

General quantum hydrodynamic model.

In Chapter 4 we make more systematic approach to the problem of the derivation of quantum hydrodynamic models. Instead of taking Gardner's closure condition like in Chapter 3, here we apply the quantum entropy minimization method recently developed by Degond and Ringhofer [36]. Before we sketch the idea of the closure, we specify the collision operator.

We assume that the kernel of the collision operator consists of the quantum thermal equilibrium distribution and that the operator preserves certain moments. Such operator belongs to the class of so-called BGK-type operators, named by Bhatnagar, Gross and Krook [16].
Our approach to define a closure is based on Levermore's entropy minimization principle. This method has been first employed in the context of classical gas dynamics [78] and has been recently extended to quantum fluids [36]. The idea is to define the equilibrium distribution as the minimizer of the quantum entropy[2] subject to the constraints of given moments. The equilibrium distribution is also called the *quantum Maxwellian* since there are some similarities to the classical Maxwellian of gas dynamics. The quantum Maxwellian M_f, as the solution of a constrained minimization problem, depends on Lagrange multipliers which can be interpreted in the $O(\varepsilon^2)$ approximation as the logarithm of the particle density, the fluid velocity, and the temperature, respectively. Expanding M_f in powers of ε^2 and assuming similarly as in [47] that spatial variations of the temperature $T = T(x,t)$ are of the order $O(\varepsilon^2)$, we derive the following quantum hydrodynamic equations up to order $O(\varepsilon^4)$,

$$\begin{aligned}
\partial_t n + \operatorname{div}(nu) &= 0, && (1.22)\\
\partial_t(nu) + \operatorname{div}(nu\otimes u) + \operatorname{div} P - n\nabla V &= 0, && (1.23)\\
\partial_t e + \operatorname{div}\big((P+eI)u\big) + \operatorname{div} S - nu\cdot\nabla V &= 0, && (1.24)
\end{aligned}$$

where I is the unit matrix in $\mathbb{R}^{d\times d}$, the energy density equals

$$e = \frac{d}{2}nT + \frac{1}{2}n|u|^2 - \frac{\varepsilon^2}{24}n\Big(\Delta\log n - \frac{1}{T}\operatorname{tr}(R^\top R)\Big),$$

with the trace "tr" of a matrix, the quantities P (stress tensor) and S are given by

$$\begin{aligned}
P &= nTI - \frac{\varepsilon^2}{12}n\Big((\nabla\otimes\nabla)\log n - \frac{1}{T}R^\top R\Big),\\
S &= -\frac{\varepsilon^2}{12}n\Big(\Big(\frac{d}{2}+1\Big)R\nabla\log n + \Big(\frac{d}{2}+2\Big)\operatorname{div} R + \frac{3}{2}\Delta u\Big)\\
&\quad + \frac{\varepsilon^2}{12}\Big(\frac{d}{2}+1\Big)n(R\nabla\log n + \operatorname{div} R),
\end{aligned}$$

and the vorticity matrix $R = (R_{ij})$ is the antisymmetric part of the velocity derivative,

$$R_{ij} = \partial_{x_j}u_i - \partial_{x_i}u_j. \qquad (1.25)$$

[2] Here, we adopted the mathematical sign convention of decreasing entropy.

A more general model, allowing arbitrarily large spatial deviations of the temperature, is derived in Section 4.2. Employing a Caldeira-Leggett-type collision operator, relaxation-time terms can be also included (see Section 4.2.1). According to (1.13), the quantum correction $(\varepsilon^2/12)n(\nabla\otimes\nabla)\log n$ can be interpreted as a force including the Bohm potential $\Delta\sqrt{n}/\sqrt{n}$ [**40**]. For $\varepsilon = 0$ in (1.22)-(1.24), we recover the classical hydrodynamic equations. For $\varepsilon > 0$ and constant temperature, we obtain the same equations as derived in [**32, 70**] where also the quantum entropy minimization method has been used. Our model differs from Gardner's quantum hydrodynamic equations (formulas (1)-(3) in [**47**]) by the vorticity term R and the dispersive velocity term in the energy equation (1.24),

$$\operatorname{div} q_S = \frac{\varepsilon^2}{8}\operatorname{div}(n\Delta u). \tag{1.26}$$

The origin of this difference lies in the different choices of the quantum Maxwellian. We refer to Section 4.2.5 for a detailed discussion.
The term q_S – but not the vorticity R – also appears in some other quantum hydrodynamic derivations. It has been derived in [**48**] from a mixed-state Wigner model and interpreted as a dispersive "heat flux" (see formula (36) in [**48**]). Moreover, it appears in the quantum hydrodynamic equations of [**52**] involving a "smoothed" potential, derived from the Wigner-Boltzmann equation by a Chapman-Enskog expansion.
An interesting feature of the dispersive term (1.26) is that it stabilizes the quantum hydrodynamic system numerically. More precisely, this term allows us to solve the general quantum hydrodynamic equations in one space dimension by using a central finite difference scheme, thus avoiding numerical viscosity.
The numerical simulations of a quantum hydrodynamic model involving the term (1.26) are presented in Section 4.5. Like before, a simple one-dimensional resonant tunneling diode is simulated. The current-voltage characteristics show multiple regions of negative differential resistance. The dispersive term (1.26) has the effect of "smoothing" the current-voltage curve, i.e., it decreases the peak-to-valley ratio.
In Section 4.4 we also examine the existence of conserved quantities of the general quantum hydrodynamic equations. Clearly, the mass is conserved. We prove that also the energy $E = \int(e + \lambda^2|\nabla V|^2/2)dx$ is conserved. This provides gradient estimates for the particle density, velocity, and temperature, which are useful in the mathematical analysis of the equations.
At the end of this introductory overview, we point out that the quantum entropy minimization principle enables a systematic derivation of quantum

macroscopic models. Namely, using this principle, not only quantum hydrodynamic, but also quantum diffusive models (quantum drift-diffusion and quantum energy-transport model) can be derived [**33, 34**].

Chapter 2

QHD models without collisions

In this chapter we derive various versions of quantum hydrodynamic models, either from the Schrödinger or from the Wigner equation. We point out that Sections 2.1-2.3 are the reviews of known results which can be found for example in [**47, 49, 53, 55**]. This chapter begins with Section 2.1, where, starting from the single-state Schrödinger equation, the zero-temperature quantum hydrodynamic model is obtained. Next, in Section 2.2 one starts with the Wigner formalism and derives the small-temperature quantum hydrodynamic models. We mention also another approach for the derivation of the quantum hydrodynamic equations starting from a mixed-state Schrödinger system. Finally, we end the review sections with a very brief description of some analytical and numerical results in the literature on the quantum hydrodynamic models. In Section 2.4 we discuss the current-voltage curves of the simplified quantum hydrodynamic models, where the potential V is considered to be given in advance instead as usual, to be self-consistently coupled to the electron density through the Poisson equation. The essential idea here is to study simplified situations where the Schrödinger equation, which is formally equivalent to the quantum hydrodynamic model, can be explicitly solved.

2.1 Zero-temperature models

The evolution of a single electron is governed by the (dimensionless) Schrödinger equation for the wave function ψ,

$$i\varepsilon\partial_t\psi = -\frac{\varepsilon^2}{2}\Delta\psi - V\psi, \quad x\in\mathbb{R}^d,\ t>0, \tag{2.1}$$

$$\psi(0,x) = \psi_I(x), \quad x\in\mathbb{R}^d. \tag{2.2}$$

We assume that the initial datum is given by the WKB state (Wentzel [**94**], Kramers [**75**], Brillouin [**22**])

$$\psi_I = \sqrt{n_I}\exp(iS_I/\varepsilon). \tag{2.3}$$

Then a simple computation [**53**] shows that the solution of (2.1)-(2.3) is given by $\psi(t,x)=\sqrt{n(t,x)}\exp(iS(t,x)/\varepsilon)$, where (n,S) is a solution of the *zero-temperature quantum hydrodynamic equations*

$$\partial_t n - \mathrm{div} J = 0, \tag{2.4}$$

$$\partial_t J - \mathrm{div}\left(\frac{J\otimes J}{n}\right) + n\nabla V + \frac{\varepsilon^2}{2}n\nabla\left(\frac{\Delta\sqrt{n}}{\sqrt{n}}\right) = 0, \tag{2.5}$$

where $x\in\mathbb{R}^d$, $t>0$ with the current density $J=-n\nabla S$ and the initial conditions

$$n(x,0)=n_I(x), \quad J(x,0)=-n_I(x)\nabla S_I(x), \qquad x\in\mathbb{R}^d.$$

The system (2.4)-(2.5) is the quantum analogue of the classical pressureless Euler equations of gas dynamics. In the semi-classical limit when $\varepsilon\to 0$, (2.4)-(2.5) reduce to the classical equations. Notice that this derivation requires an irrotational initial velocity.
In physics textbooks, often the flow equations

$$\partial_t n + \mathrm{div}(n\nabla S)=0, \quad \partial_t S + \frac{1}{2}|\nabla S|^2 - V - \frac{\varepsilon^2}{2}\frac{\Delta\sqrt{n}}{\sqrt{n}} = 0$$

are derived instead of the formulation (2.4)-(2.5). In fact, (2.5) is obtained from the second equation of the above system after spatial differentiation and multiplication by n. The above system also occurs in the derivation of quantum-classical equations for molecular dynamics [**17**]. It has the disadvantage that it is not defined if vacuum $n=0$ occurs. Then the phase S is not defined and the Bohm potential becomes singular. As shown in

[**53**], the formulation (2.4)-(2.5) has in general better properties due to the multiplication with the density n.
We remark that this derivation has been recently extended to a two-band QHD model in [**2**].
The QHD model (2.4)-(2.5) is derived for a single particle and therefore, it does not contain a temperature term. In order to include temperature, many-particle systems need to be studied. For such systems, quantum hydrodynamics is not so well established. The starting point is a statistical mixture of particles where each of them is described by a single-state QHD system. Then averaged quantities over the ensemble of quantum states are needed. This leads to a closure problem, also occurring in the passage from kinetic to classical hydrodynamic equations. In the literature, several closure assumptions have been proposed, for instance, small-temperature asymptotics, use of the Fourier law, or entropy minimization. In the following sections, we review these closure strategies in detail.

2.2 Small-temperature models

In the previous section we have derived a relation between the Schrödinger and the fluid-dynamical picture. Another point of view is given by the Wigner formalism. More precisely, let ψ be a solution of the Schrödinger equation (2.1)-(2.2) and let

$$\rho(r,s,t) = \overline{\psi(r,t)}\psi(s,t),$$

where $\overline{\psi}$ is the complex conjugate of ψ, denote the so-called density matrix. A computation shows that it satisfies the *Heisenberg* (or von Neumann) *equation*

$$i\varepsilon\partial_t\rho = -\frac{\varepsilon^2}{2}(\Delta_s - \Delta_r)\rho - (V(s,t) - V(r,t))\rho, \quad r,s \in \mathbb{R}^d,\ t > 0, \tag{2.6}$$

with the initial condition $\rho(r,s,0) = \overline{\psi_I(r)}\psi_I(s)$. Let $f(x,v,t)$ be the Fourier transform of the density matrix in the variables $r = x + \varepsilon\eta/2$, $s = x - \varepsilon\eta/2$,

$$f(x,v,t) = \frac{1}{(2\pi)^d}\int_{\mathbb{R}^d} \rho\left(x + \frac{\varepsilon}{2}\eta, x - \frac{\varepsilon}{2}\eta, t\right) e^{i\eta\cdot v} d\eta, \quad x,v \in \mathbb{R}^d,\ t \in \mathbb{R}.$$

Then, Fourier transforming the Heisenberg equation for the density matrix (which is equivalent to the Schrödinger equation (2.1)), we obtain the (one-particle) *Wigner equation*

$$\partial_t f + v\cdot\nabla_x f + \Theta[V]f = 0, \quad x,v \in \mathbb{R}^d,\ t > 0, \tag{2.7}$$

$$f(x,v,0) = f_I(x,v), \quad x,v \in \mathbb{R}^d, \tag{2.8}$$

where $\Theta[V]$ is a pseudo-differential operator [92] defined by

$$\begin{aligned}(\Theta[V]f)(x,v,t) &= \frac{1}{(2\pi)^d}\int_{\mathbb{R}^d}\int_{\mathbb{R}^d}\frac{i}{\varepsilon}\left[V\left(x+\frac{\varepsilon}{2}\eta,t\right)-V\left(x-\frac{\varepsilon}{2}\eta,t\right)\right]\\ &\quad\times f(x,v',t)e^{i\eta\cdot(v-v')}dv'd\eta. \end{aligned}\tag{2.9}$$

We refer to [84] for details of the computation.
In order to derive a QHD model, we prescribe the initial density matrix

$$\rho_I(r,s)=\overline{\psi_I(r)}\psi_I(s)\exp\left(-\frac{\theta|r-s|^2}{2\varepsilon^2}\right),\quad r,s\in\mathbb{R}^d,$$

where $\psi_I(x)$ is given with the expression (2.3) and θ is the initial temperature. Notice that the initial Wigner function corresponding to this density matrix equals

$$f_I(x,v)=\frac{1}{(2\pi)^d}\int_{\mathbb{R}^d}\overline{\psi_I\left(x+\frac{\varepsilon}{2}\eta\right)}\psi_I\left(x-\frac{\varepsilon}{2}\eta\right)e^{i\eta\cdot v-\theta|\eta|^2/2}d\eta.$$

Elementary but lengthy calculations give the moments

$$\begin{aligned}\int_{\mathbb{R}^d}f_I dv &= n_I,\\ \int_{\mathbb{R}^d}vf_I dv &= n_I\nabla S_I,\\ \frac{1}{2}\int_{\mathbb{R}^d}(v\otimes v)f_I dv &= n_I\nabla S_I\otimes\nabla S_I+n_I\theta\,\mathrm{Id}-\frac{\varepsilon^2}{4}n_I(\nabla\otimes\nabla)\log n_I,\end{aligned}$$

where Id denotes the identity matrix in $\mathbb{R}^{d\times d}$.
Now multiply the Wigner equation (2.7) by 1, v and $\frac{1}{2}(v\otimes v)$, integrate over $v\in\mathbb{R}^d$ and integrate by parts. We introduce, as in the classical case, the particle, current and energy density, respectively, by

$$n=\int_{\mathbb{R}^d}f dv,\quad J=-\int_{\mathbb{R}^d}vf dv,\quad E=\frac{1}{2}\int_{\mathbb{R}^d}(v\otimes v)f dv,$$

and define, motivated by the above moments of f_I, the temperature tensor T via

$$E=\frac{1}{2}\left(\frac{J\otimes J}{n}+nT-\frac{\varepsilon^2}{4}n(\nabla\otimes\nabla)\log n\right).\tag{2.10}$$

It can be shown that T is of the order of θ. Then we obtain the *quantum hydrodynamic equations* with temperature [55],

$$\partial_t n - \mathrm{div} J = 0, \quad x \in \mathbb{R}^d, \ t > 0, \tag{2.11}$$

$$\partial_t J - \mathrm{div}\left(\frac{J\otimes J}{n} + nT\right) + n\nabla V + \frac{\varepsilon^2}{2} n\nabla\left(\frac{\Delta\sqrt{n}}{\sqrt{n}}\right) = 0, \tag{2.12}$$

$$\partial_t E_{jk} - \partial_{x_\ell}\left[\frac{J_\ell}{n}E_{jk} + \frac{1}{2}(J_j T_{\ell k} + J_k T_{j\ell}) - \frac{\varepsilon^2}{8}\left(J_j\partial^2_{x_k x_\ell}\log n + J_k\partial^2_{x_j x_\ell}\log n\right)\right]$$
$$+ \frac{1}{2}(J_j\partial_{x_k}V + J_k\partial_{x_j}V) + \partial_{x_\ell}q_{jk\ell} = 0, \tag{2.13}$$

where the heat flux tensor q is defined by

$$q_{jk\ell} = \int_{\mathbb{R}^d}(v_j - u_j)(v_k - u_k)(v_\ell - u_\ell)f(x,v,t)dv, \quad j,k,\ell = 1,\ldots,d,$$

and $u = -J/n$ is the mean velocity of the particles. Initial conditions for n, J, and E need to be prescribed.

Again, the above system of equations has to be closed, i.e., we have to find an expression for q depending only on n, J or T (and their derivatives). The QHD equations of Gardner [47] are obtained by replacing q in the above energy equation (2.13) by

$$q^{\mathrm{cl}}_{jk\ell} = -\frac{\varepsilon^2}{8}n\partial^2_{x_j x_k}\left(\frac{J_\ell}{n}\right). \tag{2.14}$$

However, this closure condition is *not* asymptotically correct for $\theta \to 0$ since the difference $q - q^{\mathrm{cl}} = O(\theta)$ can be seen to be of the same order as $T = O(\theta)$. This difficulty can be overcome by assuming "almost coherent" initial states $\psi_I = \sqrt{n_I}\exp(iS_I^{\varepsilon,\theta}/\varepsilon)$ with $S_I^{\varepsilon,\theta} = S_I + O(\sqrt{\theta}) + O(\varepsilon^2)$ as $\theta \to 0$, $\varepsilon \to 0$. Then it can be shown [55] that the energy equation (2.13) holds with q replaced by q^{cl} up to order $O(\theta) + O(\sqrt{\theta}\varepsilon^2) + O(\varepsilon^4)$. We stress the fact that this QHD model holds for small θ *and* ε. As explained above, the equations with the closure q^{cl} are *not* asymptotically correct for small θ but *fixed* ε.

2.3 Quantum hydrodynamics

In this section we derive QHD equations for arbitrary large temperature T. The idea of the derivation is, similar as in the previous section, to multiply the Wigner equation by 1, v, and $v\otimes v$ and to integrate over the velocity space. In the following, we set

$$\langle g(v)\rangle = \int_{\mathbb{R}^d} g(v)dv$$

for any function g depending on v. The integrals $\langle f\rangle$, $\langle vf\rangle$, and $\langle v\otimes vf\rangle$ are called the zeroth, first, and second moments, respectively. Then the moment equations read as follows:

$$\begin{aligned}\partial_t\langle f\rangle + \mathrm{div}\langle vf\rangle &= 0,\\ \partial_t\langle vf\rangle + \mathrm{div}\langle v\otimes vf\rangle - \nabla V\langle f\rangle &= 0,\\ \partial_t\langle \tfrac12|v|^2 f\rangle + \mathrm{div}\langle \tfrac12 v|v|^2 f\rangle - \nabla V\cdot\langle vf\rangle &= 0.\end{aligned}$$

As a closure condition we use an $O(\varepsilon^4)$ approximation of the quantum thermal equilibrium Wigner function first derived by Wigner [**97**] (see [**47, 50**]). More precisely, we assume that the Wigner function equals the vector-displaced equilibrium distribution $f(t,x,v) = f_e(t,x,v-u(t,x))$, where $u(t,x)$ is some group velocity and

$$\begin{aligned} f_e(x,v,t) &= A(x,t)\exp\Big(-\frac{|v|^2}{2T}+\frac{V}{T}\Big)\Big[1+\varepsilon^2\Big\{\frac{1}{8T^2}\Delta V \\ &\quad + \frac{1}{24T^3}|\nabla V|^2 - \frac{1}{24T^3}\sum_{j,\ell=1}^{d} v_j v_\ell \frac{\partial^2 V}{\partial x_j\partial x_\ell}\Big\} + O(\varepsilon^4)\Big]. \end{aligned} \tag{2.15}$$

The temperature $T = T(x,t)$ is here a scalar. The function $A(x,t)$ is assumed to be slowly varying in x and t. Notice that for $\varepsilon = 0$ (and $V = 0$) the quantum thermal equilibrium distribution function reduces to the classical Maxwellian. Then the first moments are $\langle f\rangle = n$, $\langle vf\rangle = -J$ and

$$\langle v\otimes vf\rangle = \frac{J\otimes J}{n} + nT\mathrm{Id} - \frac{\varepsilon^2}{12T}n(\nabla\otimes\nabla)V + O(\varepsilon^4), \tag{2.16}$$

$$\langle v|v|^2 f\rangle = 2\frac{J}{n}(e+T) - \frac{\varepsilon^2}{12}((\nabla\otimes\nabla)V)\cdot J + O(\varepsilon^4), \tag{2.17}$$

with the quantum energy density

$$e = \frac{|J|^2}{2n} + \frac{d}{2}nT - \frac{\varepsilon^2}{24}n\Delta\log n.$$

Notice that e is the trace of the energy tensor (2.10) except of the factor $\varepsilon^2/24$ which is 1/3 of the factor in (2.10) (see the discussion below). The formula for f_e implies that n equals, up to terms of order $O(\varepsilon^2)$, $e^{V/T}$ times a constant and therefore, if the temperature is slowly varying,

$$\frac{\partial^2\log n}{\partial x_j\partial x_k} = \frac{1}{T}\frac{\partial^2 V}{\partial x_j\partial x_k} + O(\varepsilon^2). \tag{2.18}$$

Clearly, this approximation is only valid for *smooth* functions and excludes discontinuous potentials arising at heterojunctions (see the discussion below). Under this condition we can replace all second derivatives of V by second derivatives of $\log n$, only making an error of order $O(\varepsilon^4)$ in the formulas (2.16) and (2.17). This yields the *quantum hydrodynamic equations*

$$\partial_t n - \mathrm{div} J = 0, \quad x \in \mathbb{R}^d,\ t > 0, \tag{2.19}$$

$$\partial_t J - \mathrm{div}\left(\frac{J\otimes J}{n}\right) - \nabla(nT) + \frac{\varepsilon^2}{6} n\nabla\left(\frac{\Delta\sqrt{n}}{\sqrt{n}}\right) + n\nabla V = 0, \tag{2.20}$$

$$\partial_t e - \mathrm{div}\left(J(e+T) - \frac{\varepsilon^2}{12}((\nabla\otimes\nabla)\log n)\cdot J\right) + J\cdot\nabla V = 0, \tag{2.21}$$

together with initial conditions for n, J, and e. We remark that, compared to the QHD model (2.11)-(2.13), we obtain a *scalar* energy equation instead of an energy *tensor* equation as in (2.13) since we assumed here a scalar temperature.

Another difference to the equations derived in the previous section are the factors in front of the third-order derivative of n which are $1/3$ of the factors in (2.12) and (2.13). We remark that the factor 3 is *not* related to the space dimension since we are working with arbitrary dimension d. The physical reason of this discrepancy between the two models is not understood; see also the discussion in [**49**].

Let us mention another approach for the derivation of the quantum hydrodynamic equations starting from a mixed-state Schrödinger system [**56**]. A mixed quantum mechanical state consists of a sequence of single states with occupation probabilities $\lambda_k \geq 0$ ($k \in \mathbb{N}$) for the k-th state described by

$$\begin{aligned} i\varepsilon\partial_t\psi_k &= -\frac{\varepsilon^2}{2}\Delta\psi_k - V\psi_k, \quad x\in\mathbb{R}^d,\ t>0, \\ \psi_k(x,0) &= \psi_{I,k}(x), \quad x\in\mathbb{R}^d, \end{aligned}$$

and each initial wave function is given by a WKB state

$$\psi_{I,k} = \sqrt{n_{I,k}}\exp(iS_{I,k}/\varepsilon), \quad k\in\mathbb{N}.$$

The occupation probabilities satisfy $\sum_{k=1}^\infty \lambda_k = 1$. We define the electron density $n_k = |\psi_k|^2$ and the current density $J_k = -\varepsilon\mathrm{Im}(\overline{\psi_k}\nabla\psi_k)$ of the k-th state and assume that the wave function can be decomposed as

$$\psi_k(t,x) = \sqrt{n_k(t,x)}\exp(iS_k(t,x)/\varepsilon).$$

Then the single-particle current flow is irrotational since $J_k = -n_k \nabla S_k$. Using this ansatz for ψ_k in the above Schrödinger equation gives the zero-temperature QHD equations (cf. (2.4)-(2.5))

$$\begin{aligned} \partial_t n_k - \mathrm{div} J_k &= 0, \\ \partial_t J_k - \mathrm{div}\left(\frac{J_k \otimes J_k}{n_k}\right) + n_k \nabla V + \frac{\varepsilon^2}{2} n_k \nabla \left(\frac{\Delta \sqrt{n_k}}{\sqrt{n_k}}\right) &= 0, \quad x \in \mathbb{R}^d,\ t > 0, \end{aligned}$$

with the initial conditions

$$n_k(0,x) = n_{I,k}(x), \quad J_k(0,x) = -n_{I,k}(x) \nabla S_{I,k}(x), \quad x \in \mathbb{R}^d.$$

Now we define the total particle density n and current density J by

$$n = \sum_{k=1}^{\infty} \lambda_k n_k, \quad J = \sum_{k=1}^{\infty} \lambda_k J_k.$$

The flow generated by the mixed state is generally *not* irrotational anymore. Summation of the k-th state QHD equations multiplied by λ_k leads to the QHD equations (2.11)-(2.13) where the energy tensor E_{jk} and the heat flux tensor $q_{j\ell m}$ are given by (2.10), (2.14), respectively [**56**]. The temperature T is a tensor defined as the sum of the so-called current temperature T_c and osmotic temperature T_{os}, where

$$T_i = \sum_{k=1}^{\infty} \lambda_k \frac{n_k}{n} (u_{i,k} - u_i) \otimes (u_{i,k} - u_i), \quad i = c, \mathrm{os},$$

and the "current velocities" $u_{c,k}$ and "osmotic velocities" $u_{\mathrm{os,k}}$ are given by

$$u_{c,k} = -\frac{J_k}{n_k}, \quad u_c = -\frac{J}{n}, \quad u_{\mathrm{os},k} = \frac{\varepsilon}{2} \nabla \log n_k, \quad u_{\mathrm{os}} = \frac{\varepsilon}{2} \nabla \log n.$$

The system of equations (2.11)-(2.13) has to be closed since the heat flux tensor cannot (in general) be expressed in terms of n, J, and T only. In the literature, we are aware of two choices. One choice is just to assume that the temperature is a constant scalar (times the identity matrix) such that the energy equation (2.13) does not need to be considered [**63**]. Another choice is to set $q = \kappa \nabla T$, where $\kappa > 0$ denotes the heat conductivity. This closure has been used in classical hydrodynamics [**91**] and in quantum hydrodynamic simulations [**28, 47**]. We also cite [**51**] where a *dispersive* heat flux q has been derived for a different QHD model.

The QHD model is used for the simulation of quantum devices, like the resonant tunneling diode (see Section 1.2) which consists of different materials. At the interface of the materials (heterojunctions), the (mean-field) potential is calibrated by a barrier potential which models the gap between the conduction bands of each material. The barrier potential is a given function which is constant inside each material. Thus, the sum of the (mean-field) potential and the barrier potential is discontinuous. The approximation (2.18) therefore does not make sense for such potentials. Gardner and Ringhofer [**49**] have overcome this problem by deriving so-called "smooth" QHD equations. More precisely, they obtain in the Born approximation to the Bloch equation the equations (2.19)-(2.21) in which the terms

$$\frac{\varepsilon^2}{6} n\nabla\left(\frac{\Delta\sqrt{n}}{\sqrt{n}}\right) \quad \text{and} \quad \frac{\varepsilon^2}{12}(\nabla\otimes\nabla)\log n$$

are replaced by

$$\frac{\varepsilon^2}{4}\mathrm{div}(n(\nabla\otimes\nabla)\overline{V}) \quad \text{and} \quad \frac{\varepsilon^2}{4}(\nabla\otimes\nabla)\overline{V},$$

and $\overline{V} = \overline{V}(x,T)$ depends non-locally on x and T (see [**49**] for details). The QHD equations (2.19)-(2.21) are recovered in the $O(\varepsilon^2)$ approximation

$$\overline{V} = \frac{1}{3}V + O(\varepsilon^2), \quad \nabla\log n = -\frac{\nabla V}{T} + O(\varepsilon^2),$$

if n, J and T are varying very slowly [**49**].
We mention that engineers were the first to give (formal) derivations of quantum hydrodynamic models for the use in semiconductor modeling (see, for instance, [**57**] for an isothermal model and [**40**] for the full model).
Mathematical analysis of the QHD equations has been just partially understood. More precisely, the existence of solutions, both for the transient and the stationary model, has been proven only in particular situations.
The existence of solutions to the QHD equations in the isothermal case, usually including a momentum-relaxation term $-J/\tau$ with the relaxation time τ on the right-hand side of (2.20), has been achieved only under a smallness condition on the current density similar to classical subsonic flow; see [**45, 46, 54, 62, 66, 99**] for the stationary equations. In the similar spirit, the existence results for the transient model were achieved either for small times [**69**] or for initial or boundary data sufficiently close to the thermal equilibrium state [**67, 69, 79**]. Non-existence results for supersonic-type flow using special boundary conditions have been proved in [**45**] indicating that the subsonic-type condition may be necessary.

The main mathematical difficulty, besides of the highly nonlinear structure of the third-order quantum term, is the proof of positivity (or nonnegativity) of the particle density and temperature. In the stationary case, the energy estimate only provides a bound for the energy production $\int |J|^2/(\tau n)dx$ which does not exclude zeros of the particle density. For special boundary conditions in the one-dimensional case, even a non-existence result was shown [45]. Recently, the blow-up in finite time for the solutions of certain initial-boundary value problem for multi-dimensional QHD equations is proved [44].

The one-dimensional QHD equations have been solved numerically with the aim to simulate resonant tunneling diodes. Gardner [47] used the upwind method to discretize the equations, thus treating the third-order quantum term as a perturbation of the classical Euler equations. Chen [27] employed a shock-capturing Runge-Kutta discontinuous Galerkin method for the QHD conservation laws. Caussignac et al. [25] wrote the stationary equations as a first-order system and used a general-purpose solver. Pietra and Pohl [87, 88] discretized the model using central finite differences; they also studied the behavior of the solutions in the semi-classical limit $\varepsilon \to 0$. A comparison of a central finite-difference scheme and a hyperbolic relaxation scheme applied to the QHD equations has been presented in [72].

2.4 Semi-analytical expressions for current-voltage curves

In order to describe the electron transport through the modern nano-scale semiconductor devices, one has to use fully quantum mechanical models. Besides studying the transient behaviour of the devices (switching times, oscillation frequencies), it is also worth to investigate the stationary simulation results (current-voltage curves, possible bistabilities). Although the primary application of the QHD model is the simulation of quantum devices that depend on particle tunneling through potential barriers, we study here the simplified ballistic situation, where no potential barriers are present. Namely, in this section we consider the simplified one-dimensional, stationary QHD model where the real-valued potential $V(x)$ is given and not self-consistently coupled to the electron density. We take here the potential flow, i.e. we assume that the current density can be written as $J = nS_x$, where

S is called a phase. The QHD model of interest reads

$$J_x = 0, \tag{2.22}$$

$$\Big(\frac{J^2}{n} + p(n)\Big)_x + nV_x - \frac{\varepsilon^2}{2} n\Big(\frac{(\sqrt{n})_{xx}}{\sqrt{n}}\Big)_x = 0, \tag{2.23}$$

where $x \in \mathbb{R}$, ε is the (scaled) Planck constant, n is the electron density and V is the potential. We consider an isothermal or isentropic quantum fluid of charged particles. The pressure function p is given by the particle density, i.e. $p(n) = Tn$ in the isothermal case and $p(n) = Tn^\gamma$ in the isentropic case, where $\gamma > 1$ and T is a (scaled) temperature constant. In the following, we take $T = 1$. Our aim is to consider how different terms contained in the QHD model (2.22)-(2.23) influence the current-voltage curve of the device. As we have already pointed out in Section 2.1, QHD model can be obtained from Schrödinger equation, using the Madelung transform. Our intention is, instead of solving nonlinear, third-order system (2.22)-(2.23), to deal with the equivalent stationary Schrödinger equation.
Indeed, let us start from the very particular, nonlinear, stationary Schrödinger equation

$$\frac{\varepsilon^2}{2}\psi_{xx} - (h(|\psi|^2) + V(x))\psi = E\psi, \tag{2.24}$$

with the real parameter E noted as the energy of the steady-state. The enthalpy function h is given by the expression

$$h(n) = \frac{1}{T}\int_1^n \frac{p'(s)}{s} ds. \tag{2.25}$$

In the isothermal case, $h(n) = \log(n)$ holds, while for isentropic states, we have $h(n) = \gamma/(\gamma-1)(n^{\gamma-1}-1)$, for $\gamma > 1$. Performing the Madelung transform (1.11), i.e. by writing the wave function in the terms of its amplitude $\sqrt{n(x,t)}$ and the phase $S(x,t)$, then substituting back into the Schrödinger equation (2.24) and separating its real and imaginary part, one obtains the following system

$$(nS_x)_x = 0, \tag{2.26}$$

$$\frac{S_x^2}{2} + h(n) + V(x) - E - \frac{\varepsilon^2}{2}\frac{(\sqrt{n})_{xx}}{\sqrt{n}} = 0. \tag{2.27}$$

After taking the derivative of the equation (2.27) with the respect to x, multiplying by n, and using the relation $J = nS_x$, one finally obtains the

QHD equations (2.22)-(2.23). In the same way, it is easy to see that starting with the QHD model (2.22)-(2.23), dividing by $n > 0$ and integrating with the respect to x gives the stationary Schrödinger equation (2.24) where the integration constant is noted by E. So, we conclude that the QHD model (2.22)-(2.23) is equivalent to the nonlinear stationary Schrödinger equation (2.24). This equivalence is only formal, i.e. it holds only for smooth solutions with strictly positive density. Note also that here we spoked about the equivalence on the whole space, without considering the boundary conditions.
Motivated with the equivalence mentioned above, our intention is to get the expression for the current-voltage curve $J = J(U)$, where U is the applied potential, by solving explicitly the Schrödinger equation. From the Madelung ansatz (1.11) it is obvious that

$$n(x,t) = |\psi(x,t)|^2. \tag{2.28}$$

In order to motivate the expression for the current density J in terms of the wave function, we return for the moment back to the transient Schrödinger equation

$$i\varepsilon\psi_t = -\frac{\varepsilon^2}{2}\psi_{xx} + V(x)\psi, \quad x \in \mathbb{R},\ t > 0. \tag{2.29}$$

Using the fact that the wave function solves the equation (2.29) we obtain

$$\frac{d}{dt}|\psi|^2 = \frac{i\varepsilon}{2}(\psi_x\overline{\psi} - \overline{\psi}_x\psi)_x = -\varepsilon\Big(\operatorname{Im}(\psi_x\overline{\psi})\Big)_x. \tag{2.30}$$

Comparing the equation (2.30) with the continuity equation $n_t + J_x = 0$, it follows that the current density J is defined as

$$J(x,t) = \varepsilon\operatorname{Im}(\psi_x(x,t)\overline{\psi}(x,t)),\ t > 0. \tag{2.31}$$

Let the device region be represented by the spatial (scaled) interval $(0,1)$. The next step is to define appropriate boundary conditions for the Schrödinger equation, which are motivated by the boundary conditions used for the QHD model. For the moment, we take the equivalent QHD formulation (2.26)-(2.27). Naturally , we impose that

$$V(0) = 0,\ V(1) = U, \tag{2.32}$$

where $U \in \mathbb{R}$ is the applied potential. To derive the boundary conditions for n and S we make physically relevant hypotheses, following [**62**]. The

boundary data are assumed to be the superposition of the thermal equilibrium functions (n_{eq}, S_{eq}) and the applied potential U, i.e. at the boundary valids

$$n = n_{eq},\ S = S_{eq} + U. \tag{2.33}$$

The thermal equilibrium state is defined by $J = 0$ or, equivalently, $S =$ const. (as $n > 0$). By fixing the reference point for S (and S_{eq}) we can suppose that $S_{eq} = 0$. Further, we assume $n_{eq} = 1$ at the boundary. In this way we get the Dirichlet boundary conditions

$$n(0) = n(1) = 1,\ S(0) = 0,\ S(1) = U. \tag{2.34}$$

Boundary conditions (2.34) are non-local for the QHD system (2.22)-(2.23). Here we point out that the condition $S(1) = U$ can be written in the integral form

$$\int_0^1 \frac{J(s)}{n(s)} ds = U.$$

In multi-dimensional case, a system similar to (2.26)-(2.27), coupled with the Poisson equation for the potential, is studied in [**62**]. More precisely, the model considered there contains an additional relaxation term S/τ, where τ is the relaxation parameter and the boundary conditions were (2.34)-(2.32). In [**62**] it is shown that for sufficiently small $|U|$, there exists a solution (w, S, V) with strictly positive $w = \sqrt{n}$.
Using the Madelung ansatz, the boundary conditions (2.34) can be written in terms of the wave function, as follows

$$\psi(0) = 1,\ \psi(1) = e^{\frac{iU}{\varepsilon}}. \tag{2.35}$$

However, in the simulations of tunneling devices, later in this thesis other boundary conditions for (2.22)-(2.23) are also used (see Section 3.3 and Section 4.5):

$$n(0) = n(1) = 1, \quad n_x(0) = n_x(1) = 0. \tag{2.36}$$

The boundary conditions (2.36) written in terms of the wave function ψ read

$$\psi(0) = 1,\ |\psi(1)|^2 = 1, \tag{2.37}$$

$$\mathrm{Re}(\overline{\psi}\psi_x(0)) = \mathrm{Re}(\overline{\psi}\psi_x(1)) = 0. \tag{2.38}$$

As we have already pointed out, we are interested in the boundary conditions for Schrödinger equation which are meaningful from the point of view of the

QHD model. For the accurate simulation of quantum devices a careful modeling and numerical discretization of the boundary conditions are of the enormous importance. However, the Schrödinger equation is usually considered on a large, possibly unbounded domain. Due to the numerical reasons, one has to assume that the modeling and simulation are confined to a finite subregion. At the boundary of this subregion one introduces an artificial boundary condition, taking that the incoming flux of charge carriers is known. It is clear that the choice of appropriate boundary conditions is a prerequisite for obtaining any meaningful result. In recent years lot of progress towards the understanding of the transparent boundary conditions for the Schrödinger equation, suggested in the work of Lent and Kirkner [**77**] has been done. For example in [**9, 15**] the boundary value problem for the one-dimensional Schrödinger equation with the boundary conditions

$$\psi'(0) + ik\psi(0) = 2ik, \quad \psi'(1) = i\sqrt{k^2 - 2V(1)/\varepsilon^2}\psi(1), \tag{2.39}$$

where $k > 0$ is the wave vector, is analytically and numerically studied.

Different QHD models and their current-voltage curves

The goal is to study the influence of the drift, pressure, potential and quantum term on the behaviour of the current-voltage curves for chosen (simplified) QHD model (2.22)-(2.23). Our observations show that current-voltage curves of the model under consideration depend very sensitively on the choice of boundary values. As we commented above, the derivation of sensible boundary conditions forms a vital part in the modelling process. Moreover, the current-voltage curves analytically calculated in this section differ in an essential way from the curves which are numerically obtained and presented later in the thesis (see Section 3.3.3 and Section 4.5). Numerical simulations there, however, are performed for the QHD equations coupled with the Poisson equation for the potential and containing some additional terms, like for example the relaxation term $-J/\tau$, where τ is the relaxation parameter. Our impression is that these terms strongly influence both the qualitative and the quantitative behaviour of the current-voltage curves for QHD models.

The procedure we follow here is to solve the corresponding Schrödinger equation with the appropriate boundary conditions, then to calculate J and n using formulas (2.28), (2.31) respectively, and finally to draw the corresponding current-voltage curve.

The reduced QHD model

For the beginning, we consider the situation without the pressure term and where $V \equiv 0$. The QHD system of the interest reads

$$J_x = 0, \tag{2.40}$$

$$\Big(\frac{J^2}{n}\Big)_x - \frac{\varepsilon^2}{2} n \Big(\frac{(\sqrt{n})_{xx}}{\sqrt{n}}\Big)_x = 0, \tag{2.41}$$

and it is formally equivalent to the stationary Schrödinger equation

$$-\frac{\varepsilon^2}{2}\psi_{xx} = E\psi, \tag{2.42}$$

where $E \in \mathbb{R}$ is the energy of the steady-state. The equation (2.42) considered for $x \in \mathbb{R}$ is the standard free-electron problem. The solution of this differential equation is given as a linear combination of plane waves e^{ikx}, e^{-ikx}, where k is a wave number defined as $k = \sqrt{2E/\varepsilon^2}$. Therefore, the energy can be expressed in terms of k as

$$E = \frac{\varepsilon^2 k^2}{2}, \tag{2.43}$$

which means that $E \geq 0$ if k is a real number. The wave number becomes imaginary, $k \to i\kappa$, if $E < 0$. Then, the wave function $\psi(x)$ is a linear combination of $\sinh(\kappa x)$ and $\cosh(\kappa x)$ with $E = -\varepsilon^2\kappa^2/2$. These wave functions are all real and all diverge as $x \to \pm\infty$ in at least one direction. A divergent wave function is not physically acceptable, so these solutions can be used only in a restricted region of space [**30**].
Therefore, we study the problem (2.40)-(2.41) on a bounded domain $(0, 1)$. We point out that we consider (2.42)-(2.35) as the nonlinear eigenvalue problem, where the eigenvalues E will be fixed with an additional boundary condition which is assumed to be natural for the macroscopic considerations. Let us start with the case $E = 0$. This has already being considered in [**61**]. For $E = 0$, the equation (2.42) degenerates to the one-dimensional Laplace equation which has the solutions of the form $\psi(x) = Ax + B$ with the complex-valued constants A and B. Using the boundary conditions (2.35) the constants A and B can be specified and we obtain the solution

$$\psi(x) = 1 + x(\cos(U/\varepsilon) - 1) + ix\sin(U/\varepsilon).$$

The formula (2.31) gives the expression for the corresponding current-voltage curve:

$$J(U) = \varepsilon\sin(U/\varepsilon).$$

The electron density and the current-voltage curve obtained for the reduced QHD model (2.40)-(2.41) are shown in the Figure 2.1. The chosen value of the (scaled) Planck constant is $\varepsilon^2 = 10^{-1}$. The logarithmic-scaled electron density is shown for $U = 0.158$, i.e. in the peak of the corresponding current-voltage curve and for $U = 0.314$, where the current density becomes zero.

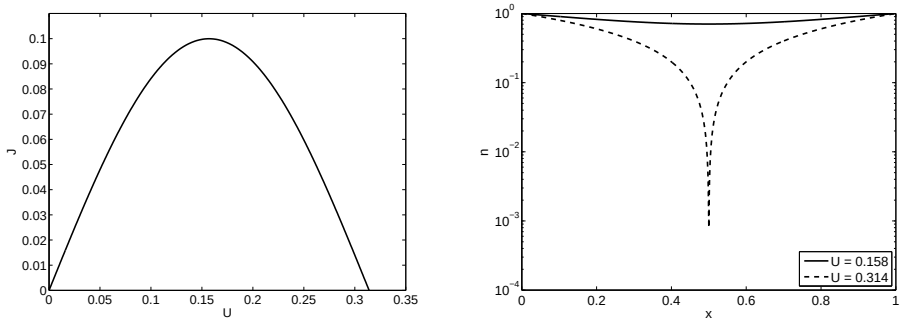

Figure 2.1: The reduced QHD model, $\varepsilon^2 = 10^{-1}$. Left: the current-voltage curve, right: the electron density.

Next, we consider the case $E > 0$. In order to fix the constant E and due to the standard boundary conditions used for QHD model (2.36), we impose, additionally to (2.35), the following boundary condition

$$n_x(0) = 0. \tag{2.44}$$

Written in the terms of the wave function, and taking into account that $\psi(0) = 1$, the condition (2.44) reads

$$\mathrm{Re}(\psi_x(0)) = 0. \tag{2.45}$$

Solving the (complex) ordinary differential equation (2.42) with the boundary conditions (2.35) and (2.45), one obtains the solution

$$\psi(x) = \cos(kx) \pm i \sin(kx),$$

with the energies E given by the expression (2.43) where $k = \pm U/\varepsilon \cdot 2l\pi$, $l \in \mathbb{Z}$. Easy calculation shows that the current-voltage curve reads

$$J_l(U) = U + 2l\pi\varepsilon, \quad l \in \mathbb{Z}.$$

For $l = 0$ one obtains the current-voltage curve $J(U) = U$ with linear dependence of the current density J upon the applied potential U. Although

trivial, this result shows that in some cases (depending on the choice of the boundary conditions) the QHD model is able to produce the current-voltage curves which are behaving according to the Ohm's law (up to some factor).

The QHD model with the linear potential

As the second example, we study the QHD model with the linear potential $V(x) = xU$, imposing the non-local boundary conditions (2.34) and we discuss the behaviour of the corresponding current-voltage curves. Notice that with the above definition of the potential V, the boundary condition (2.32) is satisfied. Firstly, we consider the case without the pressure term. Therefore, the QHD model of interest reads

$$\begin{aligned} J_x &= 0, \\ \Big(\frac{J^2}{n}\Big)_x + nU - \frac{\varepsilon^2}{2} n \Big(\frac{(\sqrt{n})_{xx}}{\sqrt{n}}\Big)_x &= 0, \quad x \in (0,1), \end{aligned}$$

The corresponding stationary Schrödinger equation is

$$-\frac{\varepsilon^2}{2}\psi_{xx} + xU\psi = E\psi, \ x \in (0,1), \ E \in \mathbb{R} \tag{2.46}$$

with the boundary conditions given by (2.35). For simplicity, we consider first the case $E = 0$. By introducing the constant

$$\alpha = 2U/\varepsilon^2, \tag{2.47}$$

substituting $\xi = \beta x$ and $\psi(x) = \varphi(\beta x)$, the Schrödinger equation can be rewritten as

$$\varphi''(\xi) - \frac{\alpha}{\beta^3}\xi\varphi(\xi) = 0. \tag{2.48}$$

By choosing $\beta = (2U/\varepsilon^2)^{1/3}$ we obtain the Airy differential equation

$$\varphi''(\xi) - \xi\varphi(\xi) = 0, \tag{2.49}$$

with the boundary conditions

$$\varphi(0) = 1, \ \varphi(\beta) = e^{\frac{iU}{\varepsilon}}. \tag{2.50}$$

Two linear independent solutions of the second-order differential equation (2.49), the Airy functions $Ai(\xi)$ and $Bi(\xi)$ are shown in the Figure 2.2. Their asymptotic representation for large $|\xi|$ due to [**1, 76**] reads:

$$Ai(\xi) = \frac{1}{2\sqrt{\pi}\xi^{1/4}} \mathrm{e}^{-\frac{2}{3}\xi^{3/2}} [1 + O(|\xi|^{-3/2})], \tag{2.51}$$

$$Bi(\xi) = \frac{1}{\sqrt{\pi}\xi^{1/4}} \mathrm{e}^{\frac{2}{3}\xi^{3/2}} [1 + O(|\xi|^{-3/2})]. \tag{2.52}$$

The solution of the boundary problem (2.49)-(2.50) is given as a linear

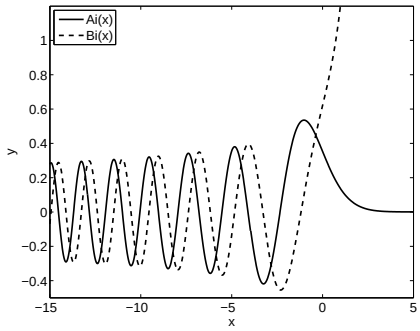

Figure 2.2: The Airy functions Ai(x) and Bi(x).

combination of the Airy functions, namely

$$\varphi(\xi) = C_1 Ai(\xi) + C_2 Bi(\xi),$$

where the complex-valued constants C_1 and C_2 are determined as the solution of the linear system

$$C_1 Ai(0) + C_2 Bi(0) = 1, \tag{2.53}$$

$$C_1 Ai(\beta) + C_2 Bi(\beta) = \mathrm{e}^{\frac{iU}{\varepsilon}}. \tag{2.54}$$

Taking into account that the current density J is constant, using the fact that the Wronskian of the Airy functions is equal $1/\pi$, direct calculation gives the expression for the current-voltage curve

$$J = \frac{1}{\pi} \cdot \varepsilon\beta \cdot \mathrm{Im}(\overline{C_1} C_2). \tag{2.55}$$

By solving the system (2.53)-(2.54), one obtains the constants C_1 and C_2 and finally the current-voltage curve reads

$$J(U) = -\frac{1}{\pi}\beta\varepsilon \frac{\sin(U/\varepsilon)}{Ai(\beta)Bi(0) - Ai(0)Bi(\beta)}. \tag{2.56}$$

Next, we consider the behaviour of the function $J = J(U)$, when $U \to 0$. The expansion of the Airy functions in the Taylor series

$$Ai(\beta) = Ai(0) + Ai'(0)\beta + O(\beta^2),$$
$$Bi(\beta) = Bi(0) + Bi'(0)\beta + O(\beta^2).$$

enables us to write the denominator of the expression (2.56) as

$$\begin{aligned} Ai(\beta)Bi(0) - Ai(0)Bi(\beta) &= (Ai(0) + Ai'(0)\beta + O(\beta^2))Bi(0) \\ &\quad - Ai(0)(Bi(0) + Bi'(0)\beta + O(\beta^2)) \\ &= \beta(Ai'(0)Bi(0) - Ai(0)Bi'(0)) + O(\beta^2). \end{aligned}$$

Since the Wronskian of the Airy functions equals $1/\pi$, we get

$$Ai(\beta)Bi(0) - Ai(0)Bi(\beta) = \beta((-1/\pi) + O(\beta)). \tag{2.57}$$

From the expression (2.57), taking into account that $\sin(x)/x \to 1$, as $x \to 0$, we obtain

$$\begin{aligned} J(U) &= -\frac{1}{\pi}\varepsilon\beta\frac{U}{\varepsilon}\frac{1}{\beta(-1/\pi + O(\beta))} \\ &= \frac{U}{(1 - \pi O(\beta))} \to 0, \text{ for } U \to 0. \end{aligned} \tag{2.58}$$

We just mention that the other way to obtain the same conclusion is to use the L'Hospital rule in the calculation of the limes of the expression (2.56), as $U \to 0$. Thus, the formula (2.56) make sense physically, since $J = 0$ at $U = 0$, as expected. The current-voltage curve obtained using the

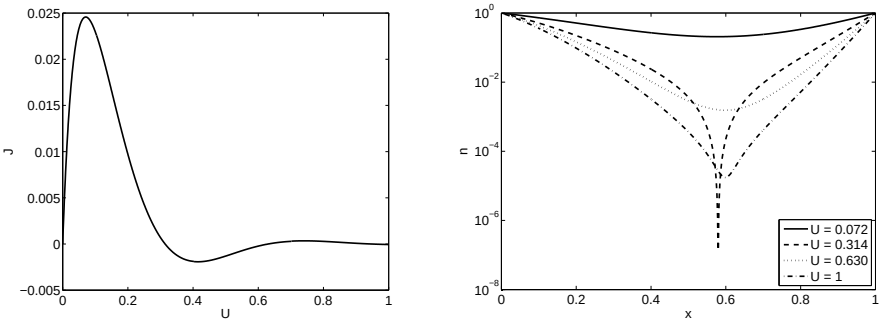

Figure 2.3: Left: The current-voltage curve, right: the electron density for the linear potential, $\varepsilon^2 = 10^{-2}$.

expression (2.56) is shown in the Figure 2.3, left. Obviously, the dependence of the produced current depends nonmonotonically on the applied voltage. The (scaled) Planck constant is chosen to be $\varepsilon^2 = 10^{-2}$. The electron density, shown in the Figure 2.3, right, using the log-scale, is presented for some characteristic points of the current-voltage curve. Namely, we were

interested to see how the electron density behaves in the first peak of the current-voltage curve ($U = 0.072$), then in the point where the current-voltage curve changes the sign for the first and second time ($U = 0.314$ and $U = 0.63$, respectively) and finally for $U = 1$. In order to consider the behaviour of $J(U)$ when $U \to \infty$, we need the asymptotics of the Airy functions $Ai(x)$ and $Bi(x)$ as $x \to \infty$ given with the formulas (2.51) and (2.52). Direct calculation shows that

$$J(U) \to 0, \text{ as } U \to \infty. \tag{2.59}$$

The result (2.59) is far from the physical behaviour of the current-voltage curve. It is expected that for large values of the increasing applied potential U, the produced current J also increases. We suppose that this ambiguity appears due to the fact that here we consider the QHD model without the relaxation term.

Next, the Figure 2.4 shows that the decreasing of the scaled Planck constant ε^2 has the consequence that the corresponding current-voltage curves are damped to zero. This follows from easy calculation of the limit $J(U)$ when $\varepsilon \to 0$, using formula (2.56).

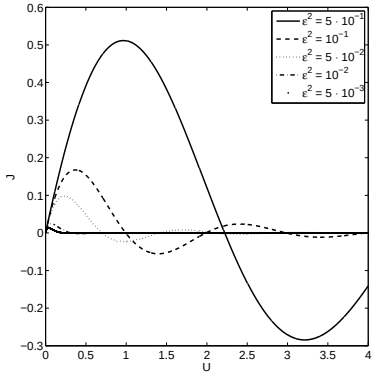

Figure 2.4: The current-voltage curve for the linear potential as $\varepsilon^2 \to 0$.

The QHD model with the linear potential and the pressure term

Next, we include the density-dependent pressure term $p(n)$ in the stationary QHD model with the linear potential, taking into account the non-local

boundary conditions (2.34). The QHD model under consideration reads

$$J_x = 0,$$
$$\Big(\frac{J^2}{n} + p(n)\Big)_x + nU - \frac{\varepsilon^2}{2} n\Big(\frac{(\sqrt{n})_{xx}}{\sqrt{n}}\Big)_x = 0, \quad x \in (0,1).$$

As we have already shown at the beginning of this section, this QHD model is formally equivalent to the following Schrödinger equation

$$\frac{\varepsilon^2}{2}\psi_{xx} - (h(|\psi|^2) + xU)\psi = E\psi,\ x \in (0,1),\ E \in \mathbb{R}. \tag{2.60}$$

Like before, due to the simplicity, here we consider the case $E = 0$. The boundary conditions written in the terms of the wave function are given by (2.35). Equation (2.60) can be written as

$$\psi'' - \alpha x\psi - \delta\psi h(|\psi^2|) = 0, \tag{2.61}$$

where the constant α is given in (2.47) and $\delta = 2/\varepsilon^2$. We solve boundary value problem (2.61)-(2.35) by routine **bvp4c** of MATLAB®, since apparently, no explicit solution can be found.
In order to consider the isothermal case we take that the enthalpy function h is scaled with some parameter η, i.e. $h(s) = \eta \log(s)$ and we consider the behaviour of the current-voltage curves when $\eta \to 0$. Figure 2.5 (left), shows that in this case, the obtained curves converge to the one obtained for the model without the pressure term (compare with the Figure 2.3, left). The current-voltage curves for the isentropic case with the different choices of the parameter γ are shown in the Figure 2.5, right.

The multi-valuedness of the unrelaxed QHD model

Finally, we consider the Schrödinger equation (2.46) for $E \neq 0$ with the boundary conditions (2.37)-(2.38) which appear in the semiconductor modelling. The boundary value problem that we intend to solve here is an eigenvalue problem with the solution pair $(\psi(x), E)$, where $E \in \mathbb{R}$. Here we follow the idea of Matthes, given in [**86**]. First, using the substitution $x = \beta y + \gamma$ with

$$\beta = \Big(\frac{\varepsilon^2}{2U}\Big)^{1/3},\ \gamma = \frac{E}{U}$$

and defining $\psi(x) = \phi(y)$, we rewrite the equation (2.46) in the form of the Airy differential equation

$$\phi_{yy} - y\phi = 0,\ y \in [y_0, y_1] \tag{2.62}$$

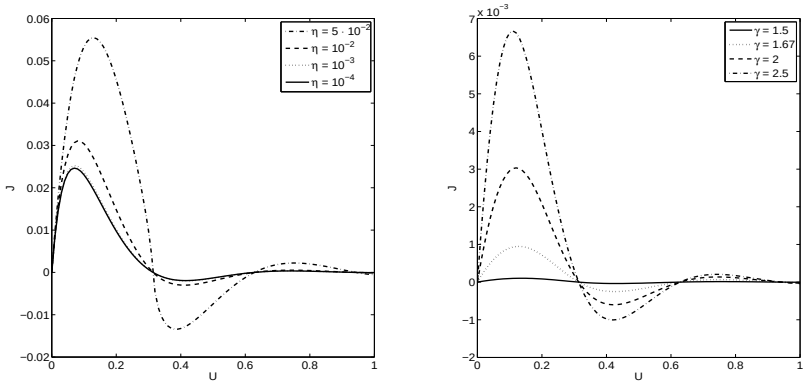

Figure 2.5: The current-voltage curves for the model with the linear potential and the pressure, $\varepsilon^2 = 10^{-2}$. Left: $h(s) = \eta \log(s)$, $\eta \to 0$, right: $h(s) = \frac{\gamma}{\gamma-1} s^{\gamma-1}$, $\gamma > 1$.

where

$$y_0 = -\frac{E}{\varepsilon^{2/3}} 2^{1/3} U^{-2/3}, \; y_1 = \frac{U-E}{\varepsilon^{2/3}} 2^{1/3} U^{-2/3}. \tag{2.63}$$

The boundary conditions (2.37)-(2.38) can be rewritten as

$$\phi(y_0) = 1, \tag{2.64}$$
$$|\phi(y_1)|^2 = 1, \tag{2.65}$$
$$\mathrm{Re}(\overline{\phi}_y(y_0)) = 0, \tag{2.66}$$
$$\mathrm{Re}(\overline{\phi}(y_1)\phi_y(y_1)) = 0. \tag{2.67}$$

where we used that $\overline{\phi}(y_0) = 1$. The solution of the equation (2.62) is given as the linear combination of the Airy functions, i.e.

$$\phi(y) = (a_1 + ib_1)Ai(y) + (a_2 + ib_2)Bi(y), \tag{2.68}$$

where $a_i, b_i \in \mathbb{R}$ for $i = 1, 2$. The condition (2.64) gives the following system:

$$a_1 Ai(y_0) + a_2 Bi(y_0) = 1, \tag{2.69}$$
$$b_1 Ai(y_0) + b_2 Bi(y_0) = 0. \tag{2.70}$$

Further on, the condition (2.66) gives the equation

$$a_1 Ai'(y_0) + a_2 Bi'(y_0) = 0, \tag{2.71}$$

Now, using the fact that the Wronskian of the Airy functions equals $1/\pi$, the conditions (2.69) and (2.71) give

$$a_1 = \pi Bi'(y_0),\ a_2 = -\pi Ai'(y_0).$$

Further on, it is obvious that constants b_1 and b_2 appear in the condition (2.70) can be written as

$$b_1 = \pi\lambda Bi(y_0),\ b_2 = -\pi\lambda Ai(y_0),$$

where $\lambda \in \mathbb{R}$. Boundary condition (2.65) gives

$$Q_1(y_0, y_1)\lambda^2 + R_1(y_0, y_1) - \frac{1}{\pi^2} = 0, \tag{2.72}$$

where

$$\begin{aligned} R_1(y_0, y_1) = {} & Ai^2(y_1)(Bi'(y_0))^2 + Bi^2(y_1)(Ai'(y_0))^2 \\ & - 2Ai(y_1)Ai'(y_0)Bi(y_1)Bi'(y_0) \end{aligned}$$

and

$$\begin{aligned} Q_1(y_0, y_1) = {} & Ai^2(y_1)Bi^2(y_0) + Bi^2(y_1)Ai^2(y_0) \\ & - 2Ai(y_1)Ai(y_0)Bi(y_1)Bi(y_0). \end{aligned}$$

Finally, the condition (2.67) can be written as

$$Q_2(y_0, y_1)\lambda^2 + R_2(y_0, y_1) = 0, \tag{2.73}$$

where

$$\begin{aligned} R_2(y_0, y_1) = {} & (Bi'(y_0))^2 Ai(y_1)Ai'(y_1) + (Ai'(y_0))^2 Bi(y_1)Bi'(y_1) \\ & - Ai'(y_0)Bi'(y_0)(Ai(y_1)Bi'(y_1) + Ai'(y_1)Bi(y_1)), \end{aligned}$$

and

$$\begin{aligned} Q_2(y_0, y_1) = {} & Bi^2(y_0)Ai(y_1)Ai'(y_1) + Ai^2(y_0)Bi(y_1)Bi'(y_1) \\ & - Ai(y_0)Bi(y_0)(Ai(y_1)Bi'(y_1) + Ai'(y_1)Bi(y_1)). \end{aligned}$$

The original problem (2.62)-(2.63) with boundary conditions (2.64)-(2.67) has a solution if and only if there exists a real λ such that (2.72) and (2.73) are satisfied. Such λ exists if and only if

$$Q_1(y_0, y_1)R_2(y_0, y_1) - Q_2(y_0, y_1)[R_1(y_0, y_1) - \frac{1}{\pi^2}] = 0, \tag{2.74}$$

and

$$Q_1(y_0, y_1) \neq 0,\ Q_1(y_0, y_1)\Big(\frac{1}{\pi^2} - R_1(y_0, y_1)\Big) \geq 0. \tag{2.75}$$

In order to simplify the notation, we define the function $\Delta\colon \mathbb{R} \times \mathbb{R} \to \mathbb{R}$ by

$$\Delta(y_0, y_1) := Q_1(y_0, y_1)R_2(y_0, y_1) - Q_2(y_0, y_1)[R_1(y_0, y_1) - \frac{1}{\pi^2}]. \tag{2.76}$$

Since the boundary points y_0 and y_1 depend upon E, we can study the solutions of the equation (2.74) as functions of E, i. e. for given U consider

$$\tilde{\Delta}(E) = \Delta\Big(-\frac{E}{\varepsilon^{2/3}}2^{1/3}U^{-2/3}, \frac{U-E}{\varepsilon^{2/3}}2^{1/3}U^{-2/3}\Big), \tag{2.77}$$

By increasing the potential U we obtain corresponding discrete energies E. For each value of E the current density J_E is calculated using the expression (2.31). Like it is shown in the Figure 2.6 (left), the obtained current-voltage curves are multivalued, since one value of the applied potential U corresponds to countable many values of energies E. In our numerical considerations we choose values of E from some fixed interval, for example, here we took that $E \in [0.01, 1]$. The dependence of values of energies E upon the applied potential U can be seen in the Figure 2.6, right.

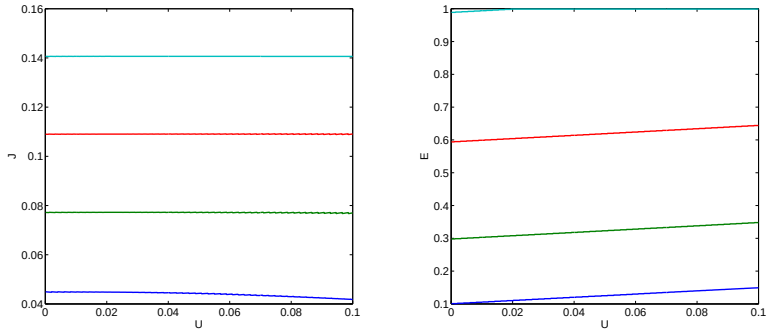

Figure 2.6: Eigenvalue problem for Schrödinger equation, $\varepsilon^2 = 10^{-2}$. Left: Current-voltage curves for different values of E, right: the dependence of E upon U.

We notice here that the use of the macroscopic boundary conditions (2.36) leads to a multi-value current-voltage curve. It seems that this multi-valuedness is an essential for the unrelaxed QHD system.

Chapter 3

QHD models using Fokker-Planck operator

This chapter is devoted to an analytical and numerical study of quantum hydrodynamic equations when they contain additional viscosity terms either originating from particle collisions or from an upwind numerical discretization. The chapter is organized as follows. In Section 3.1 we sketch the derivation of the viscous quantum hydrodynamic equations starting from the Wigner-Fokker-Planck model and we detail the scaling. Section 3.2 is devoted to the proof of the existence of solutions to the isothermal model in one space dimension. In Section 3.3 some numerical results for the isothermal and the nonisothermal one-dimensional models are presented. Next we compared the finite-difference approximations of the viscous and the inviscid model. Moreover, in Section 3.3.2 we computed the numerical viscosity and the numerical dispersion of the schemes. Finally, we present numerical simulations of a resonant tunneling diode.

3.1 Modeling—scaling

The viscous QHD equations are derived from the Wigner-Fokker-Planck equation for the distribution function $f(x,p,t)$,

$$\partial_t f + \frac{p}{m}\cdot\nabla_x f + \frac{q}{m}\theta[V]f = Q_{FP}(f), \quad (x,p)\in\mathbb{R}^6,\ t>0, \tag{3.1}$$

where (x,p) denotes the position-momentum variables, $t>0$ the time, and $\theta[V]$ is a pseudo-differential operator defined by

$$(\theta[V]f)(x,p,t) = \frac{i}{(2\pi)^{3/2}}\int_{\mathbb{R}^6}\frac{m}{\hbar}\left[V\Big(x+\frac{\hbar}{2}\eta,t\Big)-V\Big(x-\frac{\hbar}{2}\eta,t\Big)\right]f(x,p',t)\mathrm{e}^{i\eta\cdot(p-p')}d\eta dp'$$

(see [58]). The physical constants are the effective electron mass m, the elementary charge q, and the reduced Planck constant $\hbar$. The function $V(x,t)$ is the electric potential, self-consistently given by the Poisson equation

$$\varepsilon_s\Delta_x V = q\Big(\hbar^{-3}\int_{\mathbb{R}^3} f\,dp - C(x)\Big),$$

where ε_s denotes the permittivity of the semiconductor material and $C(x)$ is the doping profile. We assume that the collision operator $Q_{FP}(f)$ models the interaction of the electrons with the phonons of the crystal lattice (oscillators) and that it is given by the Fokker-Planck expression [24]

$$Q_{FP}(f) = \frac{1}{\tau_0}\mathrm{div}_p(pf) + D_{pp}\Delta_p f + 2D_{pq}\mathrm{div}_x(\nabla_p f) + D_{qq}\Delta_x f,$$

where τ_0 is a friction parameter (relaxation time) and the constants

$$D_{pp} = \frac{mk_BT_0}{\tau_0},\quad D_{pq} = \frac{\Omega\hbar^2}{12\pi k_BT_0\tau_0},\quad D_{qq} = \frac{\hbar^2}{12mk_BT_0\tau_0}$$

constitute the phase-space diffusion matrix. Here, T_0 is the lattice temperature and Ω the cut-off frequency of the reservoir oscillators. If $D_{pq}=0$ and $D_{qq}=0$, this gives the Caldeira-Leggett operator [23]. The above scattering operator has been derived under the assumptions that the thermal energy k_BT_0 is of the same order as the wave energy $\Omega\hbar$ corresponding to the cut-off frequency, and that the reservoir memory time $1/\Omega$ is much smaller than the characteristic time scale t^* of the electrons and the relaxation time τ_0. For a discussion of the Wigner-Fokker-Planck model (3.1), we refer to [10]. In order to derive macroscopic equations we apply the moment method as in [47]. The idea is to multiply (3.1) by 1, p, and $\frac{1}{2}|p|^2$ and to integrate over $\mathbb{R}^3$ with respect to $p/\hbar^3$. The resulting system of equations is closed by Gardner's shifted quantum Maxwellian [47], which is an approximation of the quantum equilibrium state according to Wigner [97, formula (25)]. Gardner's shifted Maxwellian is a quantum mechanical analogue of the classical Maxwellian which lies in the kernel of the Fokker-Planck operator. A different quantum Maxwellian derived from quantum entropy maximization

has been recently suggested by [36] and that will be considered in the Chapter 4. However, the resulting model equations are more complicated such that we prefer here the simpler choice of [47].
The only difference to the derivation in [47] is the integration of the Fokker-Planck term. This yields

$$\begin{aligned}
\langle Q_{FP}(f)\rangle &= D_{qq}\Delta_x\langle f\rangle,\\
\langle pQ_{FP}(f)\rangle &= -\frac{1}{\tau_0}\langle pf\rangle - 2D_{pq}\nabla_x\langle f\rangle + D_{qq}\Delta_x\langle pf\rangle,\\
\langle \tfrac{1}{2}|p|^2 Q_{FP}(f)\rangle &= -\tfrac{2}{\tau_0}\langle \tfrac{1}{2}|p|^2 f\rangle + 3D_{pp}\langle f\rangle - 2D_{pq}\mathrm{div}_x\langle pf\rangle + D_{qq}\Delta_x\langle \tfrac{1}{2}|p|^2 f\rangle,
\end{aligned}$$

where we used the notation

$$\langle g(p)\rangle = \hbar^{-3}\int_{\mathbb{R}^3} g(p)dp$$

for functions $g(p)$. Introducing the electron density $n = \langle f\rangle$, the electron current density $J = -(q/m)\langle pf\rangle$, and the energy density $ne = \langle |p|^2\rangle/2m$, we obtain finally the viscous QHD equations

$$\partial_t n - \frac{1}{q}\mathrm{div}J = D_{qq}\Delta n, \tag{3.2}$$

$$\begin{aligned}
&\partial_t J - \frac{1}{q}\mathrm{div}\Big(\frac{J\otimes J}{n}\Big) - \frac{qk_B}{m}\nabla(nT) + \frac{q^2}{m}n\nabla V \\
&\quad + \frac{q\hbar^2}{12m^2}\mathrm{div}(n(\nabla\otimes\nabla)\log n) = -\frac{J}{\tau_0} + \frac{2qD_{pq}}{m}\nabla n + D_{qq}\Delta J,
\end{aligned} \tag{3.3}$$

$$\begin{aligned}
&\partial_t(ne) - \frac{1}{q}\mathrm{div}\Big(\frac{J}{n}(ne+P)\Big) + J\cdot\nabla V \\
&\quad = -\frac{2}{\tau_0}\Big(ne - \frac{3}{2}nk_BT_0\Big) + \frac{2D_{pq}}{q}\mathrm{div}J + D_{qq}\Delta(ne),
\end{aligned} \tag{3.4}$$

$$\varepsilon_s^2\Delta V = q(n - C(x)), \quad x\in\mathbb{R}^3,\ t>0, \tag{3.5}$$

where $J\otimes J$ denotes the matrix with components J_jJ_k, and the stress tensor and energy density are given by, respectively,

$$\begin{aligned}
P &= nk_BTI - \frac{\hbar^2}{12m}n(\nabla\otimes\nabla)\log n,\\
ne &= \frac{m}{2q^2}\frac{|J|^2}{n} + \frac{3}{2}nk_BT - \frac{\hbar^2}{24m}n\Delta\log n.
\end{aligned}$$

The stress tensor consists of the classical pressure and a quantum "pressure" term. The energy density is the sum of kinetic energy, thermal energy, and quantum energy.

Next, we scale the above system of equations. Let L be a characteristic length, for instance the device length. We define the characteristic density, voltage, and current density, respectively, by

$$C^* = \sup|C|, \quad V^* = \frac{k_B T_0}{q}, \quad J^* = \frac{q k_B T_0 C^* t^*}{mL},$$

where the characteristic time t^* is given by $k_B T_0 = mL^2/(t^*)^2$, i.e., we assume that the thermal energy of a particle is equal to the kinetic energy needed to cross the device in time t^*. According to the conditions under which the Fokker-Planck term has been derived, we assume that the cut-off wave energy equals the thermal energy, i.e., $\Omega\hbar = k_B T_0$. Then, after introducing the scaling (notice the change of sign for the current density)

$$x \to Lx, \quad t \to t^* t, \quad C \to C^* C, \quad V \to V^* V, \quad J \to -J^* J, \quad T \to T_0 T,$$

we obtain the scaled equations

$$\partial_t n + \mathrm{div} J = \nu \Delta n, \tag{3.6}$$

$$\partial_t J + \mathrm{div}\Big(\frac{J \otimes J}{n}\Big) + \nabla(nT) - n\nabla V - \frac{\varepsilon^2}{6} n \nabla\Big(\frac{\Delta\sqrt{n}}{\sqrt{n}}\Big) \tag{3.7}$$
$$= -\frac{J}{\tau} + \nu \Delta J - \mu \nabla n,$$

$$\partial_t(ne) + \mathrm{div}\Big(\frac{J}{n}(ne + P)\Big) - J \cdot \nabla V \tag{3.8}$$
$$= -\frac{2}{\tau} n\Big(e - \frac{3}{2}\Big) + \nu \Delta(ne) - \mu \mathrm{div} J,$$

$$\lambda^2 \Delta V = n - C(x), \tag{3.9}$$

where the scaled parameters are the viscosity constant ν, the Planck constant ε, the Debye length λ, given by

$$\nu = \frac{\hbar}{\sqrt{k_B T_0 m L^2}} \frac{\hbar}{12 k_B T_0 \tau_0}, \quad \varepsilon^2 = \frac{\hbar^2}{k_B T_0 m L^2}, \quad \lambda^2 = \frac{\varepsilon_s k_B T_0}{q^2 C^* L^2},$$

and the relaxation time and interaction constant, respectively,

$$\tau = \frac{\tau_0}{t^*}, \quad \mu = \frac{\hbar}{6\pi k_B T_0 \tau_0}.$$

The scaled stress tensor and energy density can be expressed as

$$P = nTI - \frac{\varepsilon^2}{12} n(\nabla \otimes \nabla) \log n, \quad ne = \frac{|J|^2}{2n} + \frac{3}{2} nT - \frac{\varepsilon^2}{24} n \Delta \log n.$$

In the following sections we will study the one-dimensional stationary equations in a bounded domain.

3.2 Analytical results

In this section we consider the stationary viscous QHD equations with constant temperature T in one space dimension,

$$J_x = \nu n_{xx}, \tag{3.10}$$

$$\Big(\frac{J^2}{n}\Big)_x + Tn_x - nV_x - \frac{\varepsilon^2}{6} n\Big(\frac{(\sqrt{n})_{xx}}{\sqrt{n}}\Big)_x = -\frac{J}{\tau} + \nu J_{xx}, \tag{3.11}$$

$$\lambda^2 V_{xx} = n - C(x) \quad \text{in } (0,1), \tag{3.12}$$

with the physically motivated boundary conditions

$$n(0) = n(1) = 1, \quad n_x(0) = n_x(1), \quad n_{xx}(0) = n_{xx}(1), \tag{3.13}$$

$$V(0) = 0, \quad V(1) = U. \tag{3.14}$$

Notice that the term μn_x in (3.7) can be absorbed by Tn_x. The first two boundary conditions express that the total space charge vanishes at the boundary (if $C(0) = C(1) = 1$). The remaining conditions on n can be justified if the doping profile is nearly constant close to the boundary points (see Section 3.3.3). Notice that (3.10) and the boundary condition $n_x(0) = n_x(1)$ imply that the current density takes the same value at $x = 0$ and $x = 1$, namely $J(0) = J(1) = J_0$ for some constant J_0. Given the applied voltage U, the *effective* current density J_0 can be computed from the solution of the above boundary-value problem, which gives a well-defined current-voltage characteristic.

It is not difficult to see that the number of boundary conditions for the system (3.10)-(3.12) is correct. Indeed, (3.10) implies that $J = \nu n_x + J_0$ which gives

$$\Big(\frac{J^2}{n}\Big)_x - \nu J_{xx} = -2\nu^2 n\Big(\frac{(\sqrt{n})_{xx}}{\sqrt{n}}\Big)_x + \Big(\frac{J_0^2}{n}\Big)_x + 2\nu J_0 (\log n)_{xx},$$

and hence, (3.11) can be written as

$$\Big(\frac{J_0^2}{n}\Big)_x + \Big(T + \frac{\nu}{\tau}\Big)n_x - nV_x - \Big(2\nu^2 + \frac{\varepsilon^2}{6}\Big)n\Big(\frac{(\sqrt{n})_{xx}}{\sqrt{n}}\Big)_x = -\frac{J_0}{\tau} - 2J_0\nu(\log n)_{xx}. \tag{3.15}$$

Therefore, the system (3.10)-(3.12) is (formally) equivalent to the system (3.15) and (3.12) for which five boundary conditions are sufficient.

The left-hand side of (3.15) equals the usual QHD equations except that the scaled Planck constant and the scaled temperature are larger. The viscosity ν has the effect of increasing the Bohm potential and the pressure. Moreover, the right-hand side of (3.15) contains the diffusion term $2J_0\nu(\log n)_{xx}$. Thus, the viscous QHD equations can be interpreted as a quantum fluid model with larger scaled Planck constant and with a diffusion term in the variable $\log n$. We notice that QHD models with various diffusion terms in n (but not in $\log n$) have been studied in [**45**].
Our main result is the following existence theorem.

Theorem 3.1. *Let $C \in L^2(0,1)$ and let T, ε, τ, and λ be positive constants. Then there exists for any $U \in \mathbb{R}$ and any $\nu > 0$ a solution $(n, J, V) \in H^4(0,1) \times H^3(0,1) \times H^2(0,1)$ to (3.10)-(3.14) satisfying $n > 0$ in $(0,1)$. Moreover,*

$$\|\sqrt{n}\|_{H^2} + \|\log n\|_{H^2} + \left\|\frac{J_0}{n}\right\|_{L^\infty} \le c\nu^{-1},$$

where $J_0 = J - \nu n_x \in \mathbb{R}$ and $c > 0$ is a constant depending only on the data but not on ν.

3.2.1 Reformulation of the equations

The first idea for the proof, taken from [**54**], is to formulate the system (3.15) and (3.12) as a single fourth-order equation, in which the Poisson equation is taken into account. We divide (3.15) by n, differentiate the resulting equation with respect to x and employ the Poisson equation (3.12):

$$\begin{aligned}
&-\Big(2\nu^2 + \frac{\varepsilon^2}{6}\Big)\Big(\frac{(\sqrt{n})_{xx}}{\sqrt{n}}\Big)_{xx} + \Big(T + \frac{\nu}{\tau}\Big)(\log n)_{xx} \\
&\quad = \frac{n - C}{\lambda^2} + J_0^2\Big(\frac{n_x}{n^3}\Big)_x - 2J_0\nu\Big(\frac{1}{n}(\log n)_{xx}\Big)_x - \frac{J_0}{\tau}\Big(\frac{1}{n}\Big)_x. \qquad (3.16)
\end{aligned}$$

The electric potential can be recovered from (3.15), after division by n and integration, taking into account the boundary conditions $n(0) = 1$ and $V(0) = 0$,

$$\begin{aligned}
V(x) = &-\Big(2\nu^2 + \frac{\varepsilon^2}{6}\Big)\frac{(\sqrt{n})_{xx}(x)}{\sqrt{n}(x)} + \Big(T + \frac{\nu}{\tau}\Big)\log n(x) + \frac{J_0^2}{2n(x)^2} \\
&+ \frac{J_0}{\tau}\int_0^x \frac{ds}{n} + 2J_0\nu\frac{n_x(x)}{n(x)^2} + 2J_0\nu\int_0^x \frac{n_x^2}{n^3}ds \qquad (3.17) \\
&+ \Big(2\nu^2 + \frac{\varepsilon^2}{6}\Big)(\sqrt{n})_{xx}(0) - \frac{J_0^2}{2} - 2J_0\nu n_x(0).
\end{aligned}$$

Introducing the new variable $n = \mathrm{e}^w$ and observing that

$$\Big(\frac{(\sqrt{n})_{xx}}{\sqrt{n}}\Big)_{xx} = \frac{1}{2}\Big(\frac{1}{n}\big(n(\log n)_{xx}\big)_x\Big)_x = \frac{1}{2}\Big(w_{xx} + \frac{w_x^2}{2}\Big)_{xx},$$

we can write (3.16)-(3.17) as

$$\begin{aligned} &-\Big(\nu^2 + \frac{\varepsilon^2}{12}\Big)\Big(w_{xx} + \frac{w_x^2}{2}\Big)_{xx} + \Big(T + \frac{\nu}{\tau}\Big)w_{xx} \\ &\quad = \lambda^{-2}(\mathrm{e}^w - C) + J_0^2(\mathrm{e}^{-2w}w_x)_x - 2J_0\nu(\mathrm{e}^{-w}w_{xx})_x - \frac{J_0}{\tau}(\mathrm{e}^{-w})_x, \end{aligned} \tag{3.18}$$

and

$$\begin{aligned} V(x) = &-\Big(\nu^2 + \frac{\varepsilon^2}{12}\Big)\Big(w_{xx}(x) + \frac{w_x(x)^2}{2}\Big) + \Big(T + \frac{\nu}{\tau}\Big)w(x) + \frac{J_0^2}{2}\mathrm{e}^{-2w(x)} \\ &+ \frac{J_0}{\tau}\int_0^x \mathrm{e}^{-w(s)}ds + 2J_0\nu\mathrm{e}^{-w(x)}w_x(x) + 2J_0\nu\int_0^x \mathrm{e}^{-w(s)}w_x(s)^2ds \\ &+ \Big(\nu^2 + \frac{\varepsilon^2}{12}\Big)\Big(w_{xx}(0) + \frac{w_x(0)^2}{2}\Big) - \frac{J_0^2}{2} - 2J_0\nu w_x(0). \end{aligned} \tag{3.19}$$

Equation (3.18) has to be solved in the interval $(0,1)$ with the boundary conditions

$$w(0) = w(1) = 0, \quad w_x(0) = w_x(1), \quad w_{xx}(0) = w_{xx}(1). \tag{3.20}$$

We have shown the first part of the following lemma.

Lemma 3.1. *Let (n, J, V) be a smooth solution to (3.10)-(3.14) such that $n > 0$ in $(0,1)$. Then $w = \log n$ is a solution to (3.18) with boundary conditions (3.20), V solves (3.19), and J_0 is defined by (3.17) with $x = 1$, i.e.*

$$U = \frac{J_0}{\tau}\int_0^1 \frac{dx}{n} + 2J_0\nu\int_0^1 \frac{n_x^2}{n^3}dx. \tag{3.21}$$

Conversely, if $w \in H^4(0,1)$ is a solution to (3.18) with boundary conditions (3.20) and if V and J_0 are given by, respectively, (3.19) and (3.21), then $(\mathrm{e}^w, J, V) \in H^4(0,1) \times H^3(0,1) \times H^2(0,1)$ is a solution to (3.10)-(3.14), where $J := \nu\mathrm{e}^w w_x + J_0$.

Proof. It remains to show that (e^w, J, V) solves (3.10)-(3.14). In order to see this, first differentiate (3.19) twice with respect to x and take the difference to (3.18). This yields the Poisson equation (3.12). Then differentiate (3.19)

once with respect to x and multiply the resulting equation by n. This equals (3.15). Defining $J = \nu n_x + J_0$, we see that (3.15) is equivalent to (3.11). Moreover, differentiating J with respect to x gives (3.10). The boundary conditions (3.13) are a consequence of (3.20). Finally, the boundary conditions (3.14) are obtained by taking $x = 0$ and $x = 1$ in (3.19) and using (3.21). □

3.2.2 Uniform estimates

For the proof of Theorem 3.1 we need some uniform estimates. Our second idea of the existence analysis is to show that the energy production is bounded which provides the necessary estimates.

Lemma 3.2. *Let $(n, J, V) \in H^4(0,1) \times H^3(0,1) \times H^2(0,1)$ be a solution to (3.10)-(3.14) such that $n > 0$ in $(0,1)$. Then there exists a constant $c > 0$ such that*

$$\int_0^1 \Big(\frac{(J_x n - J n_x)^2}{n^3} + \frac{\varepsilon^2}{3}(\sqrt{n})_{xx}^2 + \frac{\varepsilon^2}{144}\frac{n_x^4}{n^3} + \frac{n^2}{4\lambda^2} + 4\Big(T + \frac{\nu}{\tau}\Big)(\sqrt{n})_x^2 + \frac{J_0^2}{\nu\tau n}\Big) dx \le c\nu^{-2},$$

where $c > 0$ only depends on τ, λ, U, and $\|C\|_{L^2}$.

The integrand of the above inequality can be indeed interpreted as the energy production: In [**59**] it has been shown that, with thermal equilibrium boundary conditions, the energy of the time-dependent viscous QHD equations is bounded for all time and the energy production is given by the above integral. We notice that, setting $J = nu$, the first integrand can be written as $\int_0^1 n u_x^2 dx$.

Proof. We multiply (3.10) by $T\log n - J^2/2n^2 - V - \varepsilon^2(\sqrt{n})_{xx}/6\sqrt{n}$ and integrate by parts to obtain

$$\begin{aligned}
&\int_0^1 \Big(-TJ\frac{n_x}{n} - \frac{J^2 J_x}{2n^2} + JV_x - \frac{\varepsilon^2}{6}\frac{(\sqrt{n})_{xx}}{\sqrt{n}} J_x\Big) dx + [JT\log n - JV]_0^1 \\
&\quad = \nu\int_0^1 \Big(-T\frac{n_x^2}{n} + \Big(\frac{J^2}{2n^2}\Big)_x n_x + n_x V_x - \frac{\varepsilon^2}{6}\frac{(\sqrt{n})_{xx}}{\sqrt{n}} n_{xx}\Big) dx \\
&\qquad + \nu\Big[n_x T\log n - n_x\frac{J^2}{2n^2} - n_x V\Big]_0^1. \qquad (3.22)
\end{aligned}$$

Taking into account the boundary conditions (3.13)-(3.14) and $J(0) = J(1)$, the above equation becomes

$$\int_0^1 \Big(- TJ\frac{n_x}{n} - \frac{J^2 J_x}{2n^2} + JV_x - \frac{\varepsilon^2}{6}\frac{(\sqrt{n})_{xx}}{\sqrt{n}} J_x \Big) dx - J(1)U$$
$$= \nu \int_0^1 \Big(- T\frac{n_x^2}{n} + \Big(\frac{J^2}{2n^2}\Big)_x n_x + n_x V_x - \frac{\varepsilon^2}{6}\frac{(\sqrt{n})_{xx}}{\sqrt{n}} n_{xx} \Big) dx - \nu n_x(1)U.$$

Furthermore, we multiply (3.11) by J/n and integrate by parts:

$$\int_0^1 \Big(\Big(\frac{J^2}{n}\Big)_x \frac{J}{n} + TJ\frac{n_x}{n} - JV_x + \frac{\varepsilon^2}{6}\frac{(\sqrt{n})_{xx}}{\sqrt{n}} J_x \Big) dx - \frac{\varepsilon^2}{6}\Big[\frac{(\sqrt{n})_{xx}}{\sqrt{n}} J\Big]_0^1$$
$$= \int_0^1 \Big(- \frac{J^2}{\tau n} - \nu J_x \Big(\frac{J}{n}\Big)_x \Big) dx + \Big[\nu J_x \frac{J}{n}\Big]_0^1. \tag{3.23}$$

Taking into account the boundary conditions (3.13) and $J_x = \nu n_{xx}$, the boundary terms vanish. Hence, adding (3.22) and (3.23) gives, since some terms cancel,

$$\int_0^1 \Big(- \frac{J^2 J_x}{2n^2} + \Big(\frac{J^2}{n}\Big)_x \frac{J}{n} \Big) dx + \nu \int_0^1 \Big(J_x \Big(\frac{J}{n}\Big)_x - \Big(\frac{J^2}{2n^2}\Big)_x n_x \Big) dx$$
$$+ \nu\frac{\varepsilon^2}{6} \int_0^1 \frac{(\sqrt{n})_{xx}}{\sqrt{n}} n_{xx} dx - \nu \int_0^1 n_x V_x dx + \int_0^1 \Big(\nu T\frac{n_x^2}{n} + \frac{J^2}{\tau n} \Big) dx \tag{3.24}$$
$$= J(1)U - \nu n_x(1)U = J_0 U.$$

The first integral vanishes since

$$\int_0^1 \Big(- \frac{J^2 J_x}{2n^2} + \Big(\frac{J^2}{n}\Big)_x \frac{J}{n} \Big) dx = \frac{1}{2}\int_0^1 \Big(\frac{J^3}{n^2}\Big)_x dx = \frac{1}{2}\Big[\frac{J^3}{n^2}\Big]_0^1$$
$$= \frac{1}{2}(J(1)^3 - J(0)^3) = 0.$$

The second integral equals

$$\nu \int_0^1 \Big(J_x \Big(\frac{J}{n}\Big)_x - \Big(\frac{J^2}{2n^2}\Big)_x n_x \Big) dx = \nu \int_0^1 \frac{1}{n^3}(J_x n - J n_x)^2 dx.$$

Since, using $n(0) = n(1)$ and $n_x(0) = n_x(1)$,

$$\int_0^1 \frac{n_x^2 n_{xx}}{2n^2} dx = \frac{1}{3}\int_0^1 \frac{(n_x^3)_x}{2n^2} dx = \frac{1}{3}\int_0^1 \frac{n_x^4}{n^3} dx + \frac{1}{3}\Big[\frac{n_x^3}{2n^2}\Big]_0^1 = \frac{1}{3}\int_0^1 \frac{n_x^4}{n^3} dx,$$

the third integral in (3.24) becomes

$$\nu\frac{\varepsilon^2}{12}\int_0^1\Big(\frac{n_{xx}^2}{n}-\frac{n_x^2 n_{xx}}{2n^2}\Big)dx=\nu\frac{\varepsilon^2}{3}\int_0^1\Big((\sqrt{n})_{xx}^2+\frac{n_x^4}{48n^3}\Big)dx.$$

Multiplying the Poisson equation (3.12) by $n-1$ and integrating by parts yields

$$\lambda^2\int_0^1 V_x n_x dx=-\int_0^1(n-1)(n-C(x))dx\le-\frac{1}{2}\int_0^1 n^2dx+c_1,$$

where $c_1=(1+\|C\|_{L^2}^2)/2$. Furthermore, it follows from $J=-\nu n_x+J_0$ that

$$\int_0^1\frac{J^2}{\tau n}dx=\frac{J_0^2}{\tau}\int_0^1\frac{dx}{n}+\frac{4\nu^2}{\tau}\int_0^1(\sqrt{n})_x^2dx,$$

since the integral over the mixed term $\int_0^1(\log n)_x dx$ vanishes in view of the boundary conditions $n(0)=n(1)=1$. Therefore, we obtain from (3.24), divided by ν,

$$\begin{aligned}\int_0^1\Big(\frac{1}{n^3}(J_x n-Jn_x)^2+\frac{\varepsilon^2}{3}(\sqrt{n})_{xx}^2+\frac{\varepsilon^2}{144}\frac{n_x^4}{n^3}+\frac{n^2}{2\lambda^2}+4\Big(T+\frac{\nu}{\tau}\Big)(\sqrt{n})_x^2\Big)dx\\ \le-\frac{J_0^2}{\tau\nu}\int_0^1\frac{dx}{n}+\frac{J_0U}{\nu}+\frac{c_1}{\lambda^2}.\end{aligned}\tag{3.25}$$

It remains to estimate the term J_0U/ν. For this we employ Young's inequality,

$$\frac{J_0U}{\nu}\le\frac{J_0^2}{2\tau\nu}\int_0^1\frac{dx}{n}+\frac{\tau U^2}{2\nu}\int_0^1 ndx.$$

The first term on the right-hand side can be absorbed by the corresponding term in (3.25). We employ again Young's inequality to treat the second term:

$$\begin{aligned}\frac{\tau U^2}{2\nu}\int_0^1 ndx&=\frac{\tau U^2}{2\nu}\|\sqrt{n}\|_{L^2}^2\le\frac{\tau U^2}{2\nu}\|\sqrt{n}\|_{L^4}^2\\ &\le\frac{1}{4\lambda^2}\|\sqrt{n}\|_{L^4}^4+\frac{\lambda^2\tau^2U^4}{4\nu^2}=\frac{1}{4\lambda^2}\int_0^1 n^2dx+\frac{\lambda^2\tau^2U^4}{4\nu^2}.\end{aligned}$$

Putting these inequalities into (3.25), we obtain

$$\begin{aligned}\int_0^1\Big(\frac{1}{n^3}(J_x n-Jn_x)^2+\frac{\varepsilon^2}{3}(\sqrt{n})_{xx}^2+\frac{\varepsilon^2}{144}\frac{n_x^4}{n^3}+\frac{n^2}{4\lambda^2}+4\Big(T+\frac{\nu}{\tau}\Big)(\sqrt{n})_x^2\Big)dx\\ \le-\frac{J_0^2}{2\tau\nu}\int_0^1\frac{dx}{n}+\frac{\lambda^2\tau^2U^4}{4\nu^2}+\frac{c_1}{\lambda^2}.\end{aligned}$$

This shows the lemma. □

The following a priori estimates are consequences of the previous lemma.

Lemma 3.3. *Let $(n, J, V) \in H^4(0,1) \times H^3(0,1) \times H^2(0,1)$ be a solution to (3.10)-(3.14) satisfying $n > 0$ in $(0,1)$. Then there exists a constant $c > 0$ such that*

$$|J_0| \le c\nu^{-1}, \quad |J_0| \left\| \frac{1}{\sqrt{n}} \right\|_{H^1}^2 \le c\nu^{-1},$$

where $J_0 = J - \nu n_x$ and c only depends on τ, λ, U, and $\|C\|_{L^2}$.

If $U = 0$, (3.21) shows that $J_0 = 0$ and hence, the above estimates become trivial. A consequence of the above lemma is the boundedness of the velocity J_0/n in $L^\infty(0,1)$.

Proof. Lemma 3.2 immediately gives the bound $\|\sqrt{n}\|_{L^\infty} \le c\nu^{-1}$ since $H^2(0,1)$ embeddes into $L^\infty(0,1)$. (Here and in the following, $c > 0$ denotes a generic constant not depending on ν.) Thus, since $J_0^2 \int_0^1 dx/n$ is uniformly bounded,

$$J_0^2 \le J_0^2 \int_0^1 \frac{dx}{n} \|\sqrt{n}\|_{L^\infty}^2 \le c\|\sqrt{n}\|_{L^\infty}^2 \le c\nu^{-2},$$

which shows the first assertion.
If $U > 0$ then, by (3.21), $J_0 > 0$ and

$$J_0 \int_0^1 \frac{n_x^2}{n^3} dx = \frac{U}{2\nu} - \frac{J_0}{2\tau\nu} \int_0^1 \frac{dx}{n} \le \frac{U}{2\nu}.$$

On the other hand, if $U < 0$ then $J_0 < 0$ and

$$-J_0 \int_0^1 \frac{n_x^2}{n^3} dx = -\frac{U}{2\nu} + \frac{J_0}{2\tau\nu} \int_0^1 \frac{dx}{n} \le -\frac{U}{2\nu}.$$

This shows that

$$|J_0| \int_0^1 \left| \left(\frac{1}{\sqrt{n}} \right)_x \right|^2 dx = \frac{|J_0|}{4} \int_0^1 \frac{n_x^2}{n^3} dx \le \frac{|U|}{8\nu}.$$

By Poincaré's inequality, we have

$$|J_0| \int_0^1 \Big(\frac{1}{2n} - 1 \Big) dx \le |J_0| \int_0^1 \Big(\frac{1}{\sqrt{n}} - 1 \Big)^2 dx \le c|J_0| \left\| \Big(\frac{1}{\sqrt{n}} \Big)_x \right\|_{L^2}^2 \le c\nu^{-1},$$

and hence, using the first assertion,

$$\frac{|J_0|}{2} \left\| \frac{1}{\sqrt{n}} \right\|_{L^2}^2 \le c\nu^{-1} + |J_0| \le c\nu^{-1}.$$

The second assertion is proved. □

Lemma 3.4. *Let $(n, J, V) \in H^4(0,1) \times H^3(0,1) \times H^2(0,1)$ be a solution to (3.10)-(3.14) satisfying $n > 0$ in $(0,1)$. Then there exists a constant $c > 0$ such that for all $\nu < 1$,*

$$\|\log n\|_{H^2} \le c\nu^{-1},$$

and $c > 0$ only depends on T, ε, λ, U, and $\|C\|_{L^2}$.

Proof. By Lemma 3.1, $w = \log n$ solves (3.18). Since $w \in H^2_{\mathrm{per}}(0,1)$, where $H^2_{\mathrm{per}}(0,1)$ is the space of all periodic H^2 functions, we can use w as a test function in the weak formulation of (3.18) leading to

$$\begin{aligned}\Big(\nu^2 + \frac{\varepsilon^2}{12}\Big)\int_0^1 w_{xx}^2 dx + \Big(T + \frac{\nu}{\tau}\Big)\int_0^1 w_x^2 dx \\ = -\lambda^{-2}\int_0^1 (\mathrm{e}^w - C)w dx + J_0^2 \int_0^1 \mathrm{e}^{-2w} w_x^2 dx \\ - 2J_0\nu\int_0^1 \mathrm{e}^{-w} w_{xx} w_x dx - \frac{J_0}{\tau}\int_0^1 \mathrm{e}^{-w} w_x dx.\end{aligned}$$

The last integral on the right-hand side vanishes since $w(0) = w(1)$. The function $x \mapsto -x\mathrm{e}^x$, $x \in \mathbb{R}$, has the maximal value e^{-1}. Hence, the first integral on the right-hand side can be estimated as follows, employing Poincaré's and Young's inequalities,

$$\begin{aligned}-\lambda^{-2}\int_0^1 (\mathrm{e}^w - C)w dx &\le \lambda^{-2}\int_0^1 (\mathrm{e}^{-1} + Cw)dx \le \lambda^{-2}\big(1 + \|C\|_{L^2}\|w\|_{L^2}\big) \\ &\le c + \frac{T}{2}\|w_x\|_{L^2}^2,\end{aligned}$$

where $c > 0$ depends on T. Next, we consider the second integral:

$$\begin{aligned}J_0^2\int_0^1 \mathrm{e}^{-2w} w_x^2 dx &\le \|J_0\mathrm{e}^{-w}\|_{L^\infty}|J_0|\int_0^1 \mathrm{e}^{-w} w_x^2 dx \\ &= \Big\|\frac{J_0}{n}\Big\|_{L^\infty}\cdot|J_0|\int_0^1 \frac{n_x^2}{n^3}dx \le c\nu^{-1}\cdot c\nu^{-1} = c\nu^{-2},\end{aligned}$$

using Lemma 3.3. This inequality allows to treat the remaining third integral:

$$\begin{aligned}-2J_0\nu\int_0^1 \mathrm{e}^{-w} w_{xx} w_x dx &\le \frac{\varepsilon^2}{24}\int_0^1 w_{xx}^2 dx + \frac{24\nu^2 J_0^2}{\varepsilon^2}\int_0^1 \mathrm{e}^{-2w} w_x^2 dx \\ &\le \frac{\varepsilon^2}{24}\int_0^1 w_{xx}^2 dx + c.\end{aligned}$$

Putting together the above estimates gives, for $\nu < 1$,

$$\Big(\nu^2 + \frac{\varepsilon^2}{24}\Big) \int_0^1 w_{xx}^2 dx + \Big(\frac{T}{2} + \frac{\nu}{\tau}\Big) \int_0^1 w_x^2 dx \le c\nu^{-2}.$$

Then the conclusion follows from Poincaré's inequality. □

3.2.3 Existence of solutions

Lemma 3.5. *Let $C \in L^2(0,1)$. Then there exists a solution $w \in H^4(0,1)$ to (3.18) and (3.20).*

Proof. The proof is based on Leray-Schauder's fixed-point theorem and the a priori estimate of Lemma 3.4. First, we consider weak solutions. Let $H = H_0^1(0,1) \cap H^2_{\mathrm{per}}(0,1)$. As usual, $w \in H$ is called a weak solution to (3.18) and (3.20) if, for $J_0 \in \mathbb{R}$ given, for all $\phi \in H$,

$$\begin{aligned} -\Big(\nu^2 + \frac{\varepsilon^2}{12}\Big) \int_0^1 (w_{xx} + \frac{1}{2} w_x^2) \phi_{xx} dx - \Big(T + \frac{\nu}{\tau}\Big) \int_0^1 w_x \phi_x dx \\ = \lambda^{-2} \int_0^1 (\mathrm{e}^w - C) \phi dx - J_0^2 \int_0^1 \mathrm{e}^{-2w} w_x \phi_x dx \\ + 2J_0 \nu \int_0^1 \mathrm{e}^{-w} w_{xx} \phi_x dx + \frac{J_0}{\tau} \int_0^1 \mathrm{e}^{-w} \phi_x dx. \end{aligned} \tag{3.26}$$

For the definition of the fixed-point operator, let $v \in W^{1,4}(0,1)$, $I_0 \in \mathbb{R}$, and $\sigma \in [0,1]$ be given. We wish to solve the following linear problem in H,

$$a(w, \phi) = \sigma F(\phi) \quad \text{for all } \phi \in H, \tag{3.27}$$

where for all w, $\phi \in H$,

$$\begin{aligned} a(w,\phi) &= \Big(\nu^2 + \frac{\varepsilon^2}{12}\Big) \int_0^1 w_{xx} \phi_{xx} dx + \Big(T + \frac{\nu}{\tau}\Big) \int_0^1 w_x \phi_x dx, \\ F(\phi) &= -\frac{1}{2}\Big(\nu^2 + \frac{\varepsilon^2}{12}\Big) \int_0^1 v_x^2 \phi_{xx} dx - \lambda^{-2} \int_0^1 (\mathrm{e}^v - C) dx \\ &\quad + I_0^2 \int_0^1 \mathrm{e}^{-2v} v_x \phi_x dx + 2\nu I_0 \int_0^1 (\mathrm{e}^{-v} \phi_x)_x v_x dx - \frac{I_0}{\tau} \int_0^1 \mathrm{e}^{-v} \phi_x dx. \end{aligned}$$

Notice that the product $v_x^2 \phi_{xx}$ is integrable since $v \in W^{1,4}(0,1)$. The bilinear form $a(\cdot,\cdot)$ is continuous and coercive in H since we can apply Poincaré's

inequality. Furthermore, the linear functional F is continuous. Hence, Lax-Milgram's lemma provides the existence of a unique solution $w \in H$ to (3.27). Finally, we define J_0 as the solution to (see (3.21))

$$\sigma U = J_0\Big(\frac{1}{\tau}\int_0^1 \mathrm{e}^{-w}dx + 2\nu\int_0^1 \mathrm{e}^{-w}w_x^2 dx\Big). \tag{3.28}$$

Clearly, if $U = 0$ then $J_0 = 0$.

Thus we can define the fixed-point operator $S : (W^{1,4}(0,1) \times \mathbb{R}) \times [0,1] \to W^{1,4}(0,1)\times\mathbb{R}$ by $S(v, I_0, \sigma) = (w, J_0)$. By Poincaré's inequality, $S(v, I_0, 0) = (0, 0)$. By standard arguments, S is continuous and, since the range of S is contained in $H^2(0,1)$ and $H^2(0,1)$ embeddes compactly into $W^{1,4}(0,1)$, also compact. It remains to show that there is a constant $c > 0$ such that $\|w\|_{W^{1,4}} + |J_0| \le c$ for all fixed points (w, J_0) of $S(\cdot,\cdot,\sigma)$.

Let $(w, J_0) \in H \times \mathbb{R}$ be a fixed point of S. Then $w \in H$ satisfies (3.18) in the sense of $H^{-2}(0,1)$. Since $(w_x^2)_{xx}$, $(\mathrm{e}^{-w}w_{xx})_x \in H^{-1}(0,1)$, this equation shows that $w_{xxxx} \in H^{-1}(0,1)$ and $w_{xxx} \in L^2(0,1)$. Employing (3.18) again, we obtain $w_{xxxx} \in L^2(0,1)$ and thus $w \in H^4(0,1)$, i.e., (3.18) is satisfied pointwise in $(0,1)$. Moreover, $V \in H^2(0,1)$ by (3.19). (In fact, V is much more regular but we do not need this fact.) Thus, $(n, J, V) \in H^4(0,1) \times H^3(0,1) \times H^2(0,1)$ with $n = \mathrm{e}^w > 0$ and $J = \nu n_x + J_0$ solves (3.10)-(3.14). In particular, Lemmas 3.3 and 3.4 can be applied providing uniform bounds for $|J_0|$ and $w = \log n$ in $H^2(0,1)$. More precisely, this settles the case $\sigma = 1$; however, it is not difficult to see that a similar estimate also holds for $\sigma < 1$. Hence, Leray-Schauder's fixed-point theorem gives a solution to (3.26) and thus to (3.18) and (3.20). □

3.3 Numerical results

In this section we discretize and numerically solve the viscous and the inviscid QHD equations using finite differences.

3.3.1 Numerical discretization

The stationary viscous QHD model is numerically solved in one space dimension. In this situation, the temperature in (3.7) can be replaced by the energy density and a term involving $n(\log n)_{xx}$, which can be summed with the quantum term in (3.7). This leads to the following set of equations in

the variables n, J, and ne (and the potential V):

$$J_x = \nu n_{xx}, \tag{3.29}$$

$$\frac{2}{3}\Big(\frac{J^2}{n}\Big)_x + \frac{2}{3}(ne)_x - nV_x - \frac{\varepsilon^2}{18}\big(n(\log n)_{xx}\big)_x = -\frac{J}{\tau} + \nu J_{xx} - \mu n_x, \tag{3.30}$$

$$\begin{aligned}\frac{5}{3}\Big(\frac{J\,ne}{n}\Big)_x - \Big(\frac{J^3}{3n^2}\Big)_x - JV_x - \frac{\varepsilon^2}{18}\big(J(\log n)_{xx}\big)_x \\ = -\frac{2}{\tau}\Big(ne - \frac{3}{2}n\Big) + \nu(ne)_{xx} - \mu J_x,\end{aligned} \tag{3.31}$$

$$\lambda^2 V_{xx} = n - C(x). \tag{3.32}$$

We define a uniform mesh by $x_i = ih$ $(i = 0, \dots, N)$, where $h = 1/N$ is the mesh size. In order to discretize the Neumann boundary conditions, we introduce the ghost cells $[x_{-1}, x_0]$ and $[x_N, x_{N+1}]$, where $x_{-1} = -h$ and $x_{N+1} = (n+1)h$.

First we discretize the viscous QHD equations using a central finite-difference scheme. For this, the electron density n and electric potential V are approximated at the grid points x_i, whereas the current density J and the energy density ne are discretized in the mid-points $x_{i-1/2} = (x_i + x_{i-1})/2$. We denote by n_i and V_i the approximations of $n(x_i)$ and $V(x_i)$ and by $J_{i-1/2}$ and $ne_{i-1/2}$ the approximations of $J(x_{i-1/2})$, and $ne(x_{i-1/2})$, respectively. For the sake of completeness, and since we analyze the numerical scheme in the next subsection, we make explicit the discretization. The central finite-difference scheme for (3.29) and (3.32) at $x = x_i$ reads as

$$0 = \frac{J_{i+1/2} - J_{i-1/2}}{h} - \frac{\nu}{h^2}(n_{i+1} - 2n_i + n_{i-1}), \tag{3.33}$$

$$0 = -\frac{\lambda^2}{h^2}(V_{i+1} - 2V_i + V_{i-1}) + n_i - C_i, \tag{3.34}$$

where $C_i = C(x_i)$ and $i = 1, \dots, N-1$. The central discretization of (3.30) at $x = x_{i-1/2}$ is

$$\begin{aligned}0 = {} & \frac{1}{6h}\Big(\frac{(J_{i+1/2} + J_{i-1/2})^2}{n_i} - \frac{(J_{i-1/2} + J_{i-3/2})^2}{n_{i-1}}\Big) \\ & + \frac{1}{3h}(ne_{i+1/2} - ne_{i-3/2}) - \frac{n_i + n_{i-1}}{2}\frac{V_i - V_{i-1}}{h} \\ & - \frac{\varepsilon^2}{18h^3}\Big(n_i \log\frac{n_{i+1}n_{i-1}}{n_i^2} - n_{i-1}\log\frac{n_i n_{i-2}}{n_{i-1}^2}\Big) \\ & + \frac{J_{i-1/2}}{\tau} + \frac{\mu}{h}(n_i - n_{i-1}) - \frac{\nu}{h^2}(J_{i+1/2} - 2J_{i-1/2} + J_{i-3/2}),\end{aligned} \tag{3.35}$$

and the central discretization of (3.31) at $x = x_{i-1/2}$ reads as

$$\begin{aligned} 0 = \frac{5}{12h}\Big(&\frac{(J_{i+1/2}+J_{i-1/2})(ne_{i+1/2}+ne_{i-1/2})}{n_i} \\ &- \frac{(J_{i-1/2}+J_{i-3/2})(ne_{i-1/2}+ne_{i-3/2})}{n_{i-1}}\Big) \\ &- \frac{1}{24h}\Big(\frac{(J_{i+1/2}+J_{i-1/2})^3}{n_i^2} - \frac{(J_{i-1/2}+J_{i-3/2})^3}{n_{i-1}^2}\Big) - J_{i-1/2}\frac{V_i - V_{i-1}}{h} \\ &- \frac{\varepsilon^2}{36h^3}\Big((J_{i+1/2}+J_{i-1/2})\log\frac{n_{i+1}n_{i-1}}{n_i^2} - (J_{i-1/2}+J_{i-3/2})\log\frac{n_i n_{i-2}}{n_{i-1}^2}\Big) \\ &+ \frac{2}{\tau}\Big(ne_{i-1/2} - \frac{3}{4}(n_i + n_{i-1})\Big) + \frac{\mu}{2h}(J_{i+1/2} - J_{i-3/2}) \\ &- \frac{\nu}{h^2}(ne_{i+1/2} - 2ne_{i-1/2} + ne_{i-3/2}), \end{aligned} \tag{3.36}$$

where $i = 1, \dots, N$.
We impose the following boundary conditions

$$n_0 = C_0, \quad n_N = C_N, \quad n_1 = n_{-1}, \quad n_{N-1} = n_{N+1}, \tag{3.37}$$
$$J_{1/2} = J_{-1/2}, \; J_{N+1/2} = J_{N-1/2},$$
$$ne_{1/2} = ne_{-1/2}, \; ne_{N+1/2} = ne_{N-1/2}, \tag{3.38}$$
$$V_0 = 0, \quad V_N = U. \tag{3.39}$$

With these ten conditions, the discrete system seems to be overdetermined. However, the choice of the doping profile of the tunneling diode simulated in Section 3.3.3 implies that the particle density fulfills approximately the conditions $n = C$, $J = \nu n_x = 0$, and $J_x = \nu n_{xx} = 0$ at the boundary such that the discrete system is *practically* not overdetermined.
Next, we turn to the discretization of the inviscid QHD model. Gardner suggested in [47] the upwind finite-difference scheme which we recall here. The QHD equations are here written in the variables n, $u = J/n$, and T rather than in n, J, and ne. Furthermore, the variables n, T, and V are approximated at the grid points x_i but only u is discretized at the mid-points $x_{i-1/2}$. The QHD system can be formulated in the form $(ug)_x + f = 0$, where g, $f \in \mathbb{R}^4$ are appropriate vector-valued functions, namely, writing $g = (g^{(1)}, g^{(2)}, g^{(3)}, g^{(4)})$,

$$\begin{aligned} &g^{(1)} = n, \quad g^{(2)} = nu, \\ &g^{(3)} = \frac{5}{2}nT + \frac{1}{2}nu^2 - nV - \frac{\varepsilon^2}{12}\big(n(\log n)_{xx}\big)_x, \quad g^{(4)} = 0. \end{aligned}$$

The advection terms $(ng^{(j)})_x$ are discretized using second upwind differences. More precisely, $(nu)_x$ at x_i is discretized by

$$A_1 = \frac{1}{h}(u_{i+1/2}n^{\text{up}}_{i+1/2} - u_{i-1/2}n^{\text{up}}_{i-1/2}), \tag{3.40}$$

where

$$n^{\text{up}}_{i+1/2} = \begin{cases} n_i & \text{if } u_{i+1/2} > 0 \\ n_{i+1} & \text{if } u_{i+1/2} < 0. \end{cases}$$

The term $(nu^2)_x$ is approximated at $x_{i+1/2}$ by

$$A_2 = \frac{1}{h}(u_{i+1}(nu)^{\text{up}}_{i+1} - u_i(nu)^{\text{up}}_i), \tag{3.41}$$

where

$$(nu)^{\text{up}}_{i+1} = \begin{cases} \frac{1}{2}(n_i + n_{i+1})u_{i+1/2} & \text{if } u_{i+1} > 0 \\ \frac{1}{2}(n_{i+1} + n_{i+2})u_{i+3/2} & \text{if } u_{i+1} < 0. \end{cases}$$

The remaining term $(ng^{(3)})_x$ is discretized at $x_{i+1/2}$ in a similar way noticing that $g^{(3)}(x_i)$ is approximated by

$$g^{(3)}_i = \frac{5}{2}n_iT_i + \frac{1}{8}n_i(u_{i-1/2} + u_{i+1/2})^2 - n_iV_i - \frac{\varepsilon^2}{12h^2}n_i \log\left(\frac{n_{i+1}n_{i-1}}{n_i^2}\right).$$

Gardner has imposed the following boundary conditions

$$\begin{aligned} &n(0) = C(0), \quad n(1) = C(1), \quad n_x(0) = n_x(1) = 0, \\ &T(0) = T(1) = 1, \quad V(0) = 0, \quad V(1) = U, \end{aligned}$$

which are discretized similar as in (3.37)-(3.39).
The above discrete nonlinear systems are solved by using Newton's method and the line search method of [**37**] (Algorithm A6.3.1, p. 325). For a given applied voltage, we employed the continuation method, i. e., with the solution for the applied voltage U as an initial guess, we solve the problem applying the potential $U + \triangle U$ and use this solution again as an initial guess for the next applied voltage. For the computations in Section 3.3.3, we have chosen $\triangle U = 1\,\text{mV}$ and the final voltage is usually $U = 0.5\,\text{V}$. The number of grid points is $N = 1000$ such that $h = 1/N = 10^{-3}$.

3.3.2 Numerical viscosity and numerical dispersion

In this section, we analyze the finite-difference schemes of Section 3.3.1. In particular, we derive the consistency error in order to examine the strength of numerical viscosity or dispersion introduced by the discretization.

We start with the viscous QHD model. Let (n, J, ne, V) be a smooth solution to (3.29)-(3.32). To simplify the notation we set $n_i = n(x_i)$, $n_{i+1/2} = n(x_{i+1/2})$ etc. Since we consider in this section only exact solutions, no confusion with the notation of the previous section should arise. By standard Taylor expansion, we find that (3.29) can be expanded as

$$\begin{aligned}(J_x - \nu n_{xx})(x_i) = \frac{1}{h}(J_{i+1/2} - J_{i-1/2}) - \frac{\nu}{h^2}(n_{i+1} - 2n_i + n_{i-1}) \\ - \frac{\nu h^2}{24} n_{xxxx}(x_i) + O(h^4).\end{aligned}$$

Typical values of ε^2, ν, and h are (see Section 3.3.3) $\varepsilon^2 = 10^{-2}$, $\nu = 10^{-2}$, $h = 10^{-3}$. Thus our central finite-difference discretization involves the numerical fourth-order diffusion $(\nu h^2/24) n_{xxxx} \approx 10^{-10} n_{xxxx}$.
The expansions for the terms of (3.30) read as follows:

$$\begin{aligned}\Big(\frac{J^2}{n}\Big)_x(x_{i-1/2}) &= \frac{1}{4h}\Big(\frac{(J_{i+1/2} + J_{i-1/2})^2}{n_i} - \frac{(J_{i-1/2} + J_{i-3/2})^2}{n_{i-1}}\Big) \\ &\quad + \frac{h^2}{24}\Big(\frac{J^2}{n}\Big)_{xxx}(x_{i-1/2}) + O(h^3), \\ n_x(x_{i-1/2}) &= \frac{1}{h}(n_i - n_{i-1}) - \frac{h^2}{24} n_{xxx}(x_{i-1/2}) + O(h^4), \\ \varepsilon^2\big(n(\log n)_{xx}\big)_x(x_{i-1/2}) &= \frac{\varepsilon^2}{h^3}\Big(n_i \log\Big(\frac{n_{i+1} n_{i-1}}{n_i^2}\Big) - n_{i-1}\log\Big(\frac{n_i n_{i-2}}{n_{i-1}^2}\Big)\Big) \\ &\quad + \frac{\varepsilon^2 h^2}{24} n_{xxx}(x_{i-1/2}) + O(h^3), \\ \nu J_{xx}(x_{i-1/2}) &= \frac{\nu}{h^2}(J_{i+1/2} - 2J_{i-1/2} + J_{i-3/2}) \\ &\quad - \frac{\nu^2 h^2}{12} n_{xxxxx}(x_{i-1/2}) + O(h^4).\end{aligned}$$

Thus we obtain a numerical dispersion at most of order $(h^2/24) n_{xxx} \approx 10^{-7} n_{xxx}$ which is much smaller than the physical dispersion being of order $\varepsilon^2 n_{xxx} \approx 10^{-4} n_{xxx}$.
In a similar way, one can show that the numerical viscosity and diffusion in the central discretization of (3.31) is of order $h^2 = 10^{-6}$ and therefore much smaller than ε^2 and ν. Therefore, we expect that the numerical error of the central scheme is rather small. This expectation will be verified numerically in Section 3.3.3.
Next, we turn to the upwind discretization of Gardner's QHD model. The main error comes from the discretization of the advection terms which are

only of order one. Setting $u_j^+ = \max\{u(x_j), 0\}$ and $u_j^- = -\min\{u(x_j), 0\}$, we can write the upwind discretization A_1 of $(nu)_x(x_i)$ (see (3.40)) as

$$\begin{aligned}
A_1 &= \frac{1}{h}\big((u^+_{i+1/2}n_i - u^-_{i+1/2}n_{i+1}) - (u^+_{i-1/2}n_{i-1} - u^-_{i-1/2}n_i)\big)\\
&= \frac{1}{h}\big(- u^-_{i+1/2}n_{i+1} + (u^+_{i+1/2} + u^-_{i-1/2})n_i - u^+_{i-1/2}n_{i-1}\big)\\
&= \frac{1}{h}(u_{i+1/2}n_{i+1/2} - u_{i-1/2}n_{i-1/2})\\
&\quad - \frac{1}{h}u^+_{i+1/2}(n_{i+1/2} - n_i) - \frac{1}{h}u^-_{i+1/2}(n_{i+1} - n_{i+1/2})\\
&\quad + \frac{1}{h}u^+_{i-1/2}(n_{i-1/2} - n_{i-1}) + \frac{1}{h}u^-_{i-1/2}(n_i - n_{i-1/2}).
\end{aligned}$$

The central discretization of n_{xx} gives

$$n_{i+1/2} - n_i = \frac{1}{2}(n_{i+1} - n_i) + \frac{h^2}{8}n_{xx}(x_{i+1/2}) + O(h^4),$$

and hence, we obtain

$$\begin{aligned}
A_1 &= \frac{1}{h}(u_{i+1/2}n_{i+1/2} - u_{i-1/2}n_{i-1/2})\\
&\quad - \frac{1}{2h}\big(|u_{i+1/2}|(n_{i+1} - n_i) - |u_{i-1/2}|(n_i - n_{i-1})\big)\\
&\quad - \frac{h}{8}\big(u_{i+1/2}n_{xx}(x_{i+1/2}) - u_{i-1/2}n_{xx}(x_{i-1/2})\big) + O(h^3).
\end{aligned}$$

A Taylor expansion shows that this expression can be written as

$$A_1 = (un)_x(x_i) - \frac{h}{2}(|u|n_x)_x(x_i) + O(h^2).$$

The upwind discretization A_2 of $(nu^2)_x(x_{i+1/2})$ (see (3.41)) can be written as

$$\begin{aligned}
A_2 &= \frac{1}{h}(n_{i+1}u^2_{i+1} - n_iu^2_i) + \big(u_{i+1}((nu)^{\mathrm{up}}_{i+1} - n_{i+1}u_{i+1}) - u_i((nu)^{\mathrm{up}}_i - n_iu_i)\big)\\
&= \frac{1}{h}(n_{i+1}u^2_{i+1} - n_iu^2_i) - \frac{B}{h},
\end{aligned}$$

where

$$\begin{aligned}
B &= u^+_{i+1}\Big(n_{i+1}u_{i+1} - \frac{1}{2}(n_{i+1} + n_i)u_{i+1/2}\Big)\\
&\quad - u^-_{i+1}\Big(n_{i+1}u_{i+1} - \frac{1}{2}(n_{i+2} + n_{i+1})u_{i+3/2}\Big)\\
&\quad - u^+_i\Big(n_iu_i - \frac{1}{2}(n_i + n_{i-1})u_{i-1/2}\Big) + u^-_i\Big(n_iu_i - \frac{1}{2}(n_{i+1} + n_i)u_{i+1/2}\Big).
\end{aligned}$$

Employing the approximation $u_i = (u_{i+1/2} + u_{i-1/2})/2 + u''(x_i)h^2/4 + O(h^3)$ and the relation $u^{\pm} = (|u| \pm u)/2$, we obtain after some tedious computations

$$\begin{aligned} B = \frac{1}{4}\Big(& |u_{i+1}|\big((n_{i+1}+n_{i+2})u_{i+3/2} - (n_{i+1}+n_i)u_{i+1/2}\big) \\ & - |u_i|\big((n_{i+1}+n_i)u_{i+1/2} - (n_i+n_{i-1})u_{i-1/2}\big)\Big) \\ & + \frac{1}{4}\Big(u_{i+1}\big((n_{i+1}-n_i)u_{i+1/2} - (n_{i+2}-n_{i+1})u_{i+3/2}\big) \\ & - u_i\big((n_i-n_{i-1})u_{i-1/2} - (n_{i+1}-n_i)u_{i+1/2}\big)\Big) + O(h^3). \end{aligned}$$

This term is a central finite-difference approximation of

$$h^2(|u|(nu)_x)_x + h^3(u(un_x)_x)_x \quad \text{at } x = x_{i+1/2}$$

such that

$$A_2 = (nu^2)_x(x_{i+1/2}) + h(|u|(nu)_x)_x(x_{i+1/2}) + O(h^2).$$

The above calculations show that the upwind scheme introduces diffusion terms for the variables n and nu (with diffusion coefficient $|u|$) being of the order $h = 10^{-3}$. Since the scaled velocity $|u|$ has numerically values of the order 10^3 (or larger), the artificial diffusion term is of the order $O(1)$ which is much larger than the physical diffusion being of the order $\nu = 10^{-2}$.

3.3.3 Numerical simulations of a resonant tunneling diode

The numerical scheme of Section 3.3.1 is used to simulate a simple one-dimensional resonant tunneling diode. We choose the same geometry and data as in [47]. More precisely, our resonant tunneling diode of interest consists of highly doped GaAs regions near the contacts and a lightly doped middle region of 25 nm length (see Figure 3.1). The middle region contains a quantum well of 5 nm length sandwiched between two 5 nm AlGaAs barriers. The double barrier heterostructure is placed between two 10 nm GaAs spacer layers with a doping of $5{\cdot}10^{15}\,\mathrm{cm}^{-3}$. These spacers are enclosed by two layers of 50 nm length and with doping $10^{18}\,\mathrm{cm}^{-3}$. The total length is thus 125 nm and the double barrier height is 0.209 eV. The barriers are modeled by an additional step function V_{ext} added to the electric potential. The physical constants are summarized in Table 3.1.
Gardner [47] has added the heat flux term $k_B\sigma(nT_x)_x$ to the right-hand side of the equation for the energy, where $\sigma = \kappa\tau_0 k_B T_0/m$ and $\kappa = 0.2$ is the thermal conductivity, for numerical stability. This term is *not* needed in

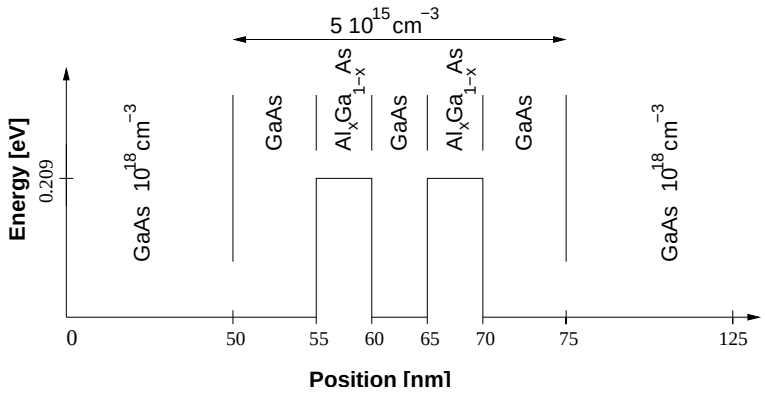

Figure 3.1: Geometry of the resonant tunneling diode with Al mole fraction $x = 0.3$.

Parameter	Physical meaning	Numerical value
q	elementary charge	$1.602 \cdot 10^{-19}$ As
m_{eff}	effective electron mass	$0.067 \cdot 9.11 \cdot 10^{-31}$ kg
m_0	electron mass at rest	$9.11 \cdot 10^{-31}$ kg
k_B	Boltzmann constant	$1.380 \cdot 10^{-23}$ J/K
$\hbar$	reduced Planck constant	$1.055 \cdot 10^{-34}$ Js
ε_S	semiconductor permittivity	$1.012 \cdot 10^{-10}$ As/Vm
T_0	lattice temperature	77 K
τ_0	momentum relaxation time	$0.9 \cdot 10^{-12}$ s
ν	viscosity	$1.589 \cdot 10^{-5}$m^2/s^2

Table 3.1: Physical parameters and their numerical values.

the numerical solution of the viscous QHD equations, but we used it in the solution of Gardner's QHD model. We notice that the expressions for the momentum relaxation and energy relaxation terms are different in Gardner's QHD model. We use the same values as in [47].
First, we present numerical results for the isothermal model (3.29), (3.30), (3.32) with constant lattice temperature $T = 77\,\text{K}$ in order to test our numerical algorithm. The stationary numerical solution was already calculated in [72] such that our results can be compared to results shown there. More precisely, in [72] the one-dimensional transient equations have been numerically discretized using a central finite-difference scheme in space and a second-order Runge-Kutta method in time, and stationary solutions are obtained by letting numerically $t \to \infty$. The disadvantage of this strategy

is that the scheme is extremely time consuming, even in one space dimension. Here we discretize directly the stationary equations using central finite differences and solve the resulting nonlinear system with a damped Newton method.
Current-voltage characteristics for the resonant tunneling diode described above are displayed in Figures 3.2 and 3.3. We observe several regions of negative differential resistance (NDR) characterizing the tunneling diode. The curve becomes "smoother" for larger values of the viscosity constant which is expected physically. However, there is a jump of the current density to a larger value after each local minimum; this jump seems to be not physical since in experiments [**74**], as well as in numerical simulations using the Schrödinger equation (see, e.g., [**38**]), sharp gradients are observed just after the current peaks. A possible explanation, already given in [**72**], is that the energy equation needs to be taken into account and that will be done below.

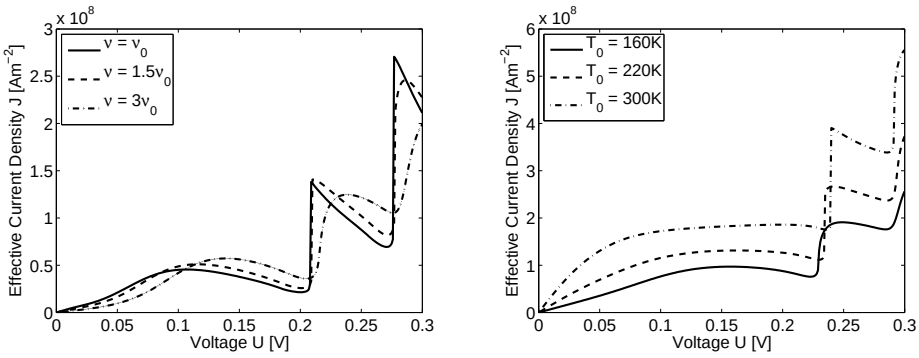

Figure 3.2: Current-voltage characteristics of a tunneling diode for various values of the viscosity with $\nu_0 = 1.589 \cdot 10^{-5}\,\mathrm{m}^2/\mathrm{s}^2$ (left) and various values of the lattice temperature (right), computed from the isothermal model.

In Figure 3.3 the current-voltage curves for various values of the effective mass constant α with $m_{\mathrm{eff}} = \alpha \cdot m_0$ are shown. The peak-to-valley ratios are given in Table 3.2.
Next, we turn to the numerical results obtained from the nonisothermal model (3.29)-(3.32). In Figure 3.4 the current-voltage characteristics are shown with lattice temperature $T_0 = 77\,\mathrm{K}$. In order to obtain NDR effects, we need to choose a smaller relaxation time than that taken in the isothermal model. The peak-to-valley ratio is too small compared to experiments which may be due to the viscosity. Again, for larger viscosity constants, the current-voltage curves become "smoother". Numerical difficulties (sup-

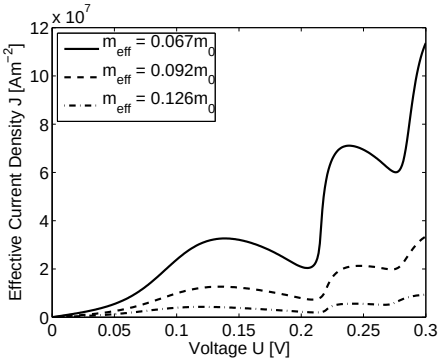

Figure 3.3: Current-voltage characteristics of a tunneling diode for various values of the effective mass computed from the isothermal model.

Effective mass	First ratio	Second ratio
$0.067\,\mathrm{m}_0$	1.750	1.180
$0.092\,\mathrm{m}_0$	1.707	1.086
$0.126\,\mathrm{m}_0$	2.205	1.108

Table 3.2: Peak-to-valley ratios from Figure 3.3 for different effective masses.

ported by the analytical estimates of Section 3.2) do not allow to perform numerically the inviscid limit $\nu \to 0$. Interestingly, the current-voltage curve shows a plateau-like behavior (see the zoom in Figure 3.5) which can be also observed experimentally [**18, 73**].

In Figure 3.6, the electron densities for the isothermal and nonisothermal model at the peak and valley current values are displayed. For the nonisothermal model, the data corresponds to the dashed curve in Figure 3.4 (left). The electron density shows a charge enhancement in the quantum well which is more pronounced in the isothermal model. At the center of the right barrier, the electron density dramatically decreases. At the peak current (left figure), the density from the isothermal model develops a "wiggle". This phenomenum is not a numerical effect since it has been observed in various numerical simulations [**72, 87**]. This "wiggle" disappears at the valley current where the density becomes very small (right figure). The electron density from the nonisothermal model is "smoother" and its minimum is larger than in the isothermal model, which stabilizes the numerical scheme.

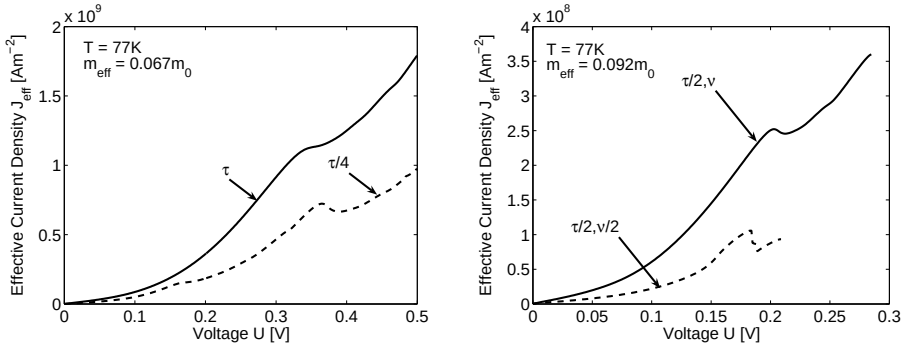

Figure 3.4: Current-voltage characteristics of a tunneling diode computed from the nonisothermal model with relaxation time $\tau = 0.9\,\mathrm{ps}$ and viscosity $\nu = 1.589 \cdot 10^{-5}\,\mathrm{m}^2/\mathrm{s}^2$.

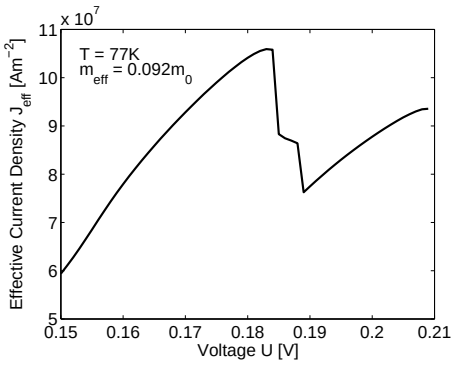

Figure 3.5: Zoom of Figure 3.4.

Next, we investigate the influence of the lattice temperature (see Figure 3.7). In order to compute the solution for $T_0 = 200\,\mathrm{K}$ and $T_0 = 300\,\mathrm{K}$ we needed a larger viscosity constant, namely 5ν. We see that there is no NDR region, even not for small lattice temperature. It seems that the viscosity dominates the quantum effects.

Finally, we notice that the number of discretization points influences the solution behavior only slightly (Figure 3.8) which is to be expected since the central scheme is of second order. On the other hand, due to the numerical viscosity introduced by the upwind scheme, the solution of Gardner's QHD model depends rather strongly on the mesh size. Moreover, as it will also be noticed in the Section 4.5, the slope of the curve in Gardner's model becomes steeper just after the first valley when the number of grid points is

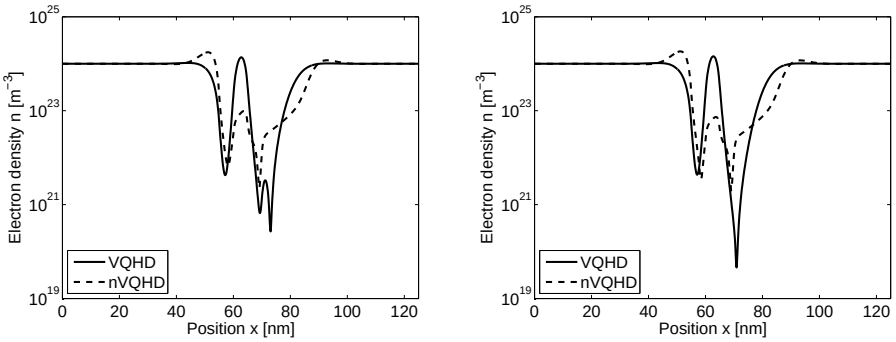

Figure 3.6: Electron density versus position with relaxation time $\tau/4 = 0.225\,\mathrm{ps}$ at the peak (left) and valley (right) current.

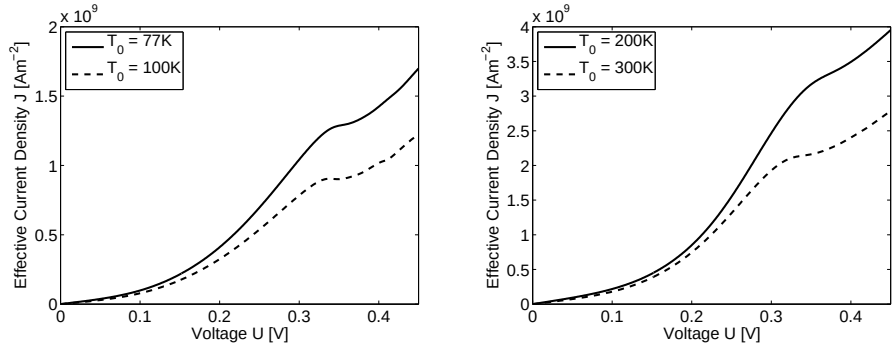

Figure 3.7: Current-voltage characteristics of a tunneling diode computed from the nonisothermal model for various values of the lattice temperature (left: $\nu = 1.589 \cdot 10^{-5}\,\mathrm{m}^2/\mathrm{s}^2$; right: $\nu = 5 \cdot 1.589 \cdot 10^{-5}\,\mathrm{m}^2/\mathrm{s}^2$).

larger. This behavior is not observed in the viscous QHD model thanks to the physical viscosity.

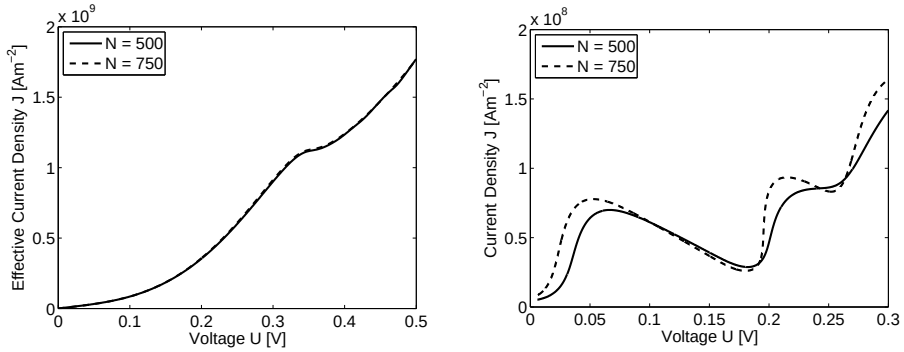

Figure 3.8: Influence of the number of discretization points on the current-voltage characteristics computed from the nonisothermal model (left) and from Gardner's QHD model (right).

Chapter 4

QHD models using BGK-type operator

In Chapter 3 we have derived the quantum hydrodynamic equations by moment method using the Wigner's approximation of the quantum thermal equilibrium as a closure condition. In this chapter we present another closure ansatz. More precisely, for the thermal equilibrium function we take the solution of the constrained quantum entropy minimization problem. This approach is based on Levermore's methodology for classical case [**78**], while the generalization on quantum systems has been done by Degond and Ringhofer in [**36**]. The chapter is organized as follows. In Section 4.1 we specify the definition of the quantum Maxwellian which is used as the closure in the moment method developed in Section 4.2. Furthermore, the same section gives the detailed derivation of the new quantum hydrodynamic model (in the text also called the generalized quantum hydrodynamic model). It follows Section 4.3, devoted to the simplified models. In Section 4.4 we prove that the energy of the system is conserved. Finally, in Section 4.5, the new quantum hydrodynamic model is numerically discretized and solved in one space dimension. Moreover, simulations of a resonant tunneling diode are presented.

4.1 Definition of the quantum Maxwellian

In order to define the quantum Maxwellian, we first recall the Wigner transform. Let A_ρ be an operator on $L^2(\mathbb{R}^d)$ with integral kernel $\rho(x, x')$, i.e.

$$(A_\rho \phi)(x) = \int_{R^d} \rho(x, x')\phi(x')dx' \quad \text{for all } \phi \in L^2(\mathbb{R}^d).$$

The Wigner transform of A_ρ is defined by

$$W(A_\rho)(x,p) = \frac{1}{(2\pi)^d}\int_{\mathbb{R}^d} \rho\Big(x+\frac{\varepsilon}{2}\eta, x-\frac{\varepsilon}{2}\eta\Big)e^{i\eta\cdot p}d\eta.$$

Its inverse W^{-1}, also called Weyl quantization, is defined as an operator on $L^2(\mathbb{R}^d)$:

$$(W^{-1}(f)\phi)(x) = \int_{\mathbb{R}^{2d}} f\Big(\frac{x+y}{2},p\Big)\phi(y)e^{ip\cdot(x-y)/\varepsilon}dpdy \quad \text{for all } \phi\in L^2(\mathbb{R}^d).$$

With these definitions we are able to introduce the *quantum exponential* and the *quantum logarithm* formally by

$$\operatorname{Exp} f = W(\exp W^{-1}(f)), \quad \operatorname{Log} f = W(\log W^{-1}(f)),$$

where exp and log are the operator exponential and logarithm, respectively. In [**34**] it has been (formally) shown that the quantum exponential and quantum logarithm are equal to the usual exponential and logarithm, respectively, up to order $O(\varepsilon^2)$,

$$\operatorname{Exp} f = \exp f + O(\varepsilon^2), \quad \operatorname{Log} f = \log f + O(\varepsilon^2). \tag{4.1}$$

The essential ingredient in the definition of the quantum Maxwellian is the relative quantum entropy. Let a quantum mechanical state be described by the Wigner function f solving the Wigner equation (1.14). Then its *relative quantum (von Neumann) entropy* is given by [**36**]

$$H(f) = \int_{\mathbb{R}^{2d}} f(x,p)\Big((\operatorname{Log} f)(x,p) - 1 + \frac{|p|^2}{2} - V(x)\Big)dxdp.$$

Whereas the classical entropy is a function on the configuration space, the above quantum entropy is a real number, underlining the non-local nature of quantum mechanics.

We define the quantum thermal equilibrium or *quantum Maxwellian* M_f for some given function $f(x,p)$ as the solution of the constrained minimization problem

$$H(M_f) = \min\left\{H(\hat{f}) : \int_{\mathbb{R}^d}\hat{f}(x,p,t)\begin{pmatrix}1\\ p\\ |p|^2/2\end{pmatrix}dp = \begin{pmatrix}n(x,t)\\ nu(x,t)\\ e(x,t)\end{pmatrix}\right\}, \tag{4.2}$$

where $x \in \mathbb{R}^d,\ t > 0$ and

$$\begin{aligned} n(x,t) &= \langle 1 \rangle(x,t) = \int_{\mathbb{R}^d} f(x,p,t)dp, \\ nu(x,t) &= \langle p \rangle(x,t) = \int_{\mathbb{R}^d} f(x,p,t)pdp, \\ e(x,t) &= \frac{1}{2}\langle |p|^2 \rangle(x,t) = \frac{1}{2}\int_{\mathbb{R}^d} f(x,p,t)|p|^2 dp. \end{aligned}$$

In [36] it is shown that the solution f^* of the constrained minimization problem (if it exists) is given by

$$M_f(x,p,t) = \mathrm{Exp}\left(A(x,t) - \frac{|p - w(x,t)|^2}{2T(x,t)}\right). \tag{4.3}$$

The Lagrange multipliers A, w, and T are uniquely determined by the moments of f. They correspond in the classical setting to the logarithm of the particle density, the velocity, and the temperature, respectively (see Lemma 4.4).

4.2 Derivation of the general QHD model

The derivation of the general QHD equations is done in several steps. First, we derive the moment equations. Then the quantum exponential is expanded in powers of ε^2 up to order $O(\varepsilon^4)$. The third step is to expand the moments accordingly. Finally, the expansions are substituted into the moment equations.

4.2.1 Moment equations

We consider the Wigner-Boltzmann equation (1.14) in the hydrodynamic scaling, i.e., we introduce the scaling

$$x' = \delta x, \quad t' = \delta t,$$

for some parameter $\delta > 0$ which is assumed to be small compared to one. Then (1.14) becomes for $f = f_\delta$ (omitting the primes)

$$\partial_t f_\delta + p \cdot \nabla_x f_\delta + \theta[V] f_\delta = \delta^{-1} Q(f_\delta), \quad (x,p) \in \mathbb{R}^{2d},\ t > 0, \tag{4.4}$$

with initial condition $f_\delta(x,p,0) = f_I(x,p)$. We assume that the collision operator has the following properties: Its kernel consists exactly of (multiples

of) M_f and

$$\int_{\mathbb{R}^d} Q(f)dp = 0, \quad \int_{\mathbb{R}^d} Q(f)pdp = 0, \quad \int_{\mathbb{R}^d} Q(f)\tfrac{1}{2}|p|^2dp = 0, \tag{4.5}$$

for all $f(x,p)$. An example satisfying these conditions is the relaxation-time or "BGK" operator $Q(f) = M_f - f$ (with scaled relaxation time $\tau = 1$) [**16**]. A more general collision operator, allowing for relaxation-time terms in the macroscopic equations, can be defined as follows. Assume that the collision operator can be written as $Q(f) = Q_0(f) + \delta Q_1(f)$, where the operator $Q_0(f)$ models elastic collisions and satisfies the conditions (4.5), and $Q_1(f)$ is given by the Caldeira-Leggett operator [**23**] (mentioned in Section 1.3, expression (1.17))

$$Q_1(f) = \frac{1}{\tau_p}(\mathrm{div}_p(pf) + \Delta_p f),$$

modeling inelastic collisions and τ_p is the momentum relaxation time. Then

$$\begin{aligned} \int_{\mathbb{R}^d} Q_1(f)dp = 0, \quad \int_{\mathbb{R}^d} Q_1(f)pdp = -\frac{nu}{\tau_p}, \\ \int_{\mathbb{R}^d} Q_1(f)\tfrac{1}{2}|p|^2dp = -\frac{2}{\tau_p}\Big(e - \frac{d}{2}n\Big), \end{aligned} \tag{4.6}$$

which is (a special case of) the momentum and energy relaxation-time terms employed in [**47**].

The formal limit $\delta \to 0$ in (4.4) yields $Q(f) = 0$, where $f = \lim_{\delta\to 0} f_\delta$, which implies that the limit f is equal to M_f. The moment equations are obtained from (4.4) by multiplication with 1, p, and $\frac{1}{2}|p|^2$, respectively, and integration over the momentum space. Since

$$\int_{\mathbb{R}^d} \theta[V]f dp = 0, \quad \int_{\mathbb{R}^d} \theta[V]fpdp = -n\nabla V, \quad \int_{\mathbb{R}^d} \theta[V]f\tfrac{1}{2}|p|^2dp = -nu\cdot\nabla V$$

(see, e.g., [**34**]), we obtain

$$\partial_t n + \mathrm{div}(nu) = 0, \tag{4.7}$$

$$\partial_t(nu) + \mathrm{div}\langle p\otimes p\rangle - n\nabla V = 0, \tag{4.8}$$

$$\partial_t e + \mathrm{div}\langle \tfrac{1}{2}|p|^2 p\rangle - nu\cdot\nabla V = 0, \tag{4.9}$$

where $(p\otimes p)_{ij} = p_i p_j$ for $i,j = 1,\dots,d$. Recall that the brackets denote integration against the Wigner function $f = M_f$, i.e. in multi-index notation,

$$\langle p^\alpha\rangle(x,t) = \int_{\mathbb{R}^d} M_f(x,p,t)p^\alpha dp,$$

for multi-indices $\alpha \in \mathbb{N}^d$. When employing the Caldeira-Leggett operator defined above, the right-hand sides of (4.7)-(4.9) equal the right-hand sides of (4.6). To close the system (4.7)-(4.9), we need to express the integrals $\langle p \otimes p \rangle$ and $\langle \frac{1}{2}|p|^2 p \rangle$ in terms of the moments n, nu, and e. This constitutes the main step of the derivation.
The following computations are simplified by working with the new variable $s = T^{-1/2}(p - w)$, where w is the Lagrange multiplier introduced in (4.3). In terms of s, the quantum Maxwellian reads as

$$M_f(x, p(s)) = \mathrm{Exp}\left(A(x) - \frac{1}{2}|s|^2\right) =: g(x, s).$$

From now on, we omit the dependence of the time t since it acts only as a parameter. The substitution $p \mapsto s$ yields

$$\langle s^\alpha \rangle(x) = T^{d/2} \int_{\mathbb{R}^d} g(x, s) s^\alpha ds.$$

In the following lemma we express the moments $\langle p^\alpha \rangle$ in terms of moments in s. This allows for a more canonical form of the QHD equations.

Lemma 4.1. *The system (4.7)-(4.9) is equivalent to*

$$\begin{aligned} \partial_t n + \mathrm{div}(nu) &= 0, && (4.10)\\ \partial_t (nu) + \mathrm{div}(nu \otimes u) + \mathrm{div}\, P - n\nabla V &= 0, && (4.11)\\ \partial_t e + \mathrm{div}\big((P + eI)u\big) + \mathrm{div}\, S - nu \cdot \nabla V &= 0, && (4.12) \end{aligned}$$

where I is the identity matrix, $u = (nu)/n$, $P = \langle (p-u) \otimes (p-u) \rangle$ is the stress tensor, and $S = \langle \frac{1}{2}(p-u)|p-u|^2 \rangle$ is the (quantum) heat flux. Moreover, the following expansions holds:

$$P = T\langle s \otimes s \rangle + O(\varepsilon^4), \quad S = \frac{1}{2} T^{3/2} \langle |s|^2 s \rangle - \Big(\frac{d}{2} + 1\Big) T^{3/2} \langle s \rangle + O(\varepsilon^4). \quad (4.13)$$

Proof. The formulation (4.10)-(4.12) follows immediately from (4.7)-(4.9) since

$$\langle p \otimes p \rangle = P + nu \otimes u \quad \text{and} \quad \langle \tfrac{1}{2}|p|^2 p \rangle = S + (P + eI)u.$$

Using the expansion (4.1), elementary integrations yield for $i, j = 1, \ldots, d$,

$$\begin{aligned} \langle 1 \rangle &= T^{d/2} e^A \int_{\mathbb{R}^d} e^{-|s|^2/2} ds + O(\varepsilon^2) = (2\pi T)^{d/2} e^A + O(\varepsilon^2), && (4.14)\\ \langle s_i \rangle &= T^{d/2} e^A \int_{\mathbb{R}^d} e^{-|s|^2/2} s_i ds + O(\varepsilon^2) = O(\varepsilon^2), && (4.15)\\ \langle s_i s_j \rangle &= T^{d/2} e^A \int_{\mathbb{R}^d} e^{-|s|^2/2} s_i s_j ds + O(\varepsilon^2) = n\delta_{ij} + O(\varepsilon^2). && (4.16) \end{aligned}$$

The relations $n = \langle 1\rangle$, $\langle w\rangle = w\langle 1\rangle = nw$, and $nu = \langle p\rangle = \langle T^{1/2}s + w\rangle = T^{1/2}\langle s\rangle + nw$ give for the second moments

$$\begin{aligned}\langle p\otimes p\rangle &= T\langle s\otimes s\rangle + \Big\langle (T^{1/2}s+w)\otimes(T^{1/2}s+w) - (T^{1/2}s)\otimes(T^{1/2}s)\Big\rangle \\ &= T\langle s\otimes s\rangle + T^{1/2}\langle s\rangle\otimes w + T^{1/2}w\otimes\langle s\rangle + w\otimes w\langle 1\rangle \\ &= T\langle s\otimes s\rangle + \frac{1}{n}\langle T^{1/2}s+w\rangle\otimes\langle T^{1/2}s+w\rangle - \frac{T}{n}\langle s\rangle\otimes\langle s\rangle \\ &= T\langle s\otimes s\rangle + nu\otimes u + O(\varepsilon^4),\end{aligned}$$

where in the last equality we have employed (4.15). Therefore, $P = \langle p\otimes p\rangle - nu\otimes u = T\langle s\otimes s\rangle + O(\varepsilon^4)$. In a similar way, we compute the third moment:

$$\begin{aligned}\frac{1}{2}\langle |p|^2 p\rangle &= \frac{1}{2}T^{1/2}\langle |T^{1/2}s+w|^2 s\rangle + \frac{1}{2}w\langle |p|^2\rangle \\ &= \frac{1}{2}T^{3/2}\langle |s|^2 s\rangle + T\langle s\otimes s\rangle w + \frac{1}{2}T^{1/2}|w|^2\langle s\rangle + ew \\ &= \frac{1}{2}T^{3/2}\langle |s|^2 s\rangle + (P+eI)w + \frac{1}{2}T^{1/2}|w|^2\langle s\rangle.\end{aligned}$$

By (4.14) and (4.15), the energy density can be expanded as

$$e = \frac{1}{2}\langle |p|^2\rangle = \frac{T}{2}\langle |s|^2\rangle + T^{1/2}w\cdot\langle s\rangle + \frac{1}{2}|w|^2\langle 1\rangle = \frac{d}{2}nT + \frac{1}{2}n|w|^2 + O(\varepsilon^2).$$

Thus, since $w = u - T^{1/2}\langle s\rangle/n$ and $P = nTI + O(\varepsilon^2)$, we obtain

$$\begin{aligned}\frac{1}{2}\langle |p|^2 p\rangle &= \frac{1}{2}T^{3/2}\langle |s|^2 s\rangle + (P+eI)u - \frac{T^{1/2}}{n}\Big(P + eI - \frac{1}{2}n|w|^2 I\Big)\langle s\rangle \\ &= \frac{1}{2}T^{3/2}\langle |s|^2 s\rangle + (P+eI)u - \frac{T^{3/2}}{n}\Big(\Big(\frac{d}{2}+1\Big)nI + O(\varepsilon^2)\Big)\langle s\rangle.\end{aligned}$$

This shows that $S = \langle\frac{1}{2}|p|^2 p\rangle - (P+eI)u = \frac{1}{2}T^{3/2}\langle |s|^2 s\rangle - (d/2+1)T^{3/2}n\langle s\rangle + O(\varepsilon^4)$. □

4.2.2 Expansion of the quantum exponential

We wish to give asymptotic expansions of P, S, and U up to order $O(\varepsilon^4)$. For this, we first need to expand the quantum Maxwellian. This is done by means of the following lemma, which is adopted from [**36**].

Lemma 4.2. *Let $f(x,p)$ be a smooth symbol. Then the quantum exponential* $\operatorname{Exp} f$ *can be expanded as follows:*

$$\operatorname{Exp} f = e^f - \frac{\varepsilon^2}{8} e^f \mathcal{Q} + O(\varepsilon^4),$$

where, using Einstein's summation convention,

$$\begin{aligned}\mathcal{Q} &= \partial_{x_ix_j}^2 f\, \partial_{p_ip_j}^2 f - \partial_{x_ip_j}^2 f\, \partial_{p_ix_j}^2 f + \frac{1}{3}\partial_{x_ix_j}^2 f\, \partial_{p_i} f\, \partial_{p_j} f \\ &\quad - \frac{2}{3}\partial_{x_ip_j}^2 f\, \partial_{p_i} f\, \partial_{x_j} f + \frac{1}{3}\partial_{p_ip_j}^2 f\, \partial_{x_i} f\, \partial_{x_j} f. \end{aligned} \tag{4.17}$$

In the situation at hand, the symbol is $f(x,p) = A(x) - |p - w(x)|^2/2T(x)$. Then we obtain the following result.

Lemma 4.3. *The quantum correction (4.17) can be written for $f(x,p) = A(x) - |p - w(x)|^2/2T(x)$ as follows:*

$$\begin{aligned}\mathcal{Q}(s) &= T^{-1}\big(X^0 + X_i^1 s_i + X_{ij}^2 s_i s_j + X_{ijk}^3 s_i s_j s_k \\ &\quad + Y^0|s|^2 + Y_i^1|s|^2 s_i + Y_{ij}^2|s|^2 s_i s_j + Z^0|s|^4\big), \end{aligned} \tag{4.18}$$

where the coefficients X^i, Y^i, and Z are defined by

$$\begin{aligned}
X^0 &= -\Delta A - \frac{1}{3}|\nabla A|^2 + \frac{1}{2T}\operatorname{tr}(\widetilde{R}^\top \widetilde{R}), \\
X_i^1 &= \frac{2}{T^{1/2}}\partial_{x_m}\Big(\frac{1}{3}A - \log T\Big)\widetilde{R}_{mi} - \frac{1}{\sqrt{T}}\Delta w_i, \\
X_{ij}^2 &= \frac{1}{3}\partial_{x_ix_j}^2 A + \frac{2}{3}\partial_{x_i}(\log T)\partial_{x_j} A - \partial_{x_i}(\log T)\partial_{x_j}(\log T) - \frac{1}{3T}(\widetilde{R}^\top \widetilde{R})_{ij} \\
X_{ijk}^3 &= \frac{1}{3T^{1/2}}\partial_{x_ix_j}^2 w_k, \\
Y^0 &= \nabla\Big(\frac{1}{2}\log T - \frac{1}{3}A\Big)\cdot\nabla(\log T) - \frac{1}{2}\Delta(\log T), \\
Y_i^1 &= \frac{1}{3T^{1/2}}\partial_{x_m}(\log T)\widetilde{R}_{mi}, \\
Y_{ij}^2 &= \frac{1}{6}\Big(\partial_{x_ix_j}^2(\log T) + \partial_{x_i}(\log T)\partial_{x_j}(\log T)\Big), \\
Z^0 &= -\frac{1}{12}|\nabla(\log T)|^2,
\end{aligned}$$

and $\widetilde{R}_{ij} = \partial_{x_j} w_i - \partial_{x_i} w_j$. The symbol "tr" denotes the trace of a matrix.

Proof. The proof consists in computing the relevant derivatives of f with respect to x_i and p_j, namely

$$\begin{aligned}
\partial_{x_i} f &= \partial_{x_i} A + T^{-1}\partial_{x_i} w_k (p-w)_k + \frac{1}{2} T^{-2}\partial_{x_i} T |p-w|^2 \\
&= \partial_{x_i} A + T^{-1/2}\partial_{x_i} w_k s_k + \frac{1}{2} T^{-1}\partial_{x_i} T |s|^2, \\
\partial^2_{x_i x_j} f &= \partial^2_{x_i x_j} A - T^{-1}\partial_{x_i} w_k \partial_{x_j} w_k - T^{-2}\partial_{x_j} T \partial_{x_i} w_k (p-w)_k + T^{-1}\partial^2_{x_i x_j} w_k (p-w)_k \\
&\quad - T^{-2}\partial_{x_i} T \partial_{x_j} w_k (p-w)_k - T^{-3}\partial_{x_i} T \partial_{x_j} T |p-w|^2 + \frac{1}{2} T^{-2}\partial^2_{x_i x_j} T |p-w|^2 \\
&= \partial^2_{x_i x_j} A - T^{-1}\partial_{x_i} w_k \partial_{x_j} w_k - T^{-3/2}\partial_{x_j} T \partial_{x_i} w_k s_k + T^{-1/2}\partial^2_{x_i x_j} w_k s_k \\
&\quad - T^{-3/2}\partial_{x_i} T \partial_{x_j} w_k s_k - T^{-2}\partial_{x_i} T \partial_{x_j} T |s|^2 + \frac{1}{2} T^{-1}\partial^2_{x_i x_j} T |s|^2, \\
\partial_{p_i} f &= -T^{-1}(p-w)_i = -T^{-1/2} s_i, \\
\partial^2_{p_i x_j} f &= T^{-1}\partial_{x_j} w_i + T^{-2}\partial_{x_j} T (p-w)_i = T^{-1}\partial_{x_j} w_i + T^{-3/2}\partial_{x_j} T s_i, \\
\partial^2_{p_i p_j} f &= -T^{-1}\delta_{ij},
\end{aligned}$$

and the products appearing in the sum (4.17), which are

$$\begin{aligned}
\partial^2_{x_i x_j} f \, \partial^2_{p_i p_j} F &= \left(-T^{-1}\Delta A - T^{-3/2}\Delta w_k + T^{-2}\|\nabla w\|^2 + 2T^{-5/2}\nabla T \cdot \nabla w_k\right) s_k \\
&\quad + \left(\frac{1}{2} T^{-2}\Delta T - T^{-3}|\nabla T|^2\right) |s|^2, \\
\partial^2_{x_i p_j} f \, \partial^2_{p_i x_j} f &= T^{-2}\partial_{x_i} w_j \partial_{x_j} w_i + 2T^{-5/2}\partial_{x_j} T \partial_{x_i} w_j s_i + T^{-3}\partial_{x_i} T \partial_{x_j} T s_i s_j, \\
\partial^2_{x_i x_j} f \, \partial_{p_i} f \, \partial_{p_j} f &= \left(T^{-1}\partial^2_{x_i x_j} A - T^{-2}\partial_{x_i} w_\ell \partial_{x_j} w_\ell\right) s_i s_j \\
&\quad + \left(T^{-3/2}\partial^2_{x_i x_j} w_k - 2T^{-5/2}\partial_{x_i} T \partial_{x_j} w_k\right) s_i s_j s_k \\
&\quad + \left(\frac{1}{2} T^{-2}\partial^2_{x_i x_j} T - T^{-3}\partial_{x_i} T \partial_{x_j} T\right) |s|^2 s_i s_j, \\
\partial^2_{x_i p_j} f \, \partial_{p_i} f \, \partial_{x_j} f &= -T^{-3/2}\partial_{x_\ell} A \partial_{x_i} w_\ell s_i - T^{-2}\partial_{x_i} T \partial_{x_j} A s_i s_j - T^{-2}\partial_{x_i} w_j \partial_{x_j} w_k s_i s_k \\
&\quad - T^{-5/2}\partial_{x_i} T \partial_{x_j} w_k s_i s_j s_k - \frac{1}{2} T^{-5/2}\partial_{x_i} w_j \partial_{x_j} T |s|^2 s_i \\
&\quad - \frac{1}{2} T^{-3}\partial_{x_i} T \partial_{x_j} T |s|^2 s_i s_j, \\
\partial^2_{p_i p_j} f \, \partial_{x_i} f \, \partial_{x_j} f &= -T^{-1}|\nabla A|^2 - 2T^{-3/2}\nabla A \cdot \nabla w_k s_k - T^{-2}\nabla A \cdot \nabla T |s|^2 \\
&\quad - T^{-2}\nabla w_k \cdot \nabla w_\ell s_k s_\ell - T^{-5/2}\nabla T \cdot \nabla w_k |s|^2 s_k - \frac{1}{4} T^{-3}|\nabla T|^2 |s|^4.
\end{aligned}$$

Inserting these expressions into (4.17) and simplifying, we arrive at (4.18). □

4.2.3 Expansion of the moments

The aim of this subsection is to specify the integrals $\langle s^\alpha \rangle$ in order to expand the moments n, nu, and e. By Lemma 4.2, we obtain

$$\begin{aligned}\langle s^\alpha \rangle &= T^{d/2} \int_{\mathbb{R}^d} g(x,s) s^\alpha ds \\ &= T^{d/2} \int_{\mathbb{R}^d} e^{A-|s|^2/2} \Big(1 - \frac{\varepsilon^2}{8} \mathcal{Q}(s)\Big) s^\alpha ds + O(\varepsilon^4) \\ &= (2\pi T)^{d/2} e^A \Big([s^\alpha] - \frac{\varepsilon^2}{8} [\mathcal{Q}(s) s^\alpha] \Big) + O(\varepsilon^4),\end{aligned}$$

where $[g]$ denotes the integral of a function $g = g(s)$ against the classical Gaussian kernel,

$$[g] = (2\pi)^{-d/2} \int_{\mathbb{R}^d} e^{-|s|^2/2} g(s) ds.$$

Notice that from the expansion

$$n = \langle 1 \rangle = (2\pi T)^{d/2} e^A \Big(1 - \frac{\varepsilon^2}{8} [\mathcal{Q}(s)]\Big) + O(\varepsilon^4) \tag{4.19}$$

it follows that

$$\langle s^\alpha \rangle = n \Big([s^\alpha] + \frac{\varepsilon^2}{8} \Big([\mathcal{Q}(s)][s^\alpha] - [\mathcal{Q}(s) s^\alpha] \Big) \Big) + O(\varepsilon^4). \tag{4.20}$$

Thus it remains to calculate the integrals $[\mathcal{Q}(s) s^\alpha]$.
Integrals of type $[s^\alpha]$ can be computed explicitly. Using

$$\int_{\mathbb{R}} t^m e^{-t^2/2} dt = \sqrt{2\pi} \times \begin{cases} 0 & \text{if } m \text{ is odd} \\ 1 & \text{if } m = 0 \text{ or } m = 2 \\ 3 & \text{if } m = 4 \\ 15 & \text{if } m = 6, \end{cases}$$

it becomes a matter of combinatorics to conclude for i, j, m, $n = 1, \ldots, d$,

$$\begin{aligned}[s_i s_j] &= \delta_{ij}, \\ [|s|^2] &= d, \\ [s_i s_j s_m s_n] &= \delta_{ij}\delta_{mn} + \delta_{im}\delta_{jn} + \delta_{in}\delta_{jm}, \\ [s_i s_j |s|^2] &= (d+2)\delta_{ij}, \\ [|s|^4] &= d(d+2), \\ [s_i s_j s_m s_n |s|^2] &= (d+4)(\delta_{ij}\delta_{mn} + \delta_{im}\delta_{jn} + \delta_{in}\delta_{jm}), \\ [s_m s_n |s|^4] &= (d+2)(d+4)\delta_{mn}.\end{aligned}$$

Then the expansion of $\mathcal{Q}(s)$, given in (4.18), yields the following formulas:

$$\begin{aligned}
[\mathcal{Q}(s)] &= X^0 + \sum_\ell X^2_{\ell\ell} + dY^0 \\
&\quad + (d+2)\sum_\ell Y^2_{\ell\ell} + d(d+2)Z^0, && (4.21)\\
[\mathcal{Q}(s)s_m] &= X^1_m + \sum_\ell \big(X^3_{m\ell\ell} + X^3_{\ell m\ell} + X^3_{\ell\ell m}\big) + (d+2)Y^1_m, && (4.22)\\
[\mathcal{Q}(s)s_m^2] &= [\mathcal{Q}(s)] + 2X^2_{mm} + 2Y^0 + 2\sum_\ell Y^2_{\ell\ell} \\
&\quad + 2(d+4)Y^2_{mm} + 4(d+2)Z^0, && (4.23)\\
[\mathcal{Q}(s)s_m s_n] &= \big(X^2_{mn} + X^2_{nm}\big) + (d+4)\left(Y^2_{mn} + Y^2_{nm}\right), && (4.24)\\
[\mathcal{Q}(s)|s|^2 s_m] &= (d+2)X^1_m + (d+4)\sum_\ell \big(X^3_{m\ell\ell} + X^3_{\ell m\ell} + X^3_{\ell\ell m}\big) \\
&\quad + (d+2)(d+4)Y^1_m. && (4.25)
\end{aligned}$$

Lemma 4.4. *The moments n, nu, and e can be expressed in terms of the Lagrange multipliers A, w, and T asymptotically as follows:*

$$\begin{aligned}
n &= (2\pi T)^{d/2}e^A - \frac{\varepsilon^2}{24T}(2\pi T)^{d/2}e^A \\
&\quad \times \Big\{ -2\Delta A - |\nabla A|^2 + (d-2)\nabla\log T\cdot\nabla A - (d-1)\Delta\log T \\
&\quad - \Big(\frac{d}{2}-1\Big)\Big(\frac{d}{2}-2\Big)|\nabla\log T|^2 + \frac{1}{2T}\mathrm{tr}\,(\widetilde{R}^\top\widetilde{R})\Big\} + O(\varepsilon^4), && (4.26)\\
nu &= nw + T^{-1}U, && (4.27)\\
e &= \frac{d}{2}nT + \frac{1}{2}n|u|^2 - \frac{\varepsilon^2}{24}n\Big\{\Delta\log n - \frac{1}{T}\mathrm{tr}\,(\widetilde{R}^\top\widetilde{R}) + \frac{d}{2}|\nabla\log T|^2 \\
&\quad - \Delta\log T - \nabla\log T\cdot\nabla\log n\Big\} + O(\varepsilon^4). && (4.28)
\end{aligned}$$

Notice that (4.26) and (4.27) imply the inverse relations

$$A = \log n - \frac{d}{2}\log T - \frac{d}{2}\log(2\pi) + O(\varepsilon^2), \quad w = u + O(\varepsilon^2). \tag{4.29}$$

In particular, the vorticity matrices $\widetilde{R}$ and R, defined in (1.25), coincide up to order $O(\varepsilon^2)$ since $\widetilde{R}_{ij} = \partial_j u_i - \partial_i u_j + O(\varepsilon^2) = R_{ij} + O(\varepsilon^2)$.

Proof. The formula for the particle density (4.26) is obtained by first substituting the expressions for the coefficients X, Y, and Z into (4.21). This

yields $[\mathcal{Q}(s)]$ in terms of A, w, and T. Inserting the result into (4.19) then gives (4.26).
In order to derive (4.27), we write, by the definition of U (see (4.13)),

$$nu = \langle T^{1/2}s + w\rangle = T^{1/2}\langle s\rangle + w\langle 1\rangle = T^{-1}U + nw.$$

Hence, $u - w = U/nT = O(\varepsilon^2)$. The above equations also show that $T^{1/2}w \cdot \langle s\rangle = nu \cdot w - n|w|^2$. Hence, using $\langle 1\rangle = n$,

$$\begin{aligned} e &= \frac{1}{2}\langle |T^{1/2}s + w|^2\rangle = \frac{T}{2}\langle |s|^2\rangle + T^{1/2}w \cdot \langle s\rangle + \frac{1}{2}|w|^2\langle 1\rangle \\ &= \frac{T}{2}\langle |s|^2\rangle + nu \cdot w - \frac{1}{2}n|w|^2 = \frac{T}{2}\langle |s|^2\rangle + \frac{1}{2}n|u|^2 - \frac{1}{2}n|u - w|^2. \end{aligned}$$

In view of (4.29), we have $|u - w|^2 = O(\varepsilon^4)$ from which we conclude

$$e = \frac{T}{2}\langle |s|^2\rangle + \frac{1}{2}n|u|^2 + O(\varepsilon^4).$$

The bracket $\langle |s|^2\rangle$ can be computed from (4.20), employing $[|s|^2] = d$,

$$\langle |s|^2\rangle = dn + \frac{\varepsilon^2}{8}n\sum_m \big([\mathcal{Q}(s)] - [\mathcal{Q}(s)s_m^2]\big) + O(\varepsilon^4).$$

Substitution of (4.21) and (4.23) into the above expression and elimination of A and w using (4.29), gives $\langle |s|^2\rangle$ in terms of n, nu, and T. This finally leads to (4.28). □

4.2.4 Expansion of the terms P, S, and U

The QHD equations (4.10)-(4.12) are determined by the following expansion of the auxiliary terms P, S, and U, defined in (4.13), in terms of the macroscopic variables n, nu, and e.

Lemma 4.5. *The following expansion holds:*

$$\begin{aligned} P &= nTI + \frac{\varepsilon^2}{12}n\Big\{\Big(\frac{d}{2}+1\Big)\nabla\log T\otimes\nabla\log T - \nabla\log T\otimes\nabla\log n \\ &\quad - \nabla\log n\otimes\nabla\log T - (\nabla\otimes\nabla)\log(nT^2) + \frac{R^\top R}{T}\Big\} \qquad (4.30) \\ &\quad + \frac{\varepsilon^2}{12}T\operatorname{div}\Big(n\frac{\nabla\log T}{T}\Big)I + O(\varepsilon^4), \\ S &= -\frac{\varepsilon^2}{12}n\Big\{\Big(\frac{d}{2}+1\Big)R\nabla\log\Big(\frac{n}{T}\Big) + \Big(\frac{d}{2}+2\Big)\operatorname{div}R + \frac{3}{2}\Delta u\Big\} \qquad (4.31) \\ &\quad + \frac{\varepsilon^2}{12}\Big(\frac{d}{2}+1\Big)n\Big\{R\nabla\log\Big(\frac{n}{T^2}\Big) + \operatorname{div}R\Big\} + O(\varepsilon^4). \qquad (4.32) \end{aligned}$$

Proof. We apply formula (4.20) to obtain for all m, $n = 1, \dots, d$,

$$\begin{aligned} P_{mn} &= nT\Big(\delta_{mn} + \frac{\varepsilon^2}{8}(\delta_{mn}[\mathcal{Q}(s)] - [\mathcal{Q}(s)s_m s_n])\Big), \\ S_m &= -\frac{\varepsilon^2}{16}nT^{3/2}[\mathcal{Q}(s)|s|^2 s_m] + \frac{\varepsilon^2}{8}\Big(\frac{d}{2}+1\Big)nT^{3/2}[\mathcal{Q}(s)s_m]. \end{aligned}$$

Then the components of P are computed by employing (4.21) and (4.24), substituting the definitions of the coefficients X, Y, and Z, and replacing A and w by n and nu according to (4.29). In a similar way, S is evaluated using (4.22) and (4.25). □

4.2.5 Discussion of the QHD equations

The differences between our QHD equations and Gardner's model can be understood as follows. In both approaches, closure is obtained by assuming that the Wigner function f is in thermal equilibrium. However, the notion of "thermal equilibrium" is different.

In order to illustrate the differences, we recall the classical situation. For a system with the Hamiltonian $h(x,p) = |p|^2/2 + V(x)$, the unconstrained thermal equilibrium distribution is given by the Gibbs measure $f_G(x,p) = \exp(-h(x,p)/T_0)$ which minimizes the relative entropy $S = \int f(\log f - 1 - h/T_0)dp$. Here, T_0 denotes a temperature constant. If mass, momentum, and energy densities are given, the constrained thermal equilibrium is realized by a suitable rescaling and a momentum-shift of the Gibbs state,

$$\widetilde{f}_G(x,p) = n(x)\,\exp\Big(-\frac{h(x,p-u(x))}{T(x)}\Big). \tag{4.33}$$

The temperature $T(x)$, which is a Lagrange multiplier coming from the minimization procedure, is determined from the given energy density. The choice of $\widetilde{f}_G$ as a thermal equilibrium function has its physical justification in the fact that it is the unique minimizer of the relative entropy S with the prescribed moments.

Analogously, a quantum system, which is characterized by its energy operator $W^{-1}(h)$ (recall that W^{-1} is the Weyl quantization), attains its minimum of the relative (von Neumann) entropy in the mixed state with Wigner function $f_Q = \mathrm{Exp}\,(-h/T_0)$. This state represents the unconstrained quantum thermal equilibrium. The expansion of f_Q in terms of the scaled Planck constant ε^2 was first given in [**97**],

$$f_Q(x,p) = \exp(-h(x,p)/T_0)(1 + \varepsilon^2 f_2(x,p)) + O(\varepsilon^4)$$

with an appropriate function f_2. As a definition of the quantum equilibrium with moment constraints, Gardner employed this expansion of f_Q and modified it as follows:

$$\widetilde{f}_Q(x,p) = n(x)\exp\Big(-\frac{h(x,p-u(x))}{T(x)}\Big)\big(1+\varepsilon^2 f_2(x,p-u(x))\big)+O(\varepsilon^4). \tag{4.34}$$

These modifications mimic the passage from the Gibbs state to (4.33) in the classical situation. The use of $\widetilde{f}_Q$ as an equilibrium function results in simple formulas for the moment equations. However, the Wigner function (4.34) is an ad hoc ansatz. Moreover, in contrast to the classical case, $\widetilde{f}_Q$ is *not* the constrained minimizer for the relative von Neumann entropy.
The equilibrium state M_f used here is a genuine minimizer of the relative quantum entropy with respect to the given moments. In the spirit of the classical situation, these equilibria seem to be more natural. The price we have to pay is the appearance of various additional terms in the expansion of M_f.
If the temperature is assumed to be constant and if only the particle density is prescribed, both approaches to define a thermal equilibrium coincide. In order to see this, we write Gardner's momentum-shifted quantum equilibrium once again[1] more explicitly than in (4.34):

$$\widetilde{f}_G(x,p,t) = e^{-V/T-|p|^2/2T} \Big\{1+\frac{\varepsilon^2}{8T^2}\Big(-\Delta V+\frac{1}{3T}|\nabla V|^2+\frac{1}{3T}p_ip_j\partial_{x_ix_j}V\Big)\Big\}+O(\varepsilon^4).$$

The equilibrium function obtained from the entropy minimization with given particle density equals (see [**70**], Remark 3.3)

$$\begin{aligned}\widetilde{f}(x,p,t) &= \operatorname{Exp}\Big(A(x,t)-\frac{|p|^2}{2T}\Big)\\ &= e^{A-|p|^2/2T}\Big\{1+\frac{\varepsilon^2}{8T}\Big(\Delta A+\frac{1}{3}|\nabla A|^2-\frac{1}{3T}p_ip_j\partial_{x_ix_j}A\Big)\Big\}+O(\varepsilon^4).\end{aligned}$$

Both approximations are essentially derived in the same way. Using $n = \int \widetilde{f}_Q dp = (2\pi T)^{d/2}e^{-V/T}+O(\varepsilon^2)$ and assuming constant (or "slowly varying") temperature, Gardner has substituted $\nabla V = -T\nabla\log n + O(\varepsilon^2)$ in the formula for $\widetilde{f}_Q$ in order to avoid the second-order derivatives of the potential. This substitution in fact yields the approximation $\widetilde{f}$ since, by (4.29), $\nabla A = \nabla\log n + O(\varepsilon^2)$, and thus, both expansions $\widetilde{f}_Q$ and $\widetilde{f}$ coincide.

[1] We mentioned it already in (2.15).

4.3 Simplified QHD models

The full QHD model is given by equations (4.10)-(4.12) with the constitutive relations (4.30)-(4.32). In this section we will discuss some simplified versions. We recall the QHD equations

$$\begin{aligned} \partial_t n + \operatorname{div}(nu) &= 0, && (4.35)\\ \partial_t (nu) + \operatorname{div}(nu \otimes u) + \operatorname{div} P - n\nabla V &= 0, && (4.36)\\ \partial_t e + \operatorname{div}\big((P+eI)u\big) + \operatorname{div} S - nu\cdot\nabla V &= 0, && (4.37) \end{aligned}$$

where e is the energy density given by (4.28), and P, S, and U are given by (4.30)-(4.32) (without the $O(\varepsilon^4)$ terms).
First, we shall assume that the temperature is slowly varying in the sense of $\nabla \log T = O(\varepsilon^2)$. Then the expressions $\varepsilon^2 \nabla \log T$ in (4.30)-(4.32) are of order $O(\varepsilon^4)$ and can therefore be neglected in our approximation:

$$\begin{aligned} P &= nTI - \frac{\varepsilon^2}{12} n\Big((\nabla\otimes\nabla)\log n - \frac{R^\top R}{T}\Big), && (4.38)\\ S &= -\frac{\varepsilon^2}{12} n\Big\{\Big(\frac{d}{2}+1\Big)R\nabla\log n + \Big(\frac{d}{2}+2\Big)\operatorname{div} R + \frac{3}{2}\Delta u\Big\}\\ &\quad + \frac{\varepsilon^2}{12}\Big(\frac{d}{2}+1\Big) n\Big\{R\nabla\log n + \operatorname{div} R\Big\}, && (4.39)\\ e &= \frac{d}{2}nT + \frac{1}{2}n|u|^2 - \frac{\varepsilon^2}{24} n\Big(\Delta\log n - \frac{1}{T}\operatorname{tr}(R^\top R)\Big), && (4.40) \end{aligned}$$

The stress tensor P consists of the classical pressure nT on the diagonal, the "quantum pressure" $(\varepsilon^2/12)n(\nabla\otimes\nabla)\log n$, and the vorticity correction $(\varepsilon^2/12)nR^\top R/T$. The term S provides additional quantum corrections not present in [47]. The energy density consists of the thermal energy, kinetic energy, and quantum energy. Again, due to the vorticity R, the energy takes a different form than the expressions in [47, 52].
Further simplifications can be obtained if the vorticity is "small", i.e. $R = O(\varepsilon^2)$. In one space dimension this term always vanishes. If $R = O(\varepsilon^2)$ then $\varepsilon^2 R$ is of order $O(\varepsilon^4)$ and can be neglected. We obtain the QHD equations

$$\begin{aligned} &\partial_t n + \operatorname{div}(nu) = 0, && (4.41)\\ &\partial_t (nu) + \operatorname{div}(nu\otimes u) + \nabla(nT)\\ &\qquad - \frac{\varepsilon^2}{12}\operatorname{div}\big(n(\nabla\otimes\nabla)\log n\big) - n\nabla V = 0, && (4.42)\\ &\partial_t e + \operatorname{div}\big((P+eI)u\big) - \frac{\varepsilon^2}{8}\operatorname{div}(n\Delta u) - nu\cdot\nabla V = 0, && (4.43) \end{aligned}$$

with the stress tensor and energy density, respectively,

$$P = nTI - \frac{\varepsilon^2}{12} n(\nabla \otimes \nabla) \log n, \quad e = \frac{d}{2} nT + \frac{1}{2} n|u|^2 - \frac{\varepsilon^2}{24} n\Delta \log n.$$

This system of equations corresponds to Gardner's QHD model (without relaxation-time terms) except for the dispersive velocity term $(\varepsilon^2/8)\mathrm{div}(n\Delta u)$. We already mentioned in the introduction that this term has been also derived by Gardner and Ringhofer [**52**] by employing a Chapman-Enskog expansion of the Wigner-Boltzmann equation. They do not obtain vorticity terms since they assume that the quantum equilibrium distribution is an even function of the momentum p. Roughly speaking, this gives (in our context) the quantum exponential $\mathrm{Exp}\,(A - |p|^2/2T)$ instead of $\mathrm{Exp}\,(A - |p-w|^2/2T)$. The Lagrange multiplier w, however, is responsible for the presence of the vorticity term R.
Interestingly, most quantum terms cancel out in the energy equation. In fact, by substituting the above expression for the energy density in (4.43), a computation yields

$$\partial_t(nT) + \mathrm{div}\,(nTu) + \frac{2}{d} nT \mathrm{div}\, u - \frac{\varepsilon^2}{6d} \mathrm{div}(n\Delta u) = 0.$$

4.4 Conserved quantities

In this section we show that the mass and energy are conserved for the system (4.10)-(4.12) with the relations (4.30)-(4.32), neglecting the $O(\varepsilon^4)$ terms. The momentum is not conserved due to the electric force given by $\int n\nabla V dx$ and the potential is given with the Poisson equation (1.12).

Lemma 4.6. *The mass $N(t) = \int n dx$ and the energy*

$$E(t) = \int_{\mathbb{R}^d} \Big(e + \frac{\lambda^2}{2} |\nabla V|^2 \Big) dx,$$

where e is defined in (4.28) (without the $O(\varepsilon^4)$ term), are conserved, i.e. $dN/dt(t) = 0$ and $dE(t)/dt = 0$ for all $t > 0$. Furthermore, the energy can be written as

$$\begin{aligned} E(t) \;=\; & \int_{\mathbb{R}^d} \Big(\frac{d}{2} nT + \frac{1}{2} n|u|^2 + \frac{\lambda^2}{2} |\nabla V|^2 + \frac{\varepsilon^2}{6} |\nabla \sqrt{n}|^2 + \frac{\varepsilon^2 d}{48} n |\nabla \log T|^2 \\ & + \frac{\varepsilon^2}{24T} n\, \mathrm{tr}(R^\top R) \Big) dx \geq 0. \end{aligned} \tag{4.44}$$

Proof. The conservation of N is clear. In order to prove that E is conserved, we differentiate E and employ the equations (4.37) and (1.12):

$$\begin{aligned}\frac{dE}{dt} &= \int_{\mathbb{R}^d}(\partial_t e + \lambda^2\nabla V\cdot\nabla\partial_t V)dx = \int_{\mathbb{R}^d}(nu\cdot\nabla V - \lambda^2 V\partial_t\Delta V)dx \\ &= \int_{\mathbb{R}^d}(-\mathrm{div}(nu)V - V\partial_t n)dx = 0,\end{aligned}$$

taking into account (4.35). Next we show the formulation (4.44). The integral of the energy density e can be written as

$$\begin{aligned}E &= \int_{\mathbb{R}^d}\Big(\frac{d}{2}nT + \frac{1}{2}n|u|^2 + \frac{\varepsilon^2 d}{48}n|\nabla\log T|^2 + \frac{\varepsilon^2}{24T}n\,\mathrm{tr}(R^\top R)\Big)dx \\ &\quad + \frac{\varepsilon^2}{24}\int_{\mathbb{R}^d}\Big(-n\Delta\log n + n\Delta\log T + n\nabla\log T\cdot\nabla\log n\Big)dx.\end{aligned}$$

The last integral equals, after an integration by parts, to

$$\frac{\varepsilon^2}{24}\int_{\mathbb{R}^d}\Big(4|\nabla\sqrt{n}|^2 - \nabla n\cdot\nabla\log T + n\nabla\log T\cdot\nabla\log n\Big)dx = \frac{\varepsilon^2}{6}\int_{\mathbb{R}^d}|\nabla\sqrt{n}|^2dx,$$

which shows (4.44). □

The energy (4.44) consists of, in this order, the thermal energy, the kinetic energy, the electrostatic energy, and that of the Bohm potential. The remaining two terms represent additional field quantum energies associated to spatial variations of the temperature and the vorticity. These last two energy terms are new, i.e., they do not appear in the QHD equations of [**47**]. In the case of the QHD equations with slowly varying temperature, i.e. equations (4.35)-(4.37) and (1.12) with the definitions (4.38)-(4.39), the energy is given by (4.44) except the term involving $|\nabla\log T|^2$. If, additionally, the vorticity is "small", i.e. in the case of the model (4.41)-(4.43) and (1.12), which is used in the numerical simulations of section 4.5, the energy is equal to (4.44) except the last two terms.
Unfortunately, we are not able to prove the conservation of the $O(\varepsilon^4)$ approximation of the quantum entropy and the positivity of the particle density (as for the model in [**36**]) since we obtain $O(\varepsilon^4)$ correction terms which do not vanish.

4.5 Numerical results

In this section we present the results from our numerical simulations of a simple one-dimensional GaAs resonant tunneling diode, using the general

QHD system. The aim is also to compare the new equations with Gardner's QHD model; in particular, the influence of the dispersive velocity term will be explored.

The geometry of the resonant tunneling diode is chosen essentially as in Section 3.3.3. For our simulations, we use the one-dimensional stationary QHD equations for small temperature variations $\nabla \log T = O(\varepsilon^2)$ coupled to the Poisson equation for the electric potential. Including the physical parameters, these equations read as follows:

$$(nu)_x = 0, \tag{4.45}$$

$$m(nu^2)_x + k_B(nT)_x - \frac{\hbar^2}{12m}(n(\log n)_{xx})_x - qnV_x = 0, \tag{4.46}$$

$$\frac{5}{2}k_B(nTu)_x + \frac{1}{2}m(nu^3)_x - \frac{\hbar^2}{8m}(nu(\log n)_{xx} + nu_{xx})_x - qnuV_x = k_B\sigma(nT_x)_x, \tag{4.47}$$

$$\varepsilon_s V_{xx} = q(n - C). \tag{4.48}$$

The physical constants in the above equations are the effective mass m, the Boltzmann constant k_B, the reduced Planck constant $\hbar$, the elementary charge q, and the semiconductor permittivity ε_s. The values of these constants are given in Section 3.3.3, Table 3.1. The parameter σ is defined by

$$\sigma = \kappa\tau_0\frac{k_BT_0}{m},$$

with the thermal conductivity κ, the relaxation time τ_0, and the lattice temperature T_0.

We have allowed the heat flux $k_B\sigma(nT_x)_x$ since this term has also been used by Gardner [**47**] in his model with which we wish to compare our numerical results. In fact, we need this term for numerical stability as it is needed in Gardner's QHD equations. We expect that the heat conductivity can be obtained by a Chapman-Enskog expansion of the Wigner-Boltzmann equation but probably, additional diffusion terms might appear.

Using a standard scaling (see, e.g., [**58**]), we obtain the scaled QHD equations where the nondimensional parameters are the scaled Planck constant and the Debye length

$$\varepsilon^2 = \frac{\hbar^2}{mk_BT_0L^2}, \quad \lambda^2 = \frac{\varepsilon_s k_BT_0}{q^2C^*L^2},$$

respectively. Here, L is the device length and C^* the maximal doping concentration. For the values we used in the numerical simulations below (see Table 3.1), we obtain $\varepsilon^2 \approx 0.011$ which justifies our expansion in ε^2.

We compare the numerical results with Gardner's QHD equations which do not contain the dispersive expression $(\varepsilon^2/8)(nu_{xx})_x$ in the velocity but additional relaxation-time terms of Baccarani-Wordeman type [**14**]:

$$(nu)_x = 0, \tag{4.49}$$

$$m(nu^2)_x + k_B(nT)_x - \frac{\hbar^2}{12m}(n(\log n)_{xx})_x - qnV_x = -\frac{mnu}{\tau_p}, \tag{4.50}$$

$$\frac{5}{2}k_B(nTu)_x + \frac{1}{2}m(nu^3)_x - \frac{\hbar^2}{8m}(nu(\log n)_{xx})_x - qnuV_x = k_B\sigma(nT_x)_x - \frac{1}{\tau_w}\Big(e - \frac{3}{2}nT_0\Big), \tag{4.51}$$

together with the Poisson equation (4.48). Here, the momentum and energy relaxation times are given by, respectively,

$$\tau_p = \tau_0\frac{T_0}{T}, \quad \tau_w = \frac{\tau_p}{2}\Big(1 + \frac{3T}{mv_s^2}\Big),$$

where $\tau_0 = 0.9{\cdot}10^{-12}s$ is the momentum relaxation time and $v_s = 2{\cdot}10^7$ cm/s is the saturation velocity. The inclusion of these terms (at least if $\tau_p = \tau_w/2$) can be justified by employing a Caldeira-Leggett scattering operator as exposed in Section 4.2.1. We observed that the relaxation-time terms in Gardner's QHD model are necessary for numerical stability; on the other hand, they lead to severe numerical difficulties when included in the general QHD equations.

The above QHD equations have to be solved in the interval $(0, 1)$ with the following boundary conditions taken from [**47**]:

$$n(0) = C(0), \quad n(1) = C(1), \quad n_x(0) = n_x(1) = 0,$$
$$u_x(0) = u_x(1) = 0, \quad T(0) = T(1) = T_0, \quad V(0) = 0, \quad V(1) = U_0,$$

where U_0 is the applied voltage.

First, we discretize the new QHD equations (4.45)-(4.48) using central finite differences on a uniform mesh with $N = 500$ points. This corresponds to a mesh size of $h = 1/500 = 0.002$. The resulting discrete nonlinear system is solved by a damped Newton method with damping parameter found by a line search method (see Algorithm A6.3.1 in [**37**]). We employ the continuation method for the applied voltage, explained already in Section 3.3.1. The voltage step is chosen as $\triangle U = 1\,\text{mV}$.

The current-voltage characteristics using the thermal conductivities $\kappa = 0.2$ and $\kappa = 0.3$ are presented in Figure 4.1. There are apparently two regions

of negative differential resistance (NDR) if $\kappa = 0.2$ and three NDR regions if $\kappa = 0.3$. It is well known for Gardner's QHD model, that the behavior of the solutions is quite sensitive to changes of the value of the thermal conductivity. We observe a similar sensitive dependence: the peak-to-valley ratio, i.e. the ratio of local maximum to local minimum current density, is larger for larger thermal conductivities.
The electron density shows a charge enhancement in the quantum well which is more pronounced for smaller κ (see Figure 4.2 left). At the center of the right barrier, the electron density dramatically decreases. After the first valley in the current-voltage curve, the density develops a "wiggle", already observed in the viscous QHD (see Section 3.3.3, Figure 3.6). For larger values of the thermal conductivity, the minimum of the particle density increases, which stabilizes the numerical scheme.

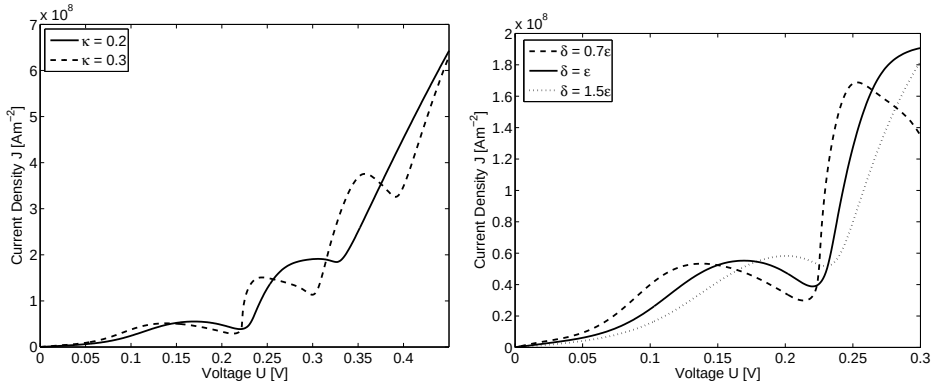

Figure 4.1: Left: Current-voltage characteristics for the general QHD system with thermal conductivities $\kappa = 0.2$ (solid line) and $\kappa = 0.3$ (dashed line). Right: Influence of the dispersive velocity term $(\delta^2/8)(nu_{xx})_x$ on the current-voltage curve for thermal conductivity $\kappa = 0.2$.

Next, we study the influence of the dispersive velocity term $(\varepsilon^2/8)(nu_{xx})_x$. For this, we replace the factor $\varepsilon^2/8$ by $\delta^2/8$ and choose various values for δ. Clearly, only $\delta = \varepsilon$ corresponds to the physical situation. The dispersive velocity term indeed regularizes the equations in the sense that the current-voltage curves become "smoother" (see Figure 4.1 right). A similar "smoothing" has been observed in Section 3.3.3 for the viscous QHD equations, but there, the smoothing originates from a diffusive and not from a dispersive term. For smaller values of δ, the peak-to-valley ratio of the first NDR region becomes larger. For $\delta = 0$, we arrive at Gardner's QHD equations without relaxation terms. We already mentioned that a central

finite-difference discretization fails for this model; therefore, the limit $\delta \to 0$ cannot be performed numerically.

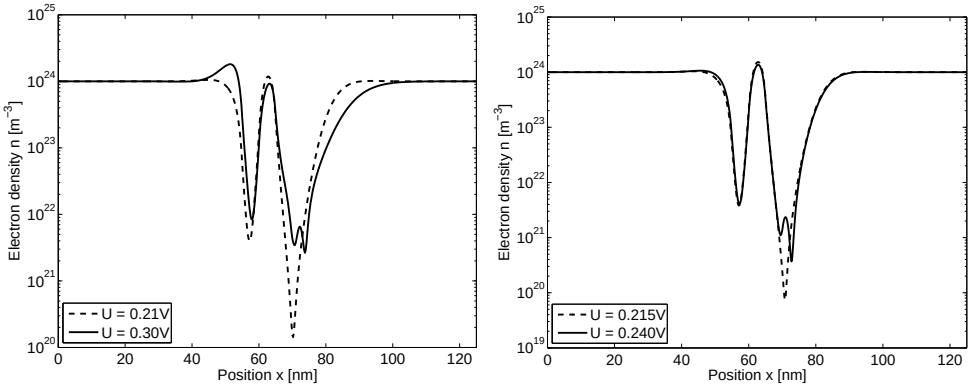

Figure 4.2: Electron density before (dashed line) and after (solid line) the first valley for thermal conductivities $\kappa = 0.2$ (left) and $\kappa = 0.3$ (right).

In Figure 4.3 the thermal energy $3/2nk_BT$ and the velocity $u = J/(qn)$ are reported. The velocity profile is very similar to that computed from Gardner's model (see Figure 4.4, $N = 500$). The velocity is high in the barriers and rather small in the well, i.e., the electrons spend more time in the quantum well than in the barriers. On the other hand, the temperature of the new QHD model differs from that obtained by Gardner's QHD model, in particular in the region between the barriers. The heating in the well in our model can be probably explained by the central scheme that we have used. Gardner's upwind scheme involves some numerical diffusion (see Section 3.3.2) which seems to bring down the thermal energy in the quantum well. We notice that $\nabla \log T$ is *not* of order $O(\varepsilon^2)$ as assumed in the derivation of the model except in the high doped contact regions.
The influence of the effective mass on the current-voltage curves are shown in Figure 4.5 (left). Corresponding to the effective masses $m = 0.067m_0$, $m = 0.092m_0$, $m = 0.126m_0$, the peak-to-valley ratios are 1.44, 1.79, 2.37, respectively. Here, m_0 denotes the electron mass at rest (see Table 3.1). The peak-to-valley ratio increases with the effective mass. Strictly speaking, the effective mass is not constant in the whole device but it is material depending. The use of a nonconstant effective mass would be more physical, but the modeling and the numerical approximation is—even in the much simpler quantum drift-diffusion model—a lot more involved [**95, 96**].
In Figure 4.5 (right) the current-voltage curve for the barrier height $B = 0.3\,\mathrm{eV}$ is shown. As expected, the peak-to-valley ratio is larger if the barrier

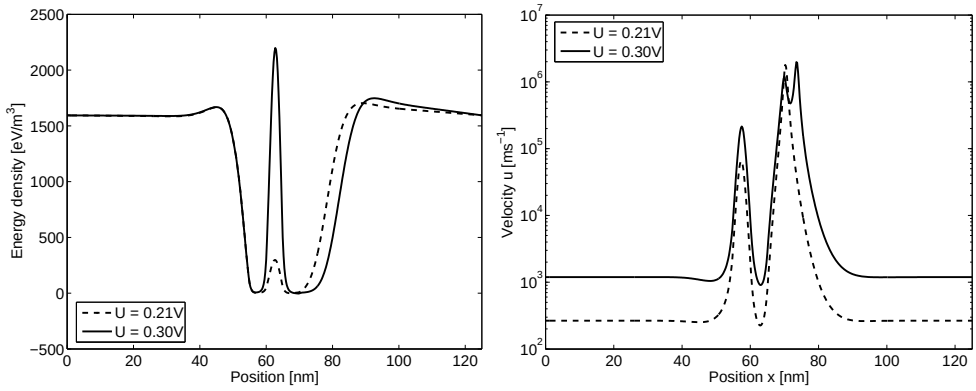

Figure 4.3: Thermal energy density (left) and velocity (right) before (dashed line) and after (solid line) the first valley computed from the general QHD model (thermal conductivity $\kappa = 0.2$).

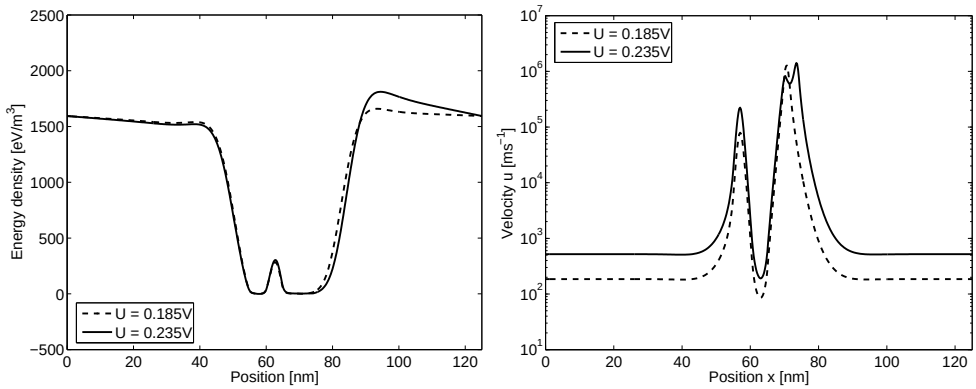

Figure 4.4: Thermal energy density (left) and velocity (right) before (dashed line) and after (solid line) the first valley computed from Gardner's QHD model (thermal conductivity $\kappa = 0.2$).

is higher (corresponding to a higher Al mole fraction); the values for the first NDR region are 1.44 for $B = 0.209\,\text{eV}$ and 2.48 for $B = 0.3\,\text{eV}$. The current densities are much smaller than in Figure 4.1, where the lower potential barrier $B = 0.209\,\text{eV}$ has been used. Interestingly, there are at least three NDR regions, whereas there are only two regions for the barrier height $B = 0.209\,\text{eV}$.

In Figure 4.6, the current-voltage curves for the general QHD equations and for Gardner's model are compared. Gardner's model is discretized using the

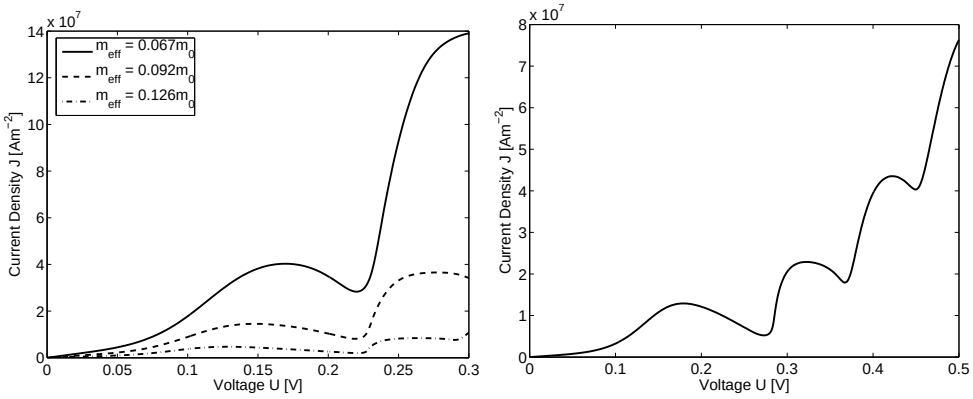

Figure 4.5: Left: Influence of the effective mass m_{eff} on the current-voltage characteristic. Right: Current-voltage characteristic for a barrier height of $B = 0.3\,\text{eV}$. In both pictures, $\kappa = 0.2$.

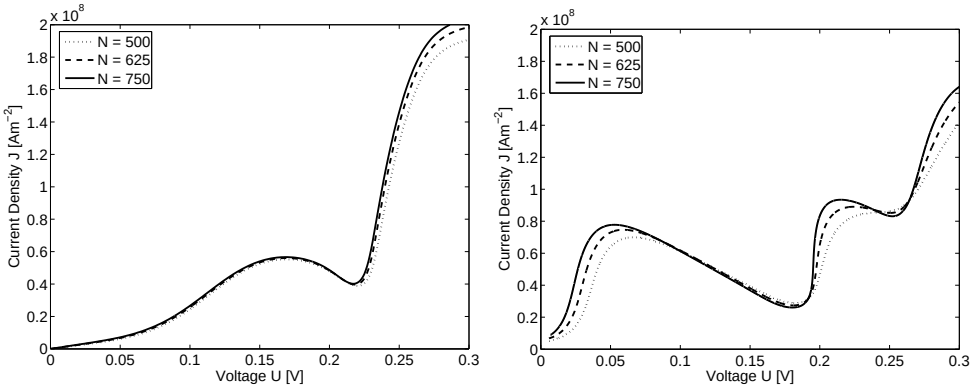

Figure 4.6: Influence of the number of discretization points on the current-voltage characteristics for the general QHD equations (left) and for Gardner's QHD model (right). In both pictures, $\kappa = 0.2$.

upwind method as in [47] (see also Section 3.3.1). The right figure with $N = 500$ points corresponds to Figure 2 of the cited paper. Notice that close to thermal equilibrium, there are well-known difficulties to compute the solution, which is not the case for our new model. Due to the numerical viscosity introduced by the upwind method, it is clear that the solution of Gardner's model depends on the mesh size. The solution to the new QHD equations is less mesh depending. In particular, the numerical results before the first valley are almost the same for $N \geq 500$ grid points. More

importantly, the slope of the curve in Gardner's model becomes steeper in the region after the valley when the mesh size h is decreased. On the other hand, the current-voltage curve of the general QHD model does not seem to develop such singular slopes. Moreover, it is possible to solve the discrete system for grid points $N > 750$ (not shown).

Conclusion and open problems

This thesis is devoted to the derivation, mathematical analysis and numerical approximation of quantum hydrodynamic models for semiconductor devices. Quantum hydrodynamic models are dispersive regularization of the classical Euler equations from fluid mechanics. The highly nonlinear structure and the quantum third-order terms make the analysis as well as numerics of these models very challenging and demanding. The central part of the thesis are the *general quantum hydrodynamic model*, derived by a moment method from the Wigner-Boltzmann equation using the entropy minimization principle and the *viscous quantum hydrodynamic model*, derived from the Wigner-Fokker-Planck equation, also by the method of moments but using different closure.

Although the entropy minimization principle enables a systematic approach to the construction of the quantum hydrodynamic models, it should be stressed that most of the mathematical properties concerning these models are not researched yet and that fact opens a large field of investigations for the future. Some of the possible, still unsolved tasks mentioned in [**36**] are: existence of solutions for the entropy minimization problem, well-posedness of the quantum hydrodynamic equations and the quantum BGK models, etc. However, a practical usage of new models does not require that all mathematical theory is settled. In this thesis it is shown that the simplified version of the general quantum hydrodynamic model is capable to produce the negative differential resistance in the simulation of the resonant tunneling diode.

Viscous quantum hydrodynamic model was developed by using particular collision operator, in order to replace numerical viscosity introduced by upwind discretization by correct physical viscosity. Due to the numerical tests performed in this thesis, the physical viscosity obtained from the Fokker-Planck collision operator was too strong and it caused the smoothing of the

current-voltage curve. Although the viscous quantum hydrodynamic model presented here is not the favourable one, our results motivate the consideration of the quantum hydrodynamic models with some different viscosities. We point out that our work here is a continuation of the idea of the viscous regularization of the classical hydrodynamic equations, already performed in [**6, 7, 12**]. In the same spirit, the viscous regularizations of the quantum hydrodynamic equations, were studied in [**45, 58, 72**]. Recently, the analysis of viscous regularizations in related Euler equations describing diffusive capillarity effects, including Korteweg-type terms with third-order derivatives, has been studied in [**21, 20**]. Interestingly, for a special choice of the capillarity function, the third-order Bohm potential is recovered. It is shown that introducing certain viscous terms enables the proof of new a priori estimates, leading to general existence results. Moreover, the strict positivity of the particle density can be proven. This observation motivate the study of the influence of various viscosities in the quantum hydrodynamic equations and their use as numerical stabilizations.

One interesting task concerning quantum hydrodynamic models would be to couple them to the mixed-state Schrödinger system in order to get hybrid quantum models. This has already been done for the classical and quantum drift-diffusion models in [**31, 38**].

At the end, we hope that the new results presented in this thesis contribute to the research of the quantum hydrodynamic models, opening in the same time some new perspectives for the future work.

Bibliography

[1] M. Abramowitz and I. A. Stegun: *Handbook of Mathematical Functions*. National Bureau of Standards, Applied Mathematics Series 55, USA, 1964.

[2] G. Alì and G. Frosali. On quantum hydrodynamic models for the two-band Kane system. *Nuovo Cimento B* 120 (12) (2005), 1279-1298.

[3] M. Ancona. Diffusion-drift modeling of strong inversion layers. *COMPEL* 6 (1987), 11-18.

[4] M. Ancona and G. Iafrate. Quantum correction to the equation of state of an electron gas in a semiconductor. *Phys. Rev. B* 39 (1989), 9536-9540.

[5] M. Ancona and H. Tiersten. Macroscopic physics of the silicon inversion layer. *Phys. Rev. B* 35 (1987), 7959-7965.

[6] A.M. Anile and S. Pennisi. Extended thermodynamics of the Blotekjaer hydrodynamical model for semiconductors. *Continuum Mech. Thermodyn.* 4 (1992), 187-197.

[7] A. M. Anile, V. Romano, and G. Russo. Extended hydrodynamical model of carrier transport in semiconductors. *SIAM J. Appl. Math.* 61 (1) (2001), 74-101.

[8] P. Argyres. Quantum kinetic equations for electrons in high electric and phonon field. *Phys. Lett. A* 171 (1992), 373-379.

[9] A. Arnold. Mathematical concepts of open quantum boundary conditions. *Transp. Theory Stat. Phys.* 30/4-6 (2001), 561-584.

[10] A. Arnold, J. Lopez, P. Markowich, and J. Soler. An analysis of quantum Fokker-Planck models: a Wigner function approach. *Rev. Mat. Iberoam.* 20 (2004), 771-814.

[11] N. Aschroft and N. Mermin. *Solid State Physics*. Sanners College, Philadelphia, 1976

[12] L. Ballestra, S. Micheletti, R. Sacco, and F. Saleri. On a viscous-hydrodynamic model for semiconductors: numerical simulation and stability analysis. *Comput. Visual. Sci.* 4 (2) (2001), 79-86.

[13] J. Barker and D. Ferry. Self-scattering path-variable formulation of high-field, time-dependent, quantum kinetic equations for semiconductor transport in the finite collision-duration regime. *Phys. Rev. Lett.* 42 (1979), 1779-1781.

[14] G. Baccarani and M. Wordeman. An investigation of steady-state velocity overshoot effects in Si and GaAs devices. *Solid-State Electronics* 28 (1985), 407-416.

[15] N. Ben Abdallah, P. Degond, and P. Markowich. On a One-Dimensional Schrödinger-Poisson Scattering Model. *ZAMP* 48-1 (1997), 135-155.

[16] P. Bhatnagar, E. Gross, and M. Krook. A model for collision processes in gases. I. Small amplitude processes in charged and neutral one-component systems. *Phys. Review* 94 (1954), 511-525.

[17] F. Bornemann, P. Nettesheim, and C. Schütte. Quantum-classical molecular dynamics as an approximation to full quantum dynamics. *J. Chem. Phys.* 105 (1996), 1074-1083.

[18] R. C. Bowen, G. Klimeck, R. Lake, W. Frensley, and T. Moise. Quantitative simulation of resonant tunneling diode. *J. Appl. Phys.* 81 (1997), 3207-3213.

[19] K. Brennan. *The Physics of Semiconductors*. Cambridge University Press, Cambridge, 1999.

[20] D. Bresch, B. Desjardins, and B. Ducomet. Quasi-neutral limit for a viscous capillary model of plasma. *Ann. Inst. H. Poincaré Anal. Non Linéaire* 22 (2005), 1-9.

[21] D. Bresch, B. Desjardins, and C. Lin. On some compressible fluid models: Korteweg, lubrication and shallow water systems. *Commun. Part. Diff. Eqs.* 28 (2003), 1009-1037.

[22] L. Brillouin. La méchanique ondulatoire de Schrödinger: une méthode générale de résolution par approximations successives. *Comptes Rendus* 183 (1926), 24-26.

[23] A. Caldeira and A. Leggett. Path integral approach to quantum Brownian motion. *Phys. A* 121A (1983), 587-616.

[24] F. Castella, L. Erdös, F. Frommlet and P. Markowich. Fokker-Planck equations as scaling limits of reversible quantum systems. *J. Stat. Phys.* 100 (2000), 543-601.

[25] P. Caussignac, J. Descloux, and A. Yamnahakki. Simulation of some quantum models for semiconductors. *Math. Models Meth. Appl. Sci.* 12 (2002), 1049-1074.

[26] L. L. Chang, L. Esaki, and R. Tsu. Resonant tunneling in semiconductor double barriers. *Appl. Phys. Lett. B* 24 (1974), 593-595.

[27] Z. Chen. A finite element method for the quantum hydrodynamic model for semiconductor devices. *Computers Math. Appl.* 31 (1996), 17-26.

[28] Z. Chen, B. Cockburn, C. Gardner, and J. Jerome. Quantum hydrodynamic simulation of hysteresis in the resonant tunneling diode. *J. Comput. Phys.* 117 (1995), 274-280.

[29] G. Cimatti, and G. Prodi. Existence results for a nonlinear elliptic system modelling a temperature dependent electrical resistor. *Ann. Mat. Pura Appl.* 152 (1988), 227-237.

[30] J. H. Davies *The Physics of low-dimensional semiconductors: an introduction.* Cambridge University Press, 1998

[31] P. Degond and A. El Ayyadi. A coupled Schrödinger drift-diffusion model for quantum semiconductor device simulations. *J. Comput. Phys. 181* 1 (2002), 222-259.

[32] P. Degond, S. Gallego, and F. Méhats. Isothermal quantum hydrodynamics: derivation, asymptotic analysis and simulation. *SIAM MMS* Vol.6 (1), (2007), 246-272.

[33] P. Degond, F. Méhats, and C. Ringhofer. Quantum hydrodynamic models derived from the entropy principle. *Contemp. Math.* 371 (2005), 107-131.

[34] P. Degond, F. Méhats, and C. Ringhofer. Quantum energy-transport and drift-diffusion models. *J. Stat. Phys.* 118 (2005), 625-665.

[35] P. Degond and C. Ringhofer. Binary quantum collision operators conserving mass, momentum and energy. *C. R. Acad. Sci. Paris, Sér. I* 336 (2003), 785-790.

[36] P. Degond and C. Ringhofer. Quantum moment hydrodynamics and the entropy principle. *J. Stat. Phys.* 112 (2003), 587-628.

[37] J. Dennis and R. Schnabel. *Numerical Methods for Unconstrained Optimization and Nonlinear Equations.* SIAM, Philadelphia, 1996.

[38] A. El Ayyadi and A. Jüngel. Semiconductor simulations using a coupled quantum drift-diffusion Schrödinger-Poisson model. *SIAM J. Appl. Math.* 66 (2005), 554-572.

[39] D. Ferry and H. Grubin. Modelling of quantum transport in semiconductor devices. *Solid State Phys.* 49 (1995), 283-448.

[40] D. Ferry and J.-R. Zhou. Form of the quantum potential for use in hydrodynamic equations for semiconductor device modeling. *Phys. Rev. B* 48 (1993), 7944-7950.

[41] W. Frensley. Wigner-function model of a resonant-tunneling semiconductor device. *Phys. Rev. B* 36 (3), (1987), 1570-1580.

[42] W. Frensley. Boundary conditions for open quantum systems driven far from equilibrium. *Rev.Modern Phys.* 62 (1990), 745-791.

[43] F. Frommlet, P. Markowich, and C. Ringhofer. A Wigner function approach to phonon scattering. *VLSI Design* 9 (1999), 339-350.

[44] I. M. Gamba, M. Gualdani, and P. Zhang. On the blowing up of solutions to a quantum hydrodynamic model on a bounded domain. Submitted to publication, 2007.

[45] I. Gamba and A. Jüngel. Positive solutions of singular equations of second and third order for quantum fluids. *Archive Rat. Mech. Anal.* 156 (2001), 183-203.

[46] I. Gamba and A. Jüngel. Asymptotic limits for quantum trajectory models. *Commun. Part. Diff. Eqs.* 27 (2002), 669-691.

[47] C. Gardner. The quantum hydrodynamic model for semiconductor devices. *SIAM J. Appl. Math.* 54 (1994), 409-427.

[48] C. Gardner. Resonant tunneling in the quantum hydrodynamic model. *VLSI Design* 3 (1995), 201-210.

[49] C. Gardner and C. Ringhofer. Smooth quantum potential for the hydrodynamic model. *Phys. Rev. E* 53 (1996), 157-167.

[50] C. Gardner and C. Ringhofer. Approximation of thermal equilibrium for quantum gases with discontinuous potentials and application to semiconductor devices. *SIAM J. Appl. Math.* 58 (1998), 780-805.

[51] C. Gardner and C. Ringhofer. The Chapman-Enskog expansion and the quantum hydrodynamic model for semiconductor devices. *VLSI Design* 10 (2000), 415-435.

[52] C. Gardner and C. Ringhofer. The Chapman-Enskog expansion and the quantum hydrodynamic model for semiconductor devices. *VLSI Design* 10 (2000), 415-435.

[53] I. Gasser and P. A. Markowich. Quantum hydrodynamics, Wigner transforms and the classical limit. *Asympt. Anal.* 14 (1997), 97-116.

[54] M. T. Gyi and A. Jüngel. A quantum regularization of the one-dimensional hydrodynamic model for semiconductors, *Adv. Diff. Eqs.* 5 (2000), 773-800.

[55] I. Gasser, P. Markowich, and C. Ringhofer. Closure conditions for classical and quantum moment hierarchies in the small-temperature limit. *Transp. Theory Stat. Phys.* 25 (1996), 409-423.

[56] I. Gasser, P. Markowich, D. Schmidt, and A. Unterreiter. Macroscopic theory of charged quantum fluids. In: P. Marcati et al. (eds.). *Mathematical Problems in Semiconductor Physics*. Research Notes in Mathematics Series 340 (1995), 42-75, Pitman.

[57] H. Grubin and J. Kreskovsky. Quantum moment balance equations and resonant tunneling structures. *Solid-State Electronics* 32 (1989), 1071-1075.

[58] M. P. Gualdani and A. Jüngel. Analysis of the viscous quantum hydrodynamic equations for semiconductors. *Europ. J. Appl. Math.* 15 (2004), 577-595.

[59] M. P. Gualdani, A. Jüngel, and G. Toscani. Exponential decay in time of solutions of the viscous quantum hydrodynamic equations. *Appl. Math. Lett.* 16 (2003), 1273-1278.

[60] F. Huang, H.-L. Li, A. Matsumura, and S. Odanaka. Well-posedness and stability of multi-dimensional quantum hydrodynamics in whole space. Preprint, Osaka University, Japan, 2004.

[61] A. Jüngel. A Note on Current-Voltage Characteristics from the Quantum Hydrodynamic Equations for Semiconductors, *Appl. Math. Lett.* 10 (4) (1996), 29-34.

[62] A. Jüngel. A steady-state quantum Euler-Poisson system for semiconductors. *Commun. Math. Phys.* 194 (1998), 463-479.

[63] A. Jüngel. *Quasi-hydrodynamic Semiconductor Equations*. Birkhäuser, Basel, 2001.

[64] A. Jüngel. *Transport Equations for Semiconductors*. Lecture Notes, Johannes Gutenberg-Universität Mainz, 2004.

[65] A. Jüngel and H.-L. Li. Quantum Euler-Poisson system: global existence and exponential decay. *Quart. Appl. Math.* 62 (2004), 569-600.

[66] A. Jüngel and H.-L. Li. Quantum Euler-Poisson systems: existence of steady states. *Archivum Math.* 40 (2004), 435-456.

[67] A. Jüngel and H.-L. Li. Quantum Euler-Poisson systems: global existence and exponential decay. *Quart. Appl. Math.* 62 (2004), 569-600.

[68] A. Jüngel, H.-L. Li, and A. Matsumura. The relaxation-time limit in the quantum hydrodynamic equations for semiconductors. *J. Diff. Eqs.* 225 (2006), 440-464.

[69] A. Jüngel, M. C. Mariani, and D. Rial. Local existence of solutions to the transient quantum hydrodynamic equations. *Math. Models Meth. Appl. Sci.* 12 (2002), 485-495.

[70] A. Jüngel and D. Matthes. A derivation of the isothermal quantum hydrodynamic equations using entropy minimization. *Z. Angew. Math. Mech.* 85 (2005), 806-814.

[71] A. Jüngel and S. Tang. A relaxation scheme for the hydrodynamic equations for semiconductors. *Appl. Num. Math.* 43 (2002), 229-252.

[72] A. Jüngel and S. Tang. Numerical approximation of the viscous quantum hydrodynamic model for semiconductors. *Appl. Numer. Math.* 56 (2006), 899-915.

[73] G. Klimeck. Quantum and semi-classical transport in NEMO 1-D. *J. Comput. Electr.* 2 (2003), 177-182.

[74] N. Kluksdahl, A. Kriman, D. Ferry, and C. Ringhofer. Self-consistent study of the resonant-tunneling diode. *Phys. Rev. B* 39 (1989), 7720-7735.

[75] H. Kramers. Wellenmechanik und halbzahlige Quantisierung. *Z. Physik* 39 (1926), 828-840.

[76] N. N. Lebedev, Special Functions and their Applications, Selected Russian Publications in the Mathematical Sciences, Prentice-Hall, 1965

[77] C. Lent and D. Kinrker. The quantum transmitting boundary method. *J.Appl.Phys.* 67 (1990), 7720-7735.

[78] C. Levermore. Moment closure hierarchies for kinetic theories. *J. Stat. Phys.* 83 (1996), 1021-1065.

[79] H.-L. Li and P. Marcati. Existence and asymptotic behavior of the multidimensional quantum hydrodynamic model for semiconductors. *Commun. Math. Phys.* 245 (2004), 215-247.

[80] M. Loffredo and L. Morato. Self-consistent hydrodynamical model for HeII near absolute zero in the framework of stochastic mechanics. *Phys. Rev. B* 35 (1987), 1742-1747.

[81] M. Loffredo and L. Morato. On the creation of quantized vortex lines in rotating HeII. *Il Nuovo Cimento* 108B (1993), 205-215.

[82] M. Lundstrom. *Fundamentals of Carrier Transport.* 2nd edition, Cambridge University Press, Cambridge, 2000.

[83] E. Madelung. Quantentheorie in hydrodynamischer Form. *Z. Physik* 40 (1927), 322-326.

[84] P. Markowich, C. Ringhofer and C. Schmeiser. *Semiconductor Equations*. Springer, Vienna, 1990.

[85] P. Mazumder, S. Kulkarni, M. Bhattacharya, J. P. Sun, and G. I. Haddad. Digital circuit applications of resonant tunneling devices. *Proceedings of the IEEE* 86 (1998), 664-686.

[86] D. Matthes. Some bifurcation problems in quantum hydrodynamics. In preparation, 2007.

[87] P. Pietra and C. Pohl. Weak limits of the quantum hydrodynamic model. In: *Proceedings of the International Workshop on Quantum Kinetic Theory*, Breckenridge, Colorado, USA, Special Issue of *VLSI Design* 9 (1999), 427-434.

[88] C. Pohl. *On the numerical treatment of dispersive equations*. PhD thesis, Technische Universität Berlin, Germany, 1998.

[89] M. A. Reed, J. W. Lee, and H. L. Tsai. Resonant tunneling through a double GaAs/AlAs superlattice barrier, single quantum well heterostructure. *Appl. Phys. Lett.* 49 (1986), 158-160.

[90] C. Ringhofer, C. Gardner, and D. Vasileska. Effective potentials and quantum fluid models: a thermodynamic approach. *Intern. J. High Speed Electronics Sys.* 13 (2003), 771-801.

[91] M. Rudan, A. Gnudi, and W. Quade. A generalized approach to the hydrodynamic model for semiconductor equations. In: G. Baccarani (ed.). *Process and Device Modeling for Microelectronics*, Elsevier, Amsterdam (1993), 109-154.

[92] M. Taylor. *Pseudodifferential Operators*. Princeton University Press, Princeton, 1981.

[93] W. Wenckebach. *Essentials of Semiconductor Physics*. John Wiley and Sons, Chichester, 1999.

[94] G. Wentzel. Eine Verallgemeinerung der Quantenbedingungen für die Zwecke der Wellenmechanik, *Z. Physik* 38 (1926), 518-529.

[95] A. Wettstein. *Quantum Effects in MOS Devices*. Series in Microelectronics 94, Hartung-Gorre, Konstanz, 2000.

[96] A. Wettstein, A. Schenk, and W. Fichtner. Quantum device-simulation with the density-gradient model on unstructured grids. *IEEE Trans. Electr. Dev.* 48 (2001), 279-284.

[97] E. Wigner. On the quantum correction for thermodynamic equilibrium. *Phys. Rev.* 40 (1932), 749-759.

[98] H. Xie, and W. Allegretto. $\mathbb{C}^{\alpha}(\overline{\Omega})$ solutions of a class of nonlinear degenerate elliptic systems arising in the thermistor problem. *SIAM J. Math. Anal.* 22 (1990), 1491-1499.

[99] B. Zhang and J. Jerome. On a steady-state quantum hydrodynamic model for semiconductors. *Nonlin. Anal.* 26 (1996), 845-856.